

**Low Band Gap Polymers Based on Isodiketopyrrolopyrroles,
Aminobenzodiones, 1,8-Benzodifuranones and Naphthodiones**

Inaugural-Dissertation

zur

Erlangung des Doktorgrades

der Mathematisch-Naturwissenschaftlichen Fakultät

der Universität zu Köln

vorgelegt von

Haichang Zhang

aus V. R. China

Köln 2013

Berichtersteller:

Prof. Dr. Bernd Tieke

Prof. Dr. Ulrich K. Deiters

Tag der Prüfung: 17.01.2014

Printed with support of the German Academic Exchange Service

(DAAD)

Abstract

In this work new monomers and polymers with donor-acceptor ability and polymers containing diketopyrrolo[3,2-*b*]pyrrole (isoDPP), benzodione and naphthodione chromophores in the main chain with deep colour, broad absorption and low band gap are prepared and investigated. The compounds might be suitable for electronic applications, especially in solar cell devices. Characteristic properties are studied using spectroscopic methods (UV/vis, fluorescence, NMR spectroscopy), gel permeation chromatography, cyclic voltammetry, elemental analysis, X-ray diffraction, differential scanning calorimetry, and thermogravimetric analysis.

Using Stille coupling, conjugated polymers containing isoDPP were prepared. The polymers exhibit a strong bathochromic shift compared with the previously reported isoDPP polymers and also show a high glass transition temperature (T_g) and excellent thermal stability. Photoirradiation studies indicate that the polymers in solution are extremely stable against UV and visible light irradiation. Spectroelectrochemical studies indicated a reversible electrochromism with isosbestic points near 710 nm.

Using Pd-catalysed Buchwald amination, some polymers based on aminobenzodiones were prepared and characterized. The polymers exhibit quite low band gaps (1.07 to 1.18 eV), high photostability and a large solvatochromic shift up to 3140 cm^{-1} . Furthermore, the polymers show broad UV/vis absorption

bands in a range from 400 to 900 nm with high extinction coefficients of 1.7 to $3.1 \times 10^4 \text{ L mol}^{-1} \text{ cm}^{-1}$.

Furthermore, four new monomers and two polymers based on naphthodifuranone (NDF) were synthesized. These compounds exhibit broad UV/vis absorption bands. Apart from that, for the first time monomers and polymers based on naphthodipyrrolidone (NDP) were synthesized in this work. The NDP-based polymers not only exhibit broad UV/vis absorption with high extinction coefficients, but also possess low band gaps. The broad absorption in the visible, combined with high colour depth and low band gap render NDP-based polymers interesting as building blocks for optoelectronic materials, especially for solar cell applications.

Zusammenfassung

Die vorliegende Arbeit beschäftigt sich mit der Synthese und den Eigenschaften neuer Monomere und Polymere mit Donor-Akzeptor-Fähigkeit sowie Polymeren, die isoDPP, Benzodione und Naphthodione in ihrer Hauptkette enthalten. Die hergestellten Polymere zeigen dunkle Farben, breite Absorptionen und kleine Bandlücken, was sie für mögliche elektronische Anwendungen interessant macht, insbesondere für Solarzellen. Mit Hilfe spektroskopischer Methoden (UV/Vis, Fluoreszenz, NMR-Spektroskopie), Gelpermeationschromatographie, Cyclovoltammetrie, Elementaranalyse, Röntgen-beugung (X-Ray), Differential-Scanning-Kalorimetrie und thermogravimetrische Analyse wurden die charakteristischen Eigenschaften untersucht.

Mittels Stille-Kupplung wurden konjugierte Polymere mit isoDPP synthetisiert. Diese Polymere weisen eine starke bathochrome Verschiebung im Vergleich zu den bisher literaturbekannten isoDPP-Polymeren auf, sowie eine hohe Glasübergangstemperatur (T_g) und eine ausgezeichnete thermische Stabilität.

Bestrahlungsversuche zeigen, dass die Polymere in Lösung äußerst stabil gegen UV- und sichtbares Licht sind. Durch spektroelektrochemische Untersuchungen konnte eine reversible Elektrochromie mit einem isobestischen Punkt nahe 710 nm nachgewiesen werden.

Einige Polymere, auf Basis von Aminobenzodionen, wurden durch Buchwald-Hartwig-Kupplung hergestellt und charakterisiert. Die Polymere weisen kleine Bandlücke (1.07-1.18 eV), eine hohe Photostabilität und eine große solvatochrome Verschiebung bis zu 3140 cm^{-1} auf. Darüber hinaus zeigen sie breite UV/Vis-Absorptionsbanden im Bereich von 400 bis 900 nm mit hohen Extinktionskoeffizienten von 1.7 bis $3.1 \cdot 10^4\text{ L mol}^{-1}\text{ cm}^{-1}$.

Außerdem wurden vier neue Monomere und zwei Polymere basierend auf Naphthodifuranon (NDF) dargestellt. Diese Verbindungen zeigen breite UV/Vis-Absorptionsbanden. Abgesehen davon wurden in dieser Arbeit zum ersten Mal Monomere und Polymere basierend auf Naphthodipyrrolidon (NDP) synthetisiert. Die NDP-enthaltenen Polymere weisen nicht nur breite UV/Vis-Absorption im Sichtbaren mit hohen Extinktionskoeffizienten, sondern auch kleine Bandlücke auf. Die breite Absorption im sichtbaren Bereich des Spektrums, kombiniert mit einer hohen Farbtiefe und einer kleinen Bandlücke machen NDP-basierte Polymere als optoelektronische Materialien interessant, insbesondere für Solarzellen.

List of abbreviations

ϵ	Extinction coefficient
Φ_f	Fluorescence quantum yield
abs	Absorption
λ	Wavelength
δ	Chemical shift
Å	Ampere
A	Acceptor
ABDF	Aminobenzodifuranone
BDF	Benzodifuranone
BDT	Benzo[1,2- <i>b</i> :4,5- <i>b'</i>]dithiophene
CV	Cyclic voltammetry
Da	Dalton
D	Donor
Da	Dalton
DCM	Dichloromethane
DTS	Dithieno[3,2- <i>b</i> :2'3'- <i>d</i>]silole
DSC	Differential scanning calorimetry
DMF	N,N-Dimethylformamide
DMSO	Dimethylsulfoxide
DPP	Diketopyrrolopyrrole
GPC	Gel permeation chromatography
h	Hour
HOMO	highest occupied molecular orbital
ICT	Intermolecular charge transfer
L	Liter
LUMO	Lowest occupied molecular orbital
min	Minute
max	Maximum
M_w	Molecular weight
NMR	Nuclear magnetic resonance
NDF	Naphthodifuranone
NDP	Naphthodipyrrolidone
nm	Nanometer
PD	Polydispersity
PL	Photoluminescence
TGA	Thermogravimetric analysis
T_g	Glass transition temperature
UV	Ultraviolet
V	Volt
Vis	Visible light

Table of contents

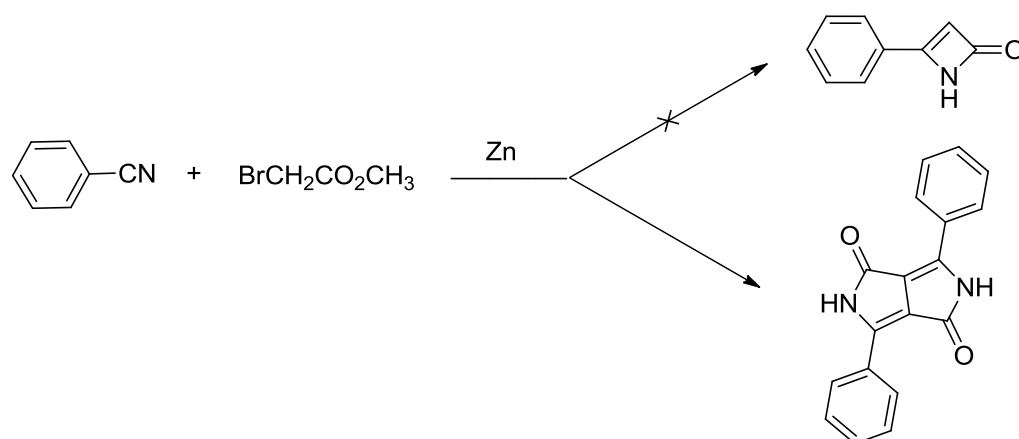
1	Introduction	1
1.1	Diketopyrrolopyrrole	1
1.2	Benzodifuranone	6
1.3	Benzodipyrrolidone	10
1.4	Naphthodifuranone	14
1.5	Concept of the work	16
2	Conjugated polymers based on isoDPP	19
2.1	Introduction	19
2.2	Synthesis of polymers	20
2.3	Conclusions	32
3	Conjugated polymers based on benzodiones	34
3.1	Introduction	34
3.2	Conjugated polymers based on amino-benzodiones via Buchwald amination	36
3.2.1	Preparation of benzodione-based monomers	36
3.3.2	Preparation of polymers	40
3.3	Polymers based on 1,8-BDF via Suzuki and Stille coupling	55
3.4	Conclusion	60
4	Conjugated polymers based on naphthodiones	62
4.1	Introduction	62
4.2	Monomers and polymers based on NDF	62
4.2.1	Monomers and polymers based on 1,10-NDF	62
4.2.1.1	Preparation of symmetrical monomers and polymers based on 1,10-NDF	62
4.2.1.1.1	Monomers	62
4.2.1.1.2	Polymers	69
4.2.1.2	Preparation of asymmetric monomers and polymers based on 1,10-NDF	79
4.2.1.2.1	Monomer	79
4.2.1.2.2	Polymers	82
4.2.2	Monomers and polymers based on 1,6-NDF	86
4.2.2.1	Monomers	86
4.2.2.2	Polymers	89
4.3	Monomers and polymers based on 1,6-NDP	92
4.3.1	Monomers	92

4.3.2	Polymers	98
4.4	Conclusion	106
5	Experimental Part	108
5.1	Materials	108
5.2	Instrumentation and general procedures	108
5.3	Synthesis	110
5.3.1	Conjugated polymers based on isoDPP	110
5.3.2	Conjugated polymers based on benzodiones	113
5.3.3	Conjugated polymers based on naphthodiones	133
5.3.3.1	Monomers and polymers based on NDF	133
5.3.3.2	Conjugated polymers based on NDP	157
6	References	169
7	Acknowledgement	178
8	List of publications	180

1 Introduction

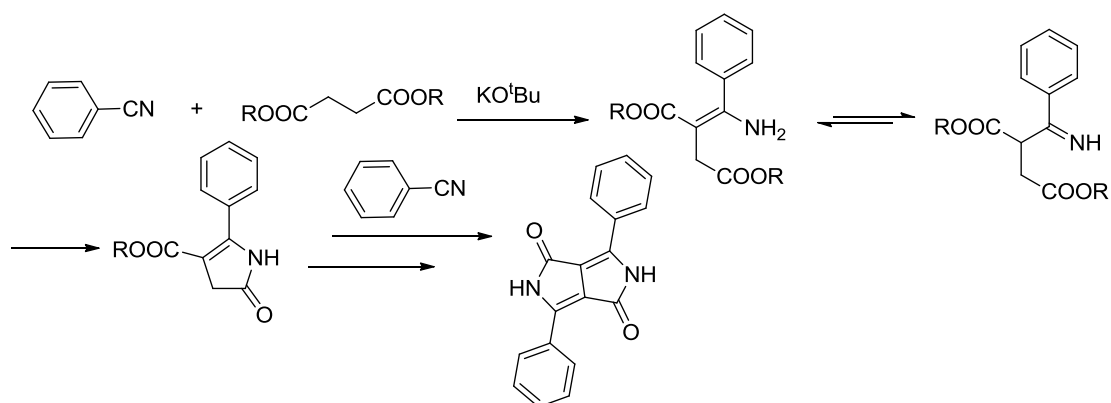
1.1 Diketopyrrolopyrrole

Diketopyrrolo[3,4-c]pyrrole (DPP) and its derivatives represent a key structural unit in an important class of yellow to red pigments with deep color, which were commercialized in the 1980s.^{1,2} A growing number of researchers focus their attention on DPPs since its monomers and DPP-containing polymers exhibit interesting light-emitting and photovoltaic properties.³⁻⁶



Scheme 1.1. Synthetic route to DPP (Farnum et al.).

DPP was first reported by Farnum et al.⁷ in 1974 with a very poor yield 5-20% (Scheme 1.1). After that, some researchers paid attention to this chromophore, and in 1983, Iqbal, Cassar, and Rochat^{8,9} reported an elegant synthetic pathway for DPP derivatives (Scheme 1.2). DPP derivatives exhibit a high luminescence, deep color, and weather resistance, which led to applications in paints, plastics, fibers and inks.



Scheme 1.2. Synthetic route to DPP via succinic esters.

The very first DPP-containing polymer was reported by Chan et al.¹⁰ in 1993 (Figure 1.1). Seven years later, a DPP polymer was prepared upon Suzuki coupling,¹¹ and another six years later, conjugated DPP polymers were prepared upon Heck coupling¹². In 2007, a report on DPP polymers prepared upon Buchwald-coupling appeared,¹³ and electrochemical polymerization¹⁴ was described in 2009. During this period, also many chemists and physicists have become interested in DPP-containing polymers.¹⁵⁻¹⁸

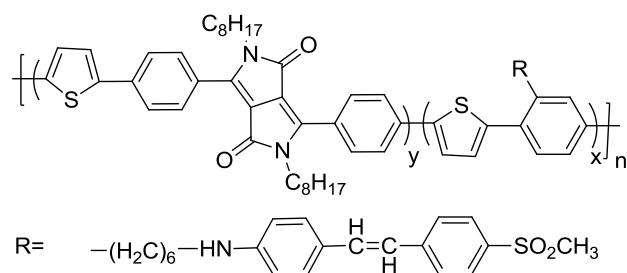


Figure 1.1. The first reported DPP-containing conjugated polymer.

Recently, thienylDPP derivatives were incorporated as an acceptor unit in the backbone of conjugated polymers. They are useful for solar cell materials, since they exhibit UV/vis absorption bands between 600 and 900 nm, small band gaps and high charge carrier mobilities.¹⁹⁻²⁴ Very recently, Yang Yang et al.²⁵ reported a DPP-containing copolymer (Figure 1.2) exhibiting a quite high power conversion efficiency (PCE) of up to 8.62 %.

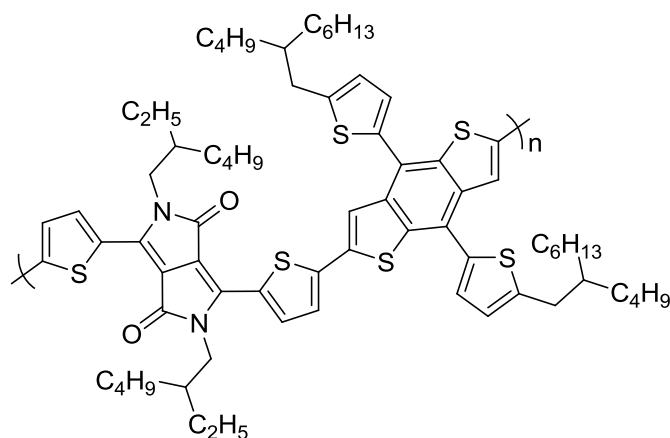


Figure 1.2. DPP based polymer with high PCE.

In 2009, Erqian Guo et al.²⁶ reported DPP derivatives (donor- π -bridge-acceptor- π -bridge- donor, D- π -A- π -D) (Figure 1.3.a), exhibiting very large two-photon absorption cross-sections (2290 GM) over a wide range of wavelengths with strong two-photon excitation red fluorescence (fluorescence quantum efficiency over 0.86). Later the same group also reported a DPP-containing polymer (Figure 1.3.b), which exhibits large two-photon absorption cross-sections (859 GM) with high fluorescence quantum efficiency of 0.67²⁷.

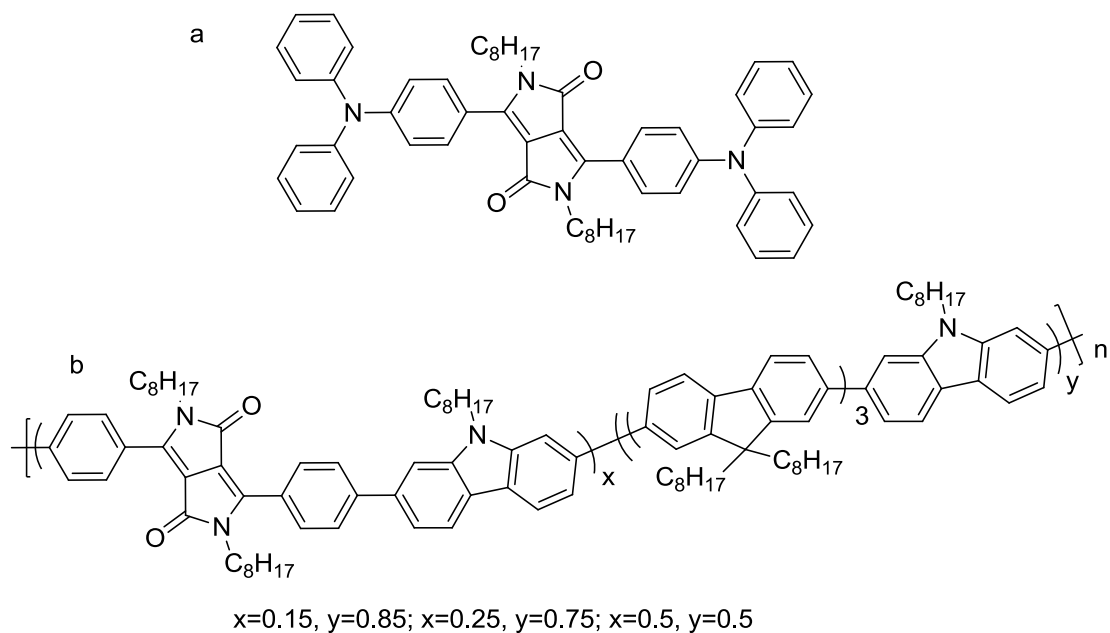
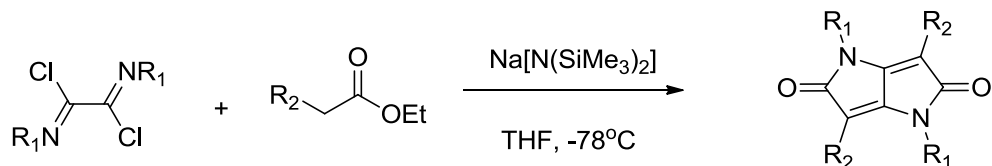


Figure 1.3. DPP-based monomer and polymers with large two-photon absorption cross-sections.

Besides diketopyrrolo[3,2-*b*]pyrrole derivatives, the regioisomeric diketopyrrolo[3,4-*c*]pyrrole (isoDPP) derivatives also represent useful organic pigments.²⁸⁻³⁰ Previously, isoDPP derivatives were prepared in three steps³¹ starting from (N-phenylacetyl)acetic acid aminoester, or in one step from pulvinic acid,^{32,33} but with very low yield. A new and efficient synthesis of *N,N'*-diphenylated isoDPP was recently described by Langer et al. (with yields up to 75 %) (Scheme 1.3).³⁴⁻³⁶



Scheme 1.3. Synthetic route to isoDPP by Langer et al.

Soon some polymers based on isoDPP were also studied. Irina Welterlich et al.³⁷ reported four polymers based on isoDPP in the main chain (Figure 1.4), which exhibit low fluorescence quantum efficiency (lower 1%), high extinction coefficients ($3.0 \times 10^4 \text{ L mol}^{-1} \text{ cm}^{-1}$), large Stokes shifts (216 nm) and broad absorption bands.

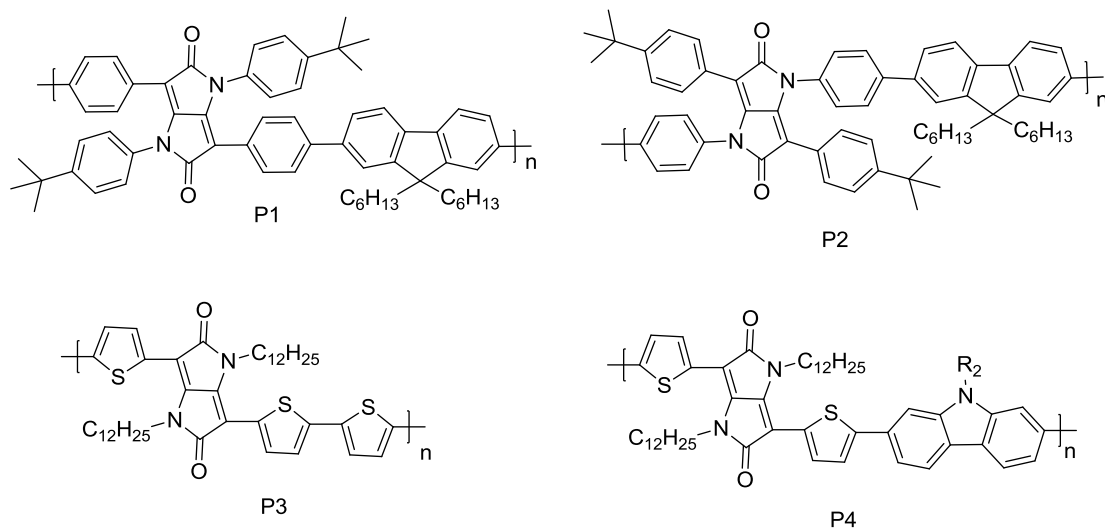


Figure 1.4. Structures of polymers based on isoDPP

Apart from that, a patent was filed on polymers containing N,N-dialkylated diaryl diketoporphyrin[3,2-b]pyrrole units. However, the yield of the dialkylated monomer was

low, only around 10 %.³⁸ A single crystal structure and some polymers based on this monomer were also reported by this group³⁹. The monomer exhibits a rather planar solid state conformation with the torsional angle between the thiophene units and the isoDPP core being 8.7°. The polymer exhibits a broad absorption, the maximum being at 642 nm as thin film, and a high PCE up to 5.1%.

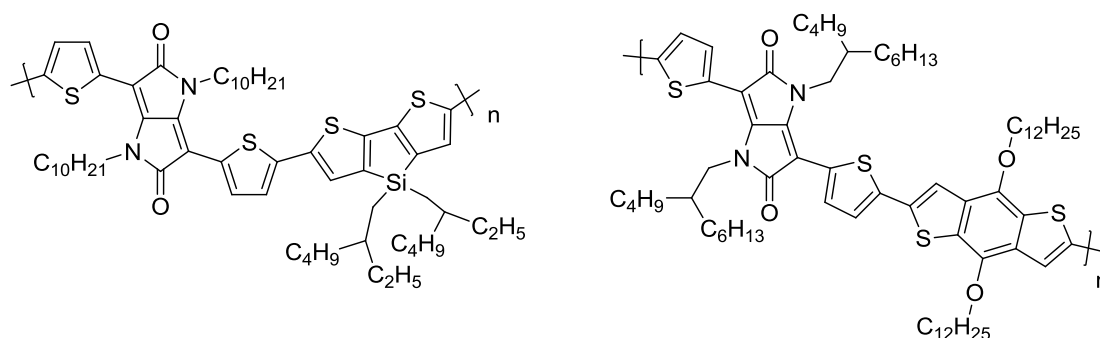
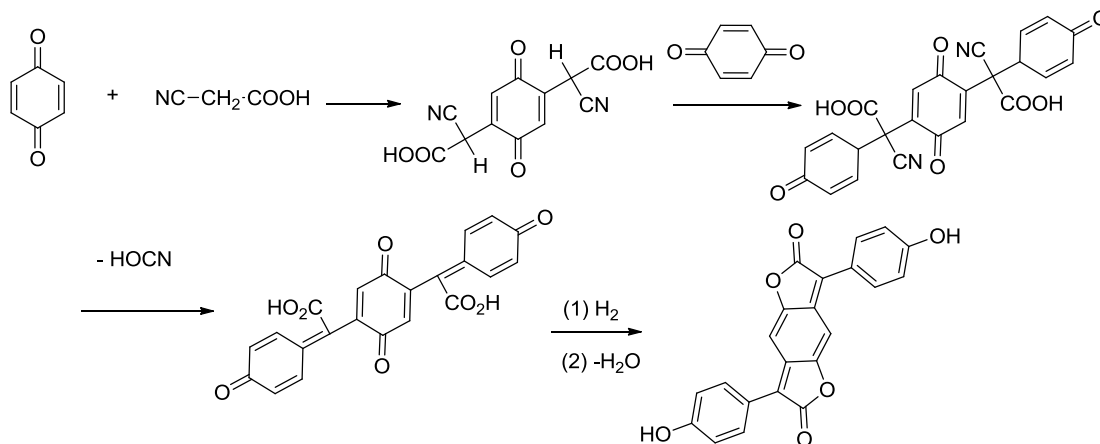


Figure 1.5. Structure of N,N-dialkylated-isoDPP based polymers.

1.2 Benzodifuranone

The first benzodifuranone (BDF) structure was reported by Greenhalgh et al.⁴⁰ in 1980, which was obtained by the reaction of benzoquinone with cyanoacetic acid leading to a double cyclization. Subsequent oxidization in air led to the conjugated molecule of benzodifuranone (Scheme 1.4). Soon the same group⁴¹ discovered that the reaction of quinone or hydroquinone with mandelic acid derivatives results in the same products. Because of their deep color, they were commercialized as disperse dyes for textiles, especially for polyesters. At the same time, some patents were also filed on this chromophore.⁴²⁻⁵³



Scheme 1.4. Synthetic route to BDF (Greenhalgh et al.).

Stephen J. Bentley et al.⁵⁴ synthesized the aminobenzodifuranone monomer (Figure 1.6) in 1996, and found that it exhibits a deep blue color. Soon this chromophore received much attention from the researchers. Aminobenzodifuranone exhibits a strong solvatochromism in different solvents. It was shown that aminobenzodifuranone exhibits positive solvatochromic shifts up to 200 nm, if the polarity of the solvents is increased.⁵⁵⁻⁵⁷

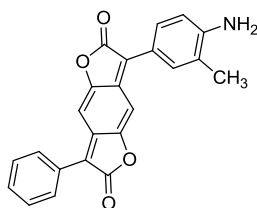


Figure 1.6. Structure of aminobenzodifuranone with large solvatochromic shift.

Ulmann⁵⁸ used a [70] fullerene-benzodifuranone acceptor dyad synthesized by a Ag⁺-mediated coupling reaction to construct a thin-film organic solar cell. He prepared a p-n heterojunction photovoltaic device consisting of a tetrabenzoporphyrin and a [70]fullerene-benzodifuranone dyad, which showed a weak but discernible contribution from light absorption of the dyad to the photocurrent under both a positive and a negative effective bias. The results indicate that the benzodifuranone attached to the acceptor contributes to light-harvesting by energy transfer.

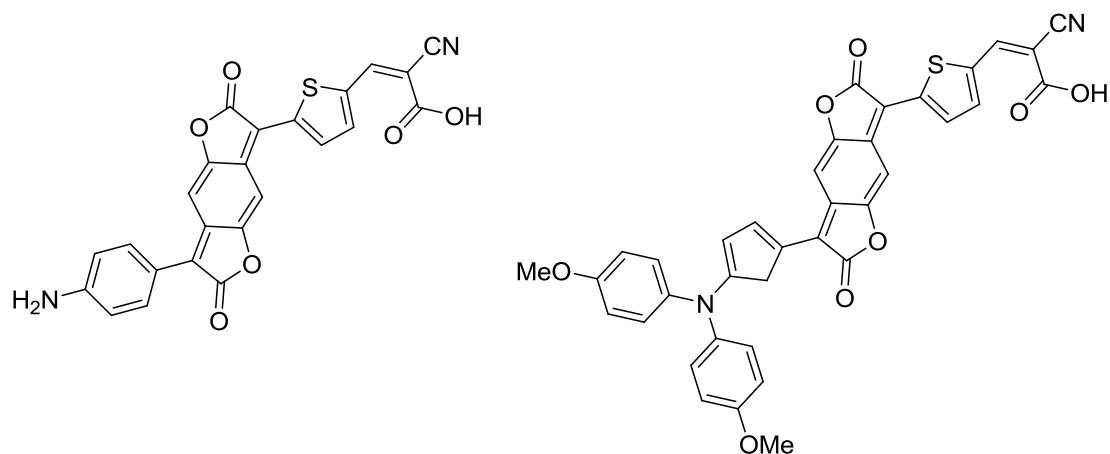


Figure 1.7. Structures of BDF with broad UV/vis absorption calculated with Gaussian formulas.

Ceron-Carraso et al.⁵⁹ designed and calculated some structures of benzodifuranone (Figure 1.7). The new structures exhibit an absorption maximum at 900 nm, if a thienyl unit is used instead of a phenyl ring. The LUMO of this kind of chromophores is always located in the benzodifuranone core. Unfortunately, these monomers have not been synthesized yet. Cai et al.⁶⁰ synthesized four symmetrical BDF monomers

and studied their third-order NLO properties at 800 nm using the femtosecond time-resolved DFMW technique. These compounds exhibit large values of X , n_2 and γ due to the high electron density in a conjugated system and a strong intramolecular charge transfer. Their response times were not more than 100 fs, which is commonly accepted to be the contribution from transient motion of the conjugated electron distribution. These features indicate potential applications of the symmetrical BDF compounds in nonlinear optics.

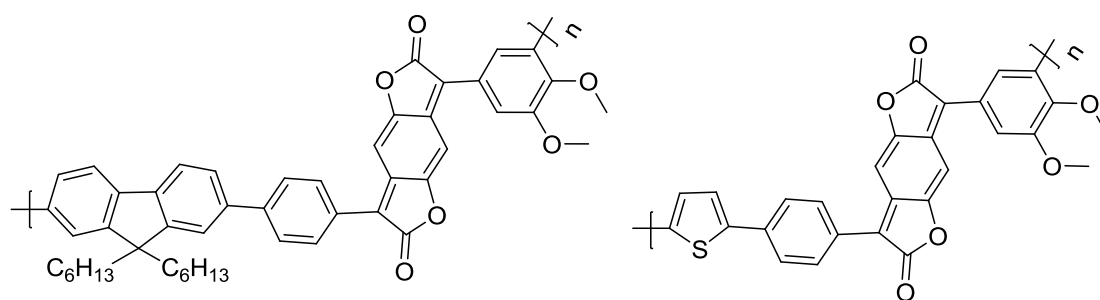


Figure 1.8. The first reported polymers based on BDF.

Very recently, Zhang and Tiede for the first time reported polymers based on unsymmetrical benzodifuranone prepared upon Suzuki and Stille coupling⁶⁰ (Figure 1.8), and polymers based on symmetrical para- and ortho-benzodifuranone which were obtained upon anodic oxidative coupling (Figure 1.9).⁶²⁻⁶⁴ The polymers exhibit broad absorption (400-700 nm) and low band gaps (1.22-1.33 eV). Unfortunately, no information is available yet on electronic devices based on benzodifuranone polymers.

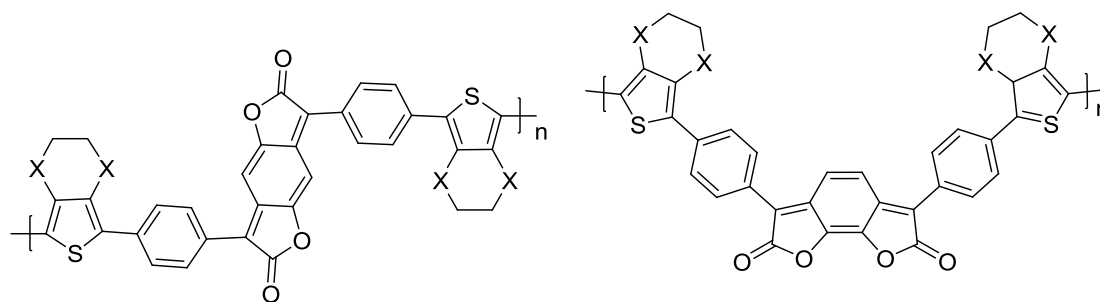
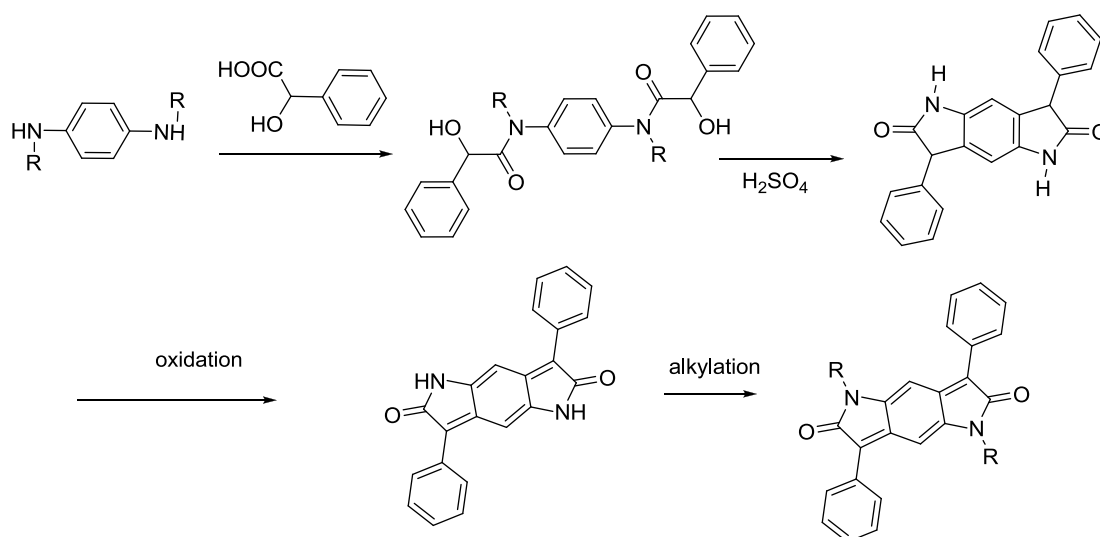


Figure 1.9. Polymer based on BDF prepared upon anodic oxidation.

1.3 Benzodipyrrolidone

Benzodipyrrolidone (BDP) is a molecule that was originally prepared as a colorant. Its structure is similar to DPP, but has the additional property of being a quinodimethane derivate. BDP was first prepared by Greenhalgh et al.⁴¹ through three step synthesis in 1994 (Scheme 1.5).



Scheme 1.5. Synthetic route to BDP by Greenhalgh et al.

Recently, Cui et al.⁶⁵ employed this chromophore to obtain two polymers based on

BDP. The examples of the polymers are displayed in Figure 1.10. The polymers exhibit excellent solubility in common organic solvents and deep color with broad absorption from 400 to 700 nm. The polymer shows n-type behavior with an electron mobility of $10^{-3} \text{ cm}^2 \text{ V}^{-1} \text{ s}^{-1}$. The authors also reported a single crystal structure of BDP which shows that the core of BDP is fully coplanar, and thus ensures full conjugation. The distance between adjacent core units of BDP is 3.56 Å, which indicates a weak π - π interaction.

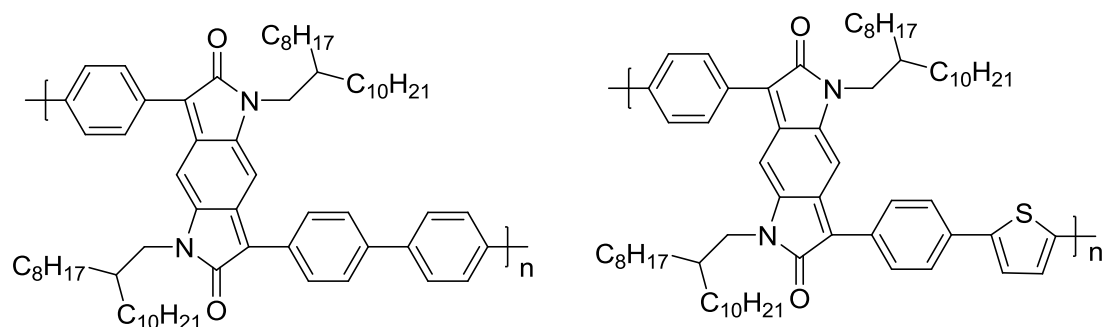


Figure 1.10. The first reported polymers based on BDP.

Deng et al.⁶⁶ studied *N*-acylation as a method for reducing the LUMO energy levels of benzodipyrrolidone-based polymers. Examples of polymers are displayed in Figure 1.11. The *N*-acylated polymers show reduced LUMO levels (about 0.3 eV) and improved reversibility of reductive doping compared with *N*-alkylated polymers. The low LUMO level and reversible reductive doping are desirable properties of conjugated materials for applications in n-type OFET devices, and as acceptors in bulk hetero-junction solar cells. This new strategy is not limited to

benzodipyrrolidone building blocks. It may also apply to other building blocks carrying lactam units.

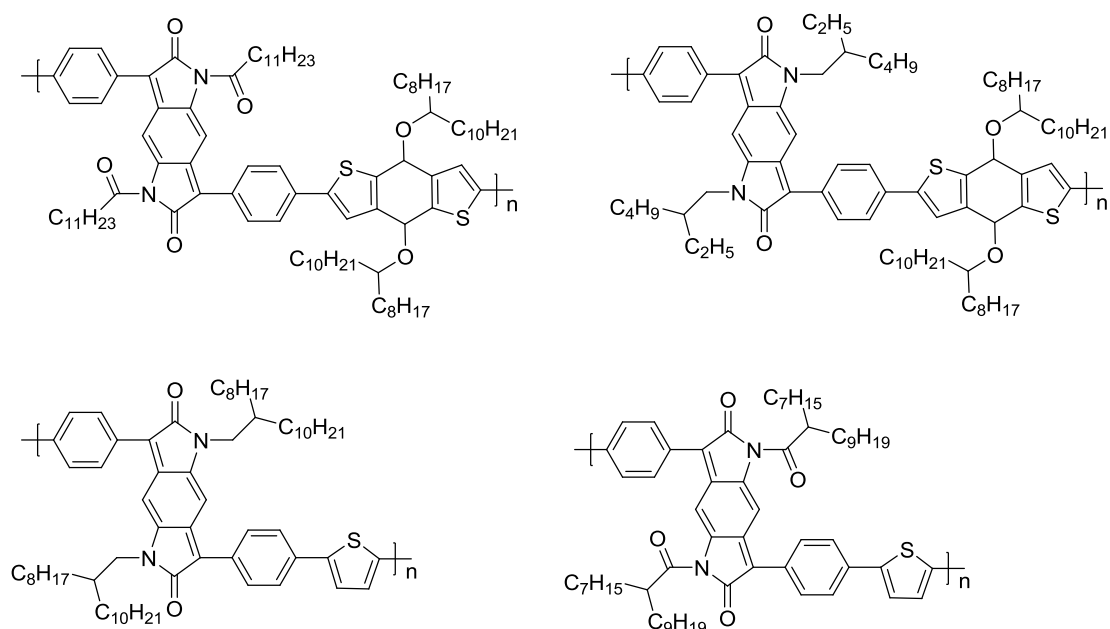


Figure 1.11. Polymers based on N-acylated and N-alkylated BDP.

Three new BDP-bithiophene copolymers were reported by Hong et al. (Figure 1.12).⁶⁷ The BDP moiety shows similar electron-accepting effects as the DPP unit in conjugated polymers, but it induces stronger intermolecular interactions due to its large ring size. The polymers exhibit a large hole mobility up to $0.03 \text{ cm}^2 \text{V}^{-1} \text{ S}^{-1}$, demonstrating that BDP is a potentially useful acceptor building block for polymer semiconductors for OFETs.

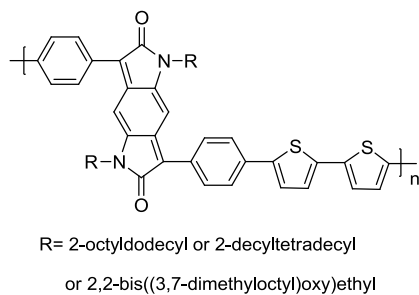


Figure 1.12. Structures of BDP-based polymers according to Hong et al.

Wei Yue et al.⁶⁸ reported a novel low band gap polymer (Figure 1.13) based on a dithienopyrrole containing unit as the donor and BDP as the acceptor. The UV/vis absorption of this covers the whole range from the visible to the near-infrared region of 350-900 nm with an electrochemical band gap of 1.44 eV, suggesting this class of materials as promising candidates for polymer solar cell applications. Furthermore they fabricated the first solar cell devices using BDP based polymers with a PCE of 2.6 %.

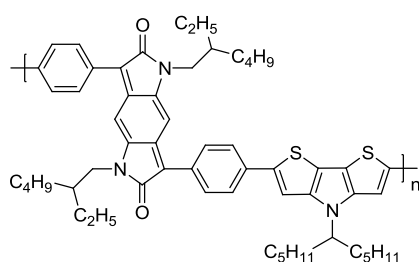


Figure 1.13. Polymer based on BDP with PCE of 2.6 %.

For the first time, Rumer et al.⁶⁹ reported a thienyl-substituted BDP monomer

synthesized through six steps, and described two polymers based on this monomer (Figure 1.14). The polymers show broad, long wavelength absorptions (500-1250 nm), deep LUMO energy levels (-4.16- -4.24 eV) and narrow bandgaps (1.03-1.17 eV). Balanced ambipolar charge transport behaviour of the polymer was also demonstrated with both hole and electron mobilities of over $0.1 \text{ cm}^2\text{V}^{-1}\text{S}^{-1}$ achieved in top gate transistor devices.

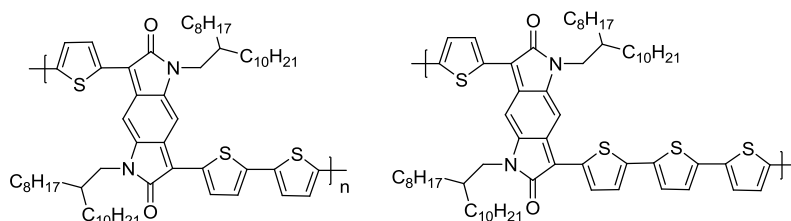
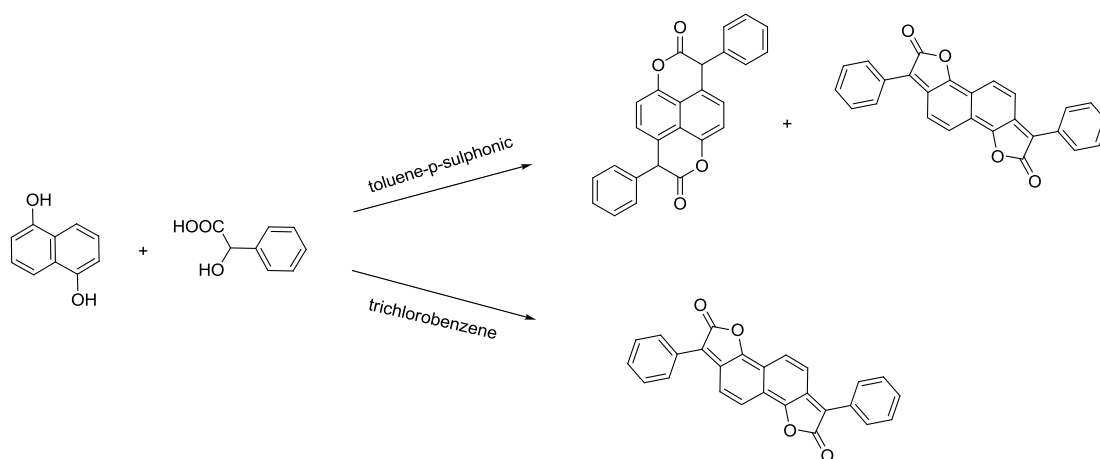


Figure 1.14. The first reported polymer based on thienyl-BDP.

1.4 Naphthodifuranone

The naphthodifuranone (NDF) structure is similar to BDF except an additional benzene ring is present in the core of NDF. The first NDF monomer was reported by Carey et al.⁷⁰ in 1957 (Scheme 1.6). The synthetic route to NDF is similar to BDF except that 1,5-dihydroxynaphthalene instead of 1,4-dihydroxybenzene is used. The authors tried to use different solvents to obtain the NDF monomer such as zinc chloride, molten toluene-p-sulphonic acid and methanesulphonic acid. Finally they found that the reaction in boiled trichlorobenzene proceeds with high yield (49 %), and free of side products, whereas the reaction in molten toluene-p-sulphonic acid yields a

mixture of 3,8-diphenylnaphtho[1,8-bc:4,5-b'c']dipyran-2,7-dione and 3,8-diphenylnaphtho[1,2-b:5,6-b']difuran-2,7-dione. Eleven years later, P. A. Smith studied this kind of monomers in his Ph.D study.⁷¹



Scheme 1.6. Synthetic route to NDF (John L. Carey et al).

Already in 2001, Hallas and Yoon^{72,73} reported a series of symmetric and unsymmetric monomers based on NDF (Figure 1.15). This kind of monomer exhibits colours from purple to blue. The asymmetrically substituted NDFs have a less hypsochromic colour shade compared with symmetrically substituted ones. Synthesis of asymmetric NDFs was difficult due to generation of many by-products by two competitive reactions, low yield and difficulty of purification. One year later, they comparatively studied the BDFs and NDFs.⁷⁴ The NDFs exhibited a much poorer build-up on polyester than the BDFs regardless of their asymmetric or symmetric structure. However, asymmetric NDFs have a better build-up than asymmetric NDFs.

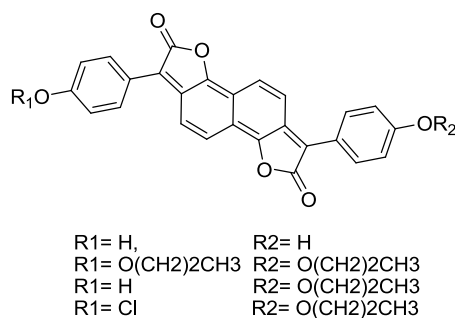


Figure 1.15. Asymmetric and symmetric structures of NDF.

1.5 Concept of the work

Among the so-called ‘high-performance pigments’, DPP, isoDPP, BDF and their derivatives have been the key chromophores in our research group over the last few years. In continuation of this work, the purpose of this dissertation is to synthesize new monomers with donor-acceptor ability, and polymers with deep color, broad absorption and low band gap, which might be suitable for electronic applications, especially in solar cell devices.

IsoDPP is a regioisomer of DPP, which exhibits strong electron acceptor ability as DPP. Up to now, only few articles reported isoDPP-containing polymers, which exhibit rather blue-shifted UV/vis absorption maxima around at 489 nm. Here, it was desired to employ monomers with planar structure such as BDT and DTS and to copolymerize it with isoDPP to obtain new donor-acceptor polymers. It was hoped that this kind of polymers has a strong bathochromic shift compared with the previously reported isoDPP polymers.

Aminobenzodifuranone is a deeply blue colored dye and a typical D-A system, in which aniline as electron donor is combined with benzodifuranone as acceptor unit. Till now, only few articles have been published about ABDF. Some articles reported a strong solvatochromism of this dye, whereas no publications could be found on aminobenzodipyrrolidones (ABDP). Up to now, polymers based on ABDF were only described by S. Ghasimi in his master thesis⁷⁵. In this dissertation, new polymers based ABDF and ABDP have been prepared and characterized using NMR, UV/vis absorption, cyclic voltammetry and gel permeation chromatography (GPC).

NDF-based dyes, which exhibit deep yellow to blue colors have been designed and synthesized in 1957. After this, only two more articles were published. In this dissertation, a series of monomers based on NDF are designed including some functional monomers with bromo end groups, which might be suitable for Stille and Suzuki coupling. Polymers based on NDF are prepared and characterized using NMR, UV/vis absorption, cyclic voltammetry and gel permeation chromatography (GPC).

The UV/vis absorption spectrum of BDP is similar to BDF since the structures of the compounds are similar. It was hoped that the UV/vis absorption spectra of the two monomers 3,8-di(4-bromophenyl)-1,6-bis-dodecyl-2,7-dioxo-1,2,6,7-tetrahydro-naphtho[1,2-*b*:5,6-*b'*]dipyrrole (1,6-NDP) and 1,6-NDF are also similar because the structures of the two molecules only differ in the presence of the N-atom instead of an

O-atom (Figure 1.16). In this dissertation, for the first time monomers and polymers based on 1,6-NDP are prepared and characterized using NMR, UV/vis absorption, cyclic voltammetry, gel permeation chromatography (GPC) and X-ray diffraction.

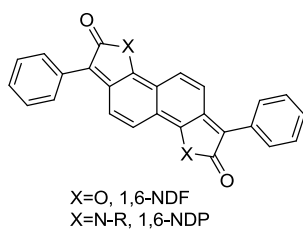


Figure 1.16. Structure of 1,6-NDF and 1,6-NDP.

2 Conjugated polymers based on isoDPP

2.1 Introduction

In recent years, extensive research efforts have been made to enhance the power conversion efficiency while up to now, the photovoltaic levels of polymer-based devices have not met commercial requirements for application. The less than ideal results are idered to be mainly caused by poor hole mobility, spectral mismatch between the polymer absorption and the terrestrial solar spectra, and short life times of the devices.^{76,77} In order to make devices with a long life time, it is necessary to use a polymer with excellent thermal stability and photostability. In order to enhance the hole mobility and the absorption of sunlight, and to obtain broader spectra of polymers, the most effective strategy is to introduce internal D-A structures by incorporating electron-rich and electron-deficient segments in the polymer backbone.⁷⁸⁻⁸⁰

Many kinds of electron-rich building blocks containing thiophene derivates have been proven to be particularly useful, among them being dithieno[3,2-*b*:2'3'-*d*]silole (DTS) and benzo[1,2-*b*:4,5-*b'*]dithiophene (BDT) as fused-ring thiophene donor building blocks. They have attracted much attention over the past few years due to their strong donor ability and large planar conjugated structure, which favors a high charge carrier mobility.⁸¹⁻⁸⁵ Furthermore, the 4-position of DTS has been replaced with a silicon atom which might induce a low-lying LUMO and low band gap in the polymers due to the effective orbital mixing of the Si- π^* orbital with the π^* orbital of the butadiene

fragment.^{82,86-88} Chu et al. synthesized D-A copolymers with DTS as donor which gave a PCE up to 7.3 %, while Hou et al. reported BDT D-A copolymers with a high PCE of 7.40 %.⁸⁹⁻⁹⁰

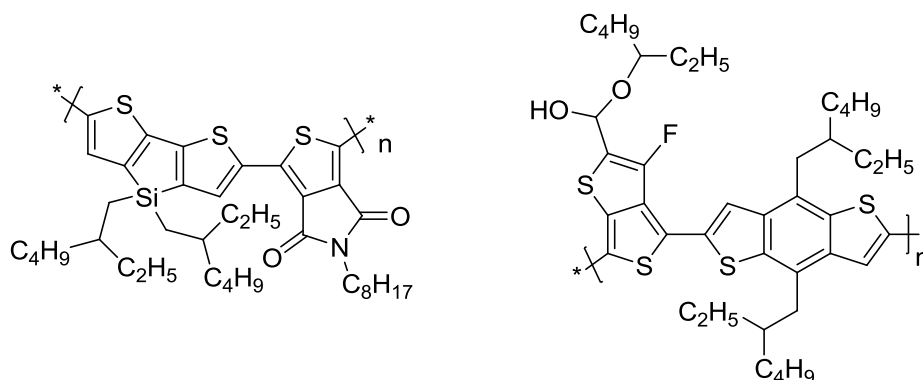


Figure 2.1. Polymers based on DTS or BDT with high PCE.

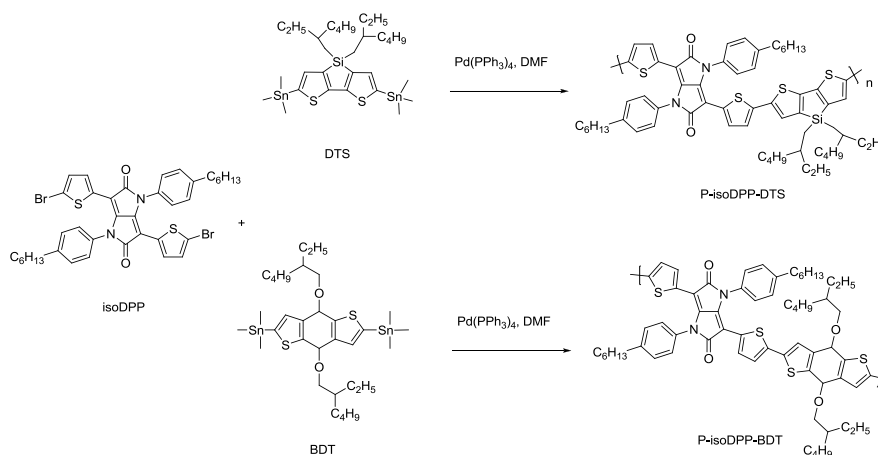
IsoDPP is a regioisomer of DPP as an interesting acceptor unit, which received much attention by the researchers. Up to now, very few monomers based on isoDPP have been reported, and only a few reports appeared on polymers based on isoDPP.³⁷⁻³⁹

In the following, two new polymers consisting of isoDPP as electron accepting unit, and DTS or BDT with large planar conjugated structure as the electron-donating building block are described.

2.2 Synthesis of polymers

The two D-A polymers were prepared by Stille coupling of monomer dibromo-substituted-isoDPP (**isoDPP**) with 4,4'-bis(2-ethylhexyl)-5,5'-bis-(trimethyltin)-dithieno[3,2-b:2',3'-d]silole (**DTS**) (**P-IsoDPP-DTS**), and **isoDPP** and

(4,8-bis(2-ethylhexyloxy)benzo[1,2-*b*:4,5-*b'*]dithiophene-2,6-diyl)bis(trimethyl-stannane) (**BDT**) (**P-IsoDPP-BDT**), the yields being 62-64 % (Scheme 2.1). **P-IsoDPP-DTS** shows excellent solubility in common organic solvents such as toluene, dichlorobenzene and tetrahydrofurane, while **P-IsoDPP-BDT** is only moderately soluble in dipolar aprotic solvents such as dimethylformamide and dichloromethane. The weight-average molecular weights (M_w) of the polymers are 14.8 kDa (**P-IsoDPP-DTS**) and 5.7 kDa (**P-IsoDPP-BDT**) and the polydispersity indices (PDI) are 1.7 (**P-IsoDPP-DTS**) and 1.5 (**P-IsoDPP-BDT**), respectively. The molecular structures were analyzed using $^1\text{H-NMR}$ spectroscopy (Experimental Part). The chemical shifts at about 0.80-2.76 ppm are typical for the protons of the alkyl group, while the broad signal with a chemical shift at about 6.60-7.70 ppm originates from the protons of phenyl and thiophene groups. The signals at about 3.69-3.79 ppm can be ascribed to the protons of the methylene group attached to the oxygen of the BDT unit.



Scheme 2.1. Synthetic routes to **P-IsoDPP-DTS** and **P-IsoDPP-BDT**.

2.3 Results and discussion

Single crystals of monomer isoDPP were prepared with 0.2*0.1*0.03 mm size from benzene solution, and their crystal structure was determined by X-ray diffraction (Figure 2.2). The unit cell with two molecules was found to be monoclinic with a $P2_1/c$ space group and the crystallographic center of symmetry being located at the midpoint of C17 and C17a. The core of isoDPP is fully coplanar, which ensures full conjugation. There is a 14.3° dihedral angle between the thiophene units and the isoDPP core, which is 4.4° larger than the torsional angle between the thiophene units and the N-terminal hexyl chain of thienyl-DPP.⁹¹ This indicates that thienyl-isoDPP is less coplanar than thienyl-DPP. The dihedral angle between the lactam phenyl ring and the isoDPP core is 76.6° . If this is true for the polymer, π - π interactions between adjacent isoDPP units and also between adjacent polymer chains become highly unlikely. The bond lengths from C2 to C3 to C4 to N1 to C17a to C17 were found to be 1.448, 1.492, 1.411, 1.386 and 1.446 Å. Due to the large distance of adjacent isoDPP cores of 6.969 Å, a direct π - π interaction can be ruled out. In DPP the relevant distance is only 3.614 Å, causing strong π - π interactions.⁹¹

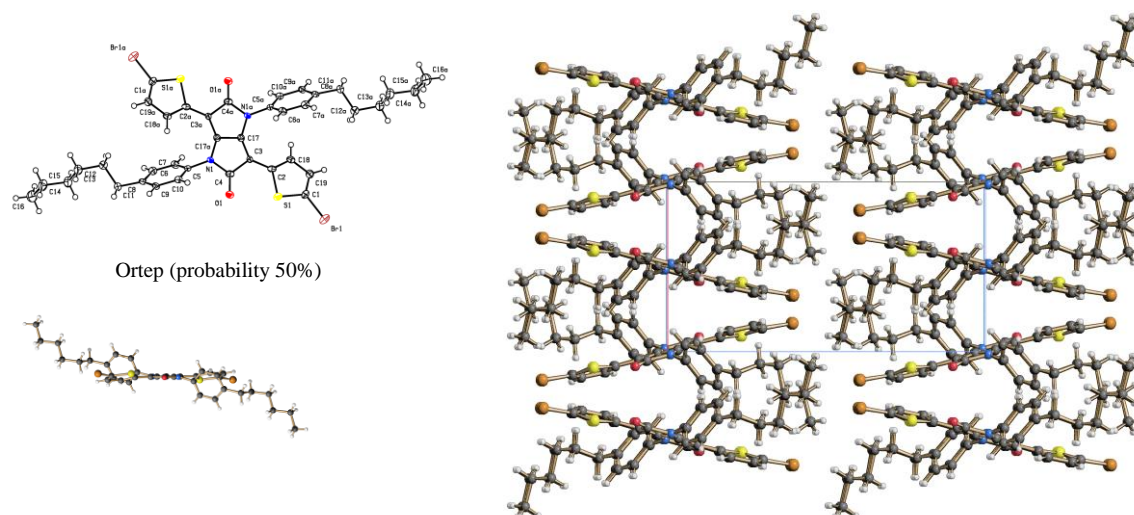


Figure 2.2. Single crystal structure of **isoDPP**.

Optical properties.

In Figure 2.3, the UV/vis absorption and fluorescence spectra of the polymers and UV-vis absorption spectrum of the monomer **isoDPP** in dichloromethane are shown. The polymer solutions are deeply colored. The extinction coefficients of the strongest bands are $64877 \text{ L mol}^{-1} \text{ cm}^{-1}$ for **P-IsoDPP-DTS**, and $26485 \text{ L mol}^{-1} \text{ cm}^{-1}$ for **P-IsoDPP-BDT**, respectively. **P-IsoDPP-DTS** forms a blue solution with an absorption maximum at 587 nm, while the solution of **P-IsoDPP-BDT** is purple, the main absorption of the π -conjugated backbone occurring at 509 nm. Compared with monomer **isoDPP**, the absorption of **P-IsoDPP-DTS** is red-shifted by 151 nm, while the red-shift of **P-IsoDPP-BDT** is 73 nm. The red-shift originates from the extended π -conjugation of the backbone and, in addition, can be ascribed to D-A interactions between the dithienyl-DTS or dithienyl-BDT units and the adjacent isoDPP core (without the two thienyl groups) giving rise to an enhanced intramolecular charge

transfer (ICT). The absorption maxima of **P-IsoDPP-BDT** and **P-IsoDPP-DTS** are 30 and 98 nm red-shifted compared with the copolymer synthesized by Welterlich et al., which contained thienyl comonomer units instead of BDT or DTS. The red shift can be ascribed to a stronger D-A character originating from the DTS and BDT units. In addition, the higher molecular weight, which induces a longer π - π^* -conjugated system may also play a role. The difference in the red-shift of **P-IsoDPP-DTS** and **P-IsoDPP-BDT** has two origins. First, the DTS unit provides **P-IsoDPP-DTS** with a low-lying LUMO and a low band gap due to effective mixing of the Si- π^* orbital with the π^* orbital of the butadiene fragment,^{82,86-88} and second the BDT-containing polymer has a low molecular weight with less extended π -system. Further red-shift of the absorption may be possible, if a higher molecular weight can be obtained, and if the N-phenyl units of isoDPP are replaced by N-alkyl chains. This would improve π -stacking of the chromophores and decrease the band gap. The two polymers exhibit a weak fluorescence with maxima at 744 nm for **P-IsoDPP-DTS**, and 660 nm for **P-IsoDPP-BDT**, respectively (Figure 2.3). The fluorescence quantum yields are very low (0.13 % for **P-IsoDPP-DTS**, and 0.82 % for **P-IsoDPP-BDT**) resulting in unsmooth fluorescence spectra in dichloromethane solution.

Table 2.1. Optical properties of polymers.

Polymer	λ_{\max} [nm]		λ_{em} [nm]	Stokes shift	Φ_f [%]	Extinct coeff ϵ (λ_{\max}) [L mol ⁻¹ cm ⁻¹]
	in DCM	in thin film				
P-IsoDPP-DTS	587	620	744	204	0.13 ^a	64887 (587 nm)
P-IsoDPP-BDT	371, 509	523	660	158	0.82 ^a	26485 (502 nm)

^a compared with Rhodamine 6G in ethanol.

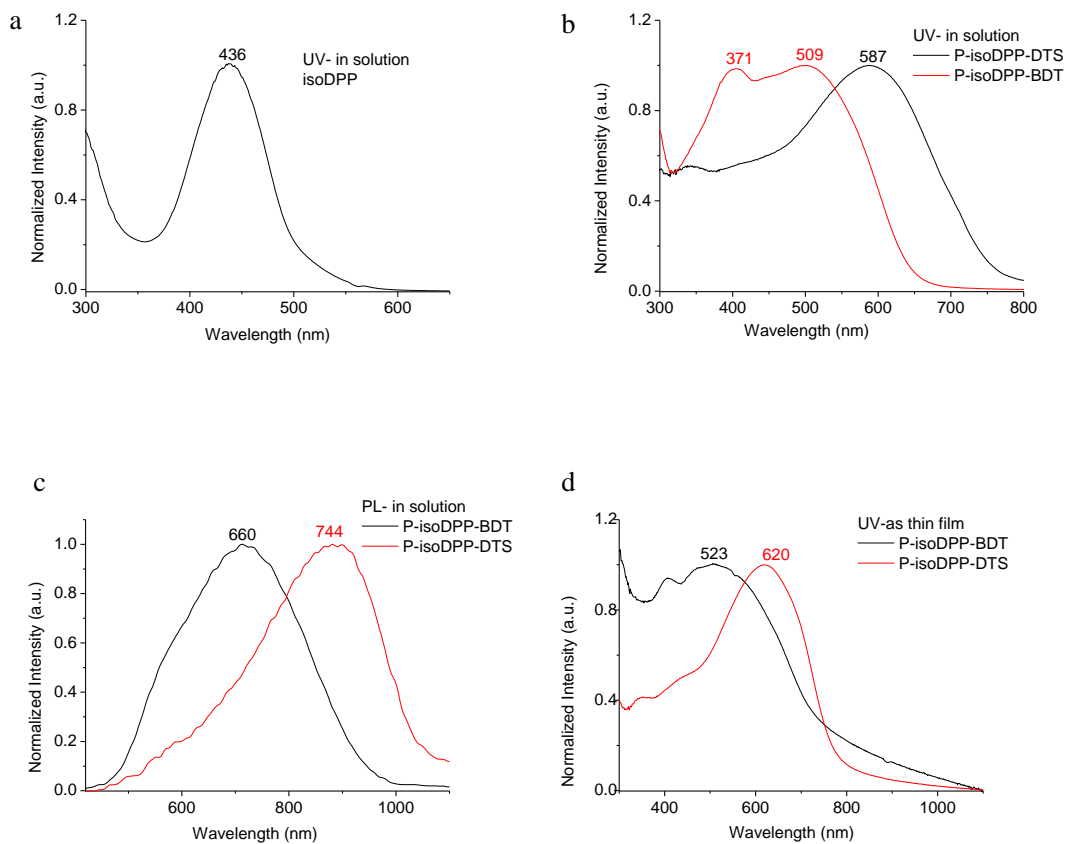


Figure 2.3. UV/vis absorption spectra of monomer **isoDPP** and polymers in dichloromethane solution (a,b), emission spectra of polymers in dichloromethane solution (c), and UV/vis absorption spectra of polymers in thin films (d).

UV/vis absorption spectra of the polymer films are very broad and red-shifted (33 nm for **P-IsoDPP-DTS**, and 14 nm for **P-IsoDPP-BDT**) compared with the solution spectra. The long-wavelength tail of the absorption bands is extended to the infrared. This indicates a more planar conformation, whereas an increase of the π - π interchain association seems unlikely because of the strong tilt of the phenyl units of isoDPP shown by the structure analysis. The polymer absorption bands are very broad ranging

from 400 nm to 800 nm, which might be advantageous for solar cell applications, since the absorption is extended to the region where the solar photon flux is most intense (that is in the 600-800 nm range).^{92,93} The optical bandgaps (E_g^{opt}) calculated from the absorption edges of the **P-IsoDPP-DTS** and **P-IsoDPP-BDT** films are 1.42 eV and 1.39 eV, respectively. The photophysical data are summarized in Table 2.1.

Photostability of polymers

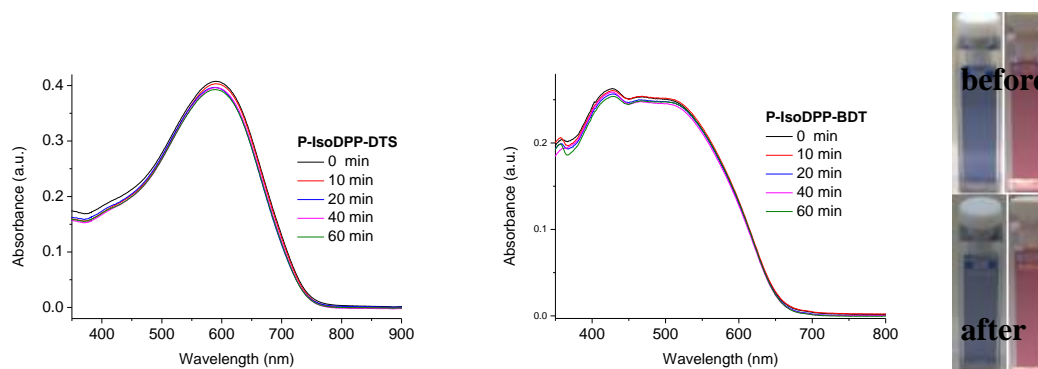


Figure 2.4. UV/Vis absorption spectra of polymers (left: **P-IsoDPP-DTS**; right: **P-IsoDPP-BDT**) before and after irradiation in toluene. Photographs of polymers (left: **P-IsoDPP-DTS**; right: **P-IsoDPP-BDT**) in toluene before and after irradiation are also shown.

In order to investigate the photostability of the polymers, we used a 200 W Hg lamp (Oriel Instruments 6283) and irradiated **P-IsoDPP-DTS** and **P-IsoDPP-BDT** in toluene, respectively. As shown in Figure 2.4, the absorption maxima of **P-IsoDPP-DTS** and **P-IsoDPP-BDT** are only slightly diminished after irradiation for 60 min. This indicates that **P-IsoDPP-DTS** and **P-IsoDPP-BDT** are very stable in UV-light. IsoDPP-based polymers are much more stable in the UV-light than

DPP-based polymers.⁹⁴

Electrochemical Properties.

The electrochemical properties of the two polymers were investigated using cyclic voltammetry. The HOMO and LUMO energy levels of the polymers were estimated from the onset of the oxidation and reduction curves, respectively. (see Figure 2.5 and Table 2.2). **P-IsoDPP-BDT** shows a single broad and irreversible oxidative peak with maximum at +0.71 V and a quasi-reversible reduction peak at -1.74 V which is reverted at -1.54 V. Anodic oxidation of **P-IsoDPP-DTS** takes place at a low potential of 0.35 V, and further peaks appear at 0.58 and 1.08 V. The oxidation behavior is irreversible. The cathodic wave sets in at a potential of -1.43 V.

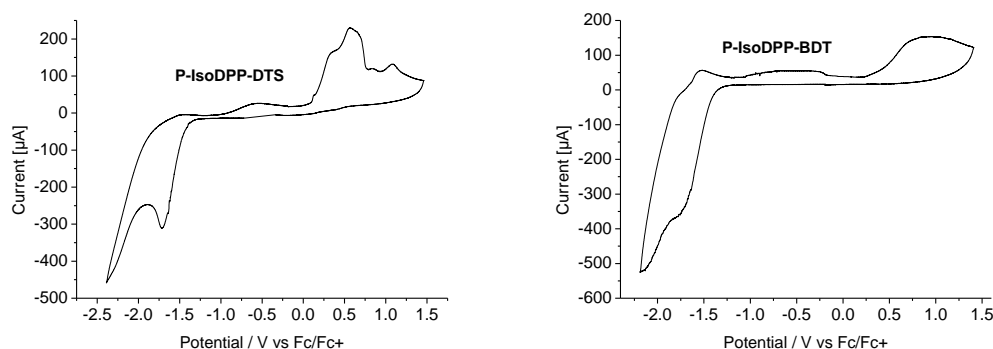


Figure 2.5. Cyclic voltammograms of **P-IsoDPP-BDT** (left) and **P-IsoDPP-DTS** (right) as thin films deposited on ITO. Solution: 0.1 M TBAPF₆/acetonitrile. Potential calculated versus ferrocene. Scan rate: 100 mV s⁻¹; T= 20 °C.

From the onset of anodic and cathodic waves HOMO and LUMO values as well as electrochemical bandgaps (E_g^{ec}) were calculated. As shown in Table 2.2, the E_g^{ec} of **P-IsoDPP-DTS** is 0.17 eV smaller than for **P-IsoDPP-BDT** since the silicon atom of DTS might cause a low-lying LUMO and a low band gap in the polymer due to the effective orbital mixing of Si- π^* orbital with the π^* orbital of the butadiene fragment.^{82,86-88} The electrochemical bandgaps are slightly larger than the optical ones due to the interfacial barrier for charge injection.⁹⁵

Table 2.2. Band gap data of polymers^a

Polymer	$\lambda_{abs,onset}$ of film [nm]	Oxidation onset [V]	Reduction onset [V]	E_g^{opt}/E_g^{ec} [eV]
		{HOMO [eV]}	{LUMO [eV]}	
P-IsoDPP-DTS	818	0.10 {-4.90}	-1.43{-3.37}	1.51/1.53
P-IsoDPP-BDT	798	0.28 {-5.08}	-1.39 {-3.41}	1.55/1.67

^aThe optical bandgap E_{opt} was measured at the onset of absorption of polymer film ($E_{opt} = 1240/\lambda_{abs,onset}$ eV). The HOMO-LUMO gap was calculated according to the equation $-E_{LUMO} = E_{onset(red)} + 4.8$ eV, and $-E_{HOMO} = E_{onset(ox)} + 4.8$ eV. $E_{onset(ox)}$ and $E_{onset(red)}$ are onset potentials for oxidation and reduction processes vs. Fc/Fc⁺ couple.

Theoretical calculation.

For a better understanding of the electronic structures of the polymers, quantum chemistry calculations using the density functional theory (B3LYP/6-31G^{*}) method were performed. In order to make computation possible, we choose repeating units with methyl instead of 2-ethylhexyl substituents as simplified models. The optimized structures reveal that there are 19.1^o (**P-IsoDPP-DTS**) and 18.9^o (**P-IsoDPP-BDT**)

dihedral angles between the thiophene units and the isoDPP core. This is about 4.5° larger than the dihedral angles determined from the crystal structure analysis. The dihedral angles between the thienyl-isoDPP and DTS or BDT units are 20.8° and 16.1° for the model compounds of **P-IsoDPP-DTS** and **P-IsoDPP-BDT**, respectively. It seems that **P-IsoDPP-BDT** is more planar than **P-IsoDPP-DTS**. This is surprising, because the absorption maximum of **P-IsoDPP-DTS** is more red-shifted than for **P-IsoDPP-BDT**. The reason probably is that the silicon atom of the DTS unit changes the HOMO-LUMO band gap due to the effective orbital mixing of the Si- π^* orbital with the π^* orbital of the butadiene fragment.

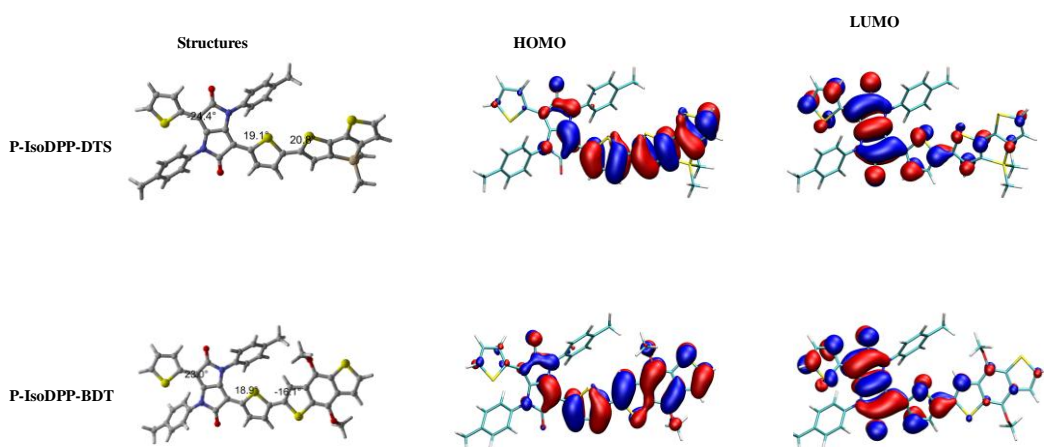


Figure 2.6. Structures and molecular orbital surfaces of the HOMO and LUMO of the repeating units of polymers, obtained at the B3LYP/6-31G* level.

As shown in Figure 2.6, we found that the LUMO orbitals of the two polymers are localized at the thienyl-isoDPP unit, while the HOMO orbitals are delocalized nearly along the conjugated backbones. This indicates that the LUMO electrons are localized at the thienyl-isoDPP units, while the HOMO electrons are delocalized along the

backbone. There exists an electron transfer from the conjugated backbone to the thienyl-isoDPP unit when the polymers are excited. The phenyl groups attached to the isoDPP core have very little contribution to the HOMO and LUMO orbitals of the polymers.

Spectroelectrochemistry of P-IsoDPP-DTS.

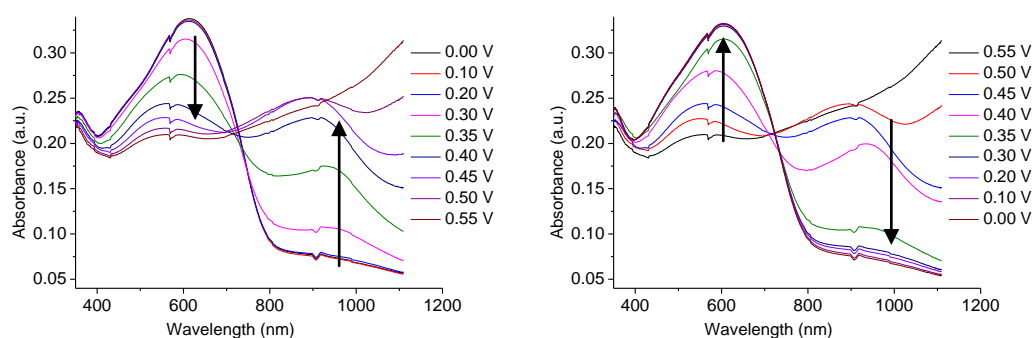


Figure 2.7. Spectroelectrochemical analysis of **P-IsoDPP-DTS** film electrodeposited on an ITO anode. Solvent: 0.1 M TBAPF₆/acetonitrile; T= 20 °C. Potential calculated versus ferrocene (left, from 0.00 V to 0.55 V; right, from 0.55 V to 0.00 V).

While measuring the CV diagrams it was noticed that the polymers change color upon anodic oxidation. Therefore the electrochromic behavior was investigated with a UV-vis spectrometer at various applied potentials (Figure 2.7). Because of the poor solubility of **P-IsoDPP-BDT**, we choose only **P-IsoDPP-DTS** to study spectroelectrochemistry. **P-IsoDPP-DTS** was dissolved in dichloromethane (6 mg / ml) and drop-casted on clean ITO-coated glass slides. The spectroelectrochemical study

was carried out using TBAPF₆ as supporting electrolyte in acetonitrile solution. The neutral **P-IsoDPP-DTS** showed one strong intense absorption band with maximum at 620 nm originating from π - π^* transition. If the potential was increased, the absorption band decreased, and a new band at 915 nm with long wavelength tail ranging into the infrared appeared. At about 710 nm an isosbestic point occurred. The new band can be ascribed to the formation of cation radicals and dications along the polymer backbone, which is similar to DPP polymers and other conjugated polymers.²¹ The experiment matches well the occurrence of the first oxidative wave at 0.35 V seen in the CV of **P-IsoDPP-DTS**. At decreasing potential, the π - π^* transition of the oxidized polymer film at 915 nm decreased, and the band at 620 nm increased again. The spectroelectrochemical experiment was associated with a reversible color change from blue to dark blue.

Thermal Properties.

The thermal properties of the two polymers were studied using DSC and TGA (Figure 2.8). From the DSC trace no melting transition is apparent in the range from 50 to 200°C. This indicates that crystallisation (or chain aggregation) of the polymer chains or alkyl side groups does not occur. High T_g are observed for **P-IsoDPP-DTS** at 153.2°C, and for **P-IsoDPP-BDT** at 143.5°C, respectively. The high T_g values can be ascribed to the hairy rod structure of the backbone with strongly reduced segmental mobility. TGA analysis shows that the copolymers exhibit excellent thermal stability with 5 % weight loss occurring for **P-IsoDPP-DTS** at 378 °C, and for

P-IsoDPP-BDT at 341 °C, respectively. **P-IsoDPP-DTS** is more stable than **P-IsoDPP-BDT** since the molecular weight of **P-IsoDPP-BDT** is much lower. The high value of T_g and the excellent thermal stability, which should prevent morphological changes and suppress the formation of aggregates, are desirable for potential optoelectronic applications of the polymers.

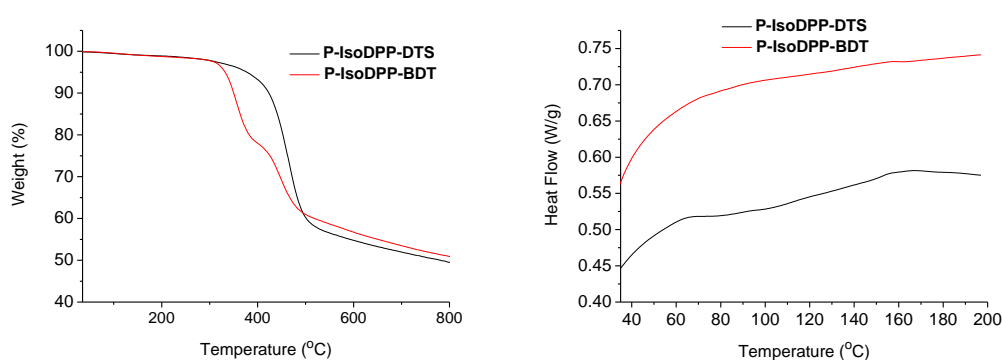


Figure 2.8. TGA (heating rate 20 °C/min) and DSC trace (heating rate 10 °C/min) of polymers.

2.3 Conclusions

Two new polymers consisting of isoDPP and BDT or DTS units were prepared using established palladium-catalyzed Stille-coupling. It was found that the absorption of the polymers is considerably red-shifted (30 nm for **P-IsoDPP-BDT** and 98 nm for **P-IsoDPP-DTS**) compared with previously synthesized isoDPP-based polymers containing 2,5-thienylene comonomer units instead of DTS or BDT.³⁷ Long-wavelength absorption of π -conjugated polymers may originate from a high

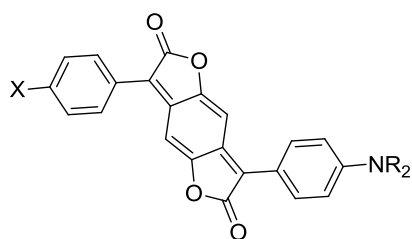
planarity of the π -system, a high molecular weight giving rise to a long and extended π -system, π - π -interactions between adjacent chains, or charge-transfer interactions within the backbone and between adjacent chains. In addition, oxidation or reduction of the backbone with formation of cations, anions and/or radicals may also cause a red-shift. The theoretical calculation indicates that the π -plane of the isoDPP core, the adjacent thienyl group, and the BDT or DTS comonomer units are tilted against each other by only a few degrees so that the polymer chains are more planar and the HOMO orbitals are delocalized along the backbone. The LUMO orbitals, however, are mainly localized at the thienyl-isoDPP core unit, so that the excitation of the polymers causes a strong electron transfer from the backbone to the thienyl-isoDPP core (acceptor) units. The crystal structure analysis of **isoDPP** confirms the small tilt between the thienyl and isoDPP units, but shows a very large tilt of the N-phenyl groups by about 76° . If this is also true for the polymer, π - π interactions between adjacent isoDPP units and also between adjacent polymer chains become highly unlikely.

In summary, the polymers exhibit high T_g , excellent thermo- and photostability, broad and intense absorption with maxima between 523 nm and 620 nm, absorption coefficients up to 64887 and 26485 L mol⁻¹ cm⁻¹, and small band gaps of 1.53 eV and 1.67 eV, respectively. This renders the polymers interesting for optoelectronic applications, for example in solar cells.

3 Conjugated polymers based on benzodiones

3.1 Introduction

Benzodiones and their derivatives have received much attention recently because of their quinoidal structure as promising candidates for electron-deficient materials. BDF and BDP are high-performance pigments serving as important building blocks for near-infrared (NIR) absorption. They were first developed in the mid-1970s and commercialized as disperse dyes owing to their deep color and high photochemical stability. Depending on the substitution pattern, BDFs exhibit red to blue colors. Monomeric aminobenzodifuranone (ABDF) (Figure 3.1) is a deeply blue colored dye with strong solvatochromism which has attracted our attention. Till now, only few articles have been published on ABDF. Some articles reported a strong solvatochromism of this colorant, whereas no articles appeared on aminobenzodipyrrolidones. Up to now, polymers based on ABDF were only recently described by S. Ghasimi in his master thesis.⁷⁵ In this chapter, five aminobenzodione-based π -conjugated polymers were synthesized and characterized.



X=H, Cl, CH₃, OCH₃
R=H, CH₃, CH₂CH₃, Pr

Figure 3.1. Structure of aminobenzodifuranone.

1,8-BDF is an isomer of 1,5-BDF (for the chemical structure see Scheme 3.1).

Due to the poor solubility of 1,8-BDF, it is difficult to use this chromophore for polymerization in solution, eg., upon Suzuki coupling. Up to now, only two polymers based on 1,8-BDF with purple color were reported, which were synthesized electrochemically (Figure 3.2). In this chapter a new method to obtain a polymer based on 1,8-BDF is reported.

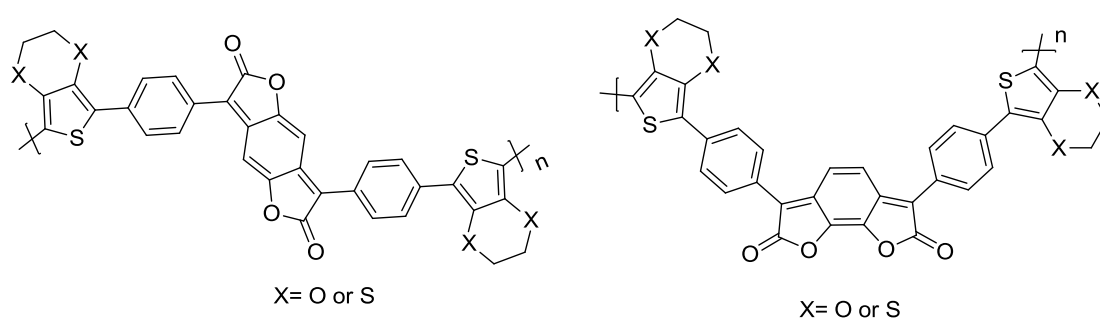
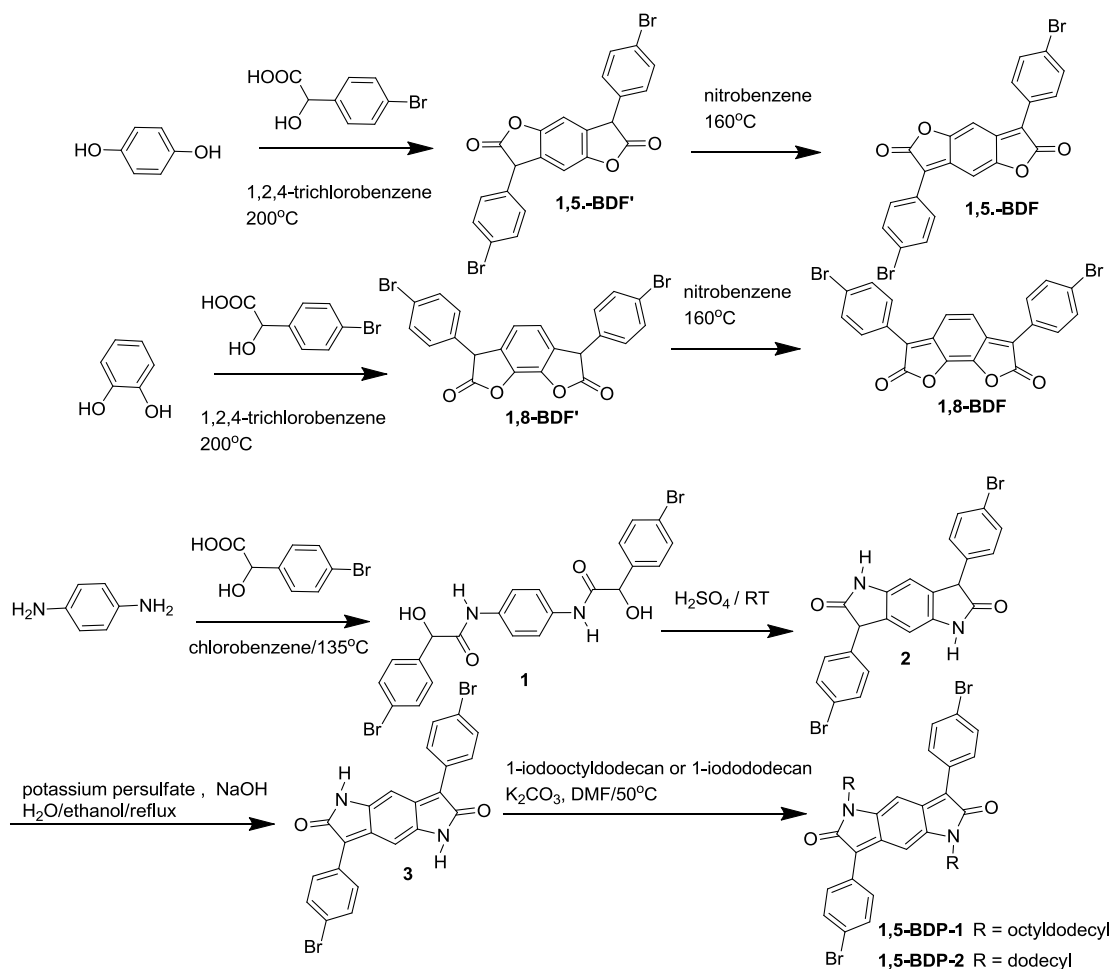


Figure 3.2. Polymers based on 1,5-BDF (left) and 1,8-BDF (right) obtained upon electrochemical polymerization.

3.2 Conjugated polymers based on amino-benzodiones via Buchwald amination

3.2.1 Preparation of benzodione-based monomers

The synthetic route to BDF-based monomers is described in Scheme 3.1. Monomers **1,5-** and **1.8-BDF** were obtained upon condensation of 1 eq. dihydroquinone with 3 eq. 4-bromomandelic acid in 1,2,4-trichlorobenzene at 200 °C. The final deep color originates from the quinonoid structure of the central core unit, which is obtained upon oxidation of the benzene unit with nitrobenzene. Both of these two chromophores are not well soluble in common organic solvents except hot DMF. **1,5-BDP1** and **1,5-BDP-2** were originally prepared as colorants and are similar in structure to DPP, but have the additional twist of being a quinodimethane derivate, which have recently attracted much attention. The monomers **1,5-BDP-1** and **1,5-BDP-2** were obtained from p-phenylenediamine with mandelic acid in chlorobenzene, followed by ring closure in sulfuric acid at room temperature. The final deep color originates from the quinonoid structure of the central core unit, which is obtained upon oxidation of the phenylene unit with potassium persulfate.



Scheme 3.1. Synthetic routes to benzodifuranone- and benzodipyrrolidone-based monomers.

Single crystal analysis of monomer 1,5-BDP-2

Single crystals of monomer **1,6-BDP-2** of 0.3*0.04*0.02 mm in size were grown upon slow diffusion of dichloromethane solution. The solid state packing, molecular structure and interactions were investigated using X-ray diffraction (Figure 3.3). The unit cell with one molecule (Figure 3.3.a) was found to be triclinic with space group P-1, the crystallographic center of symmetry being located at the midpoint of C7 and C9 (Figure 3.3.c). Just as in DPP, the core of **1,6-BDP-2** is almost planar, which

ensures full conjugation. The torsional angle between the 4-bromophenyl ring and the 1,6-BDP core is 38° . The crystal packing shows that the molecules adopt a weak, intermolecularly slipped π - π stacking separated by the distance of 3.56 Å (Figure 3.3.a).

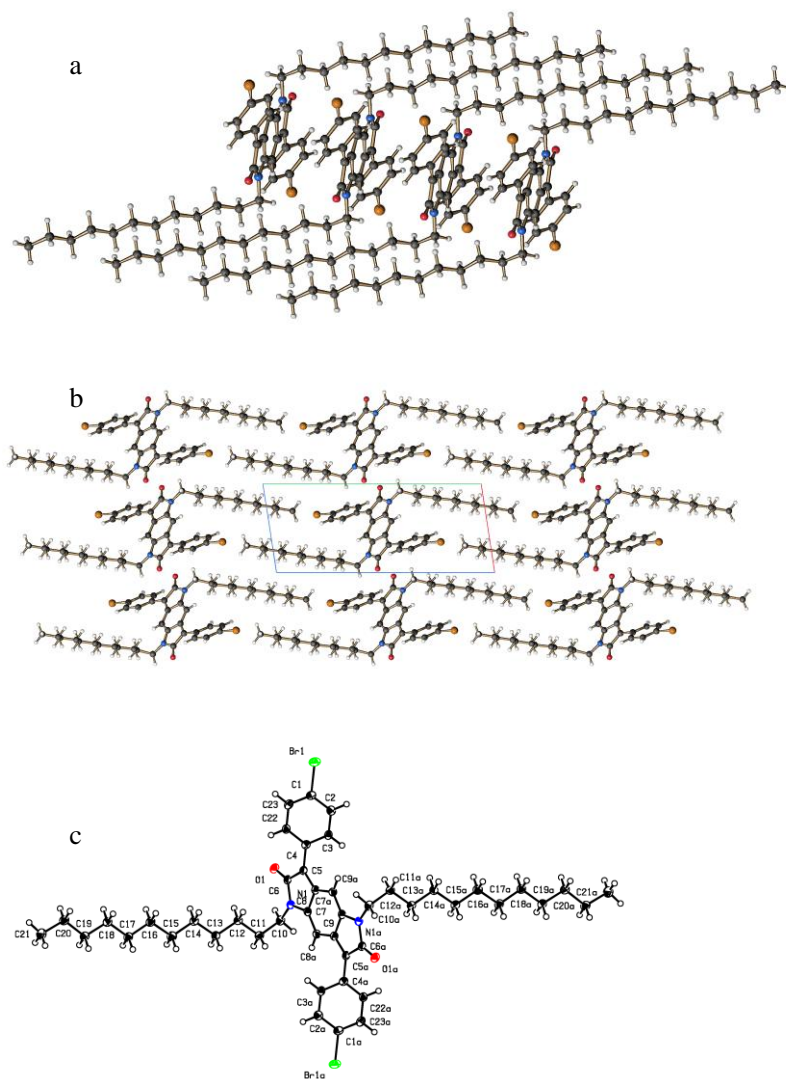


Figure 3.3. Single crystal structure of **1,5-BDP-2**.

Photostability of benzodione-based monomers

The monomers benzodiones show strong absorption maxima about 480 nm in toluene.

The photostability was studied by exposing toluene solutions of the polymers to a

200W Hg-lamp at a distance of 20 cm and measuring the decrease of the optical UV/vis absorption at 480 nm vs. time. The plots of $\ln(A_t/A_0)$ ($A_{t,0}$ = absorbance at time t and time $t=0$) vs. time for irradiation of polymers lead to nearly straight lines (Figure 3.4). From the initial slope the rate constants k of the photoreaction of $2.7 \cdot 10^{-3} \text{ min}^{-1}$ (**1,5-BDF**), $7.4 \cdot 10^{-3} \text{ min}^{-1}$ (**1,8-BDF**) and $4.4 \cdot 10^{-3} \text{ min}^{-1}$ (**1,5-BDP-1**) were derived. This indicates that a 1,5-benzodione-based monomer is more stable than a 1,8-benzodione-based one, and a BDF-based monomer is more stable than a BDP-based one.

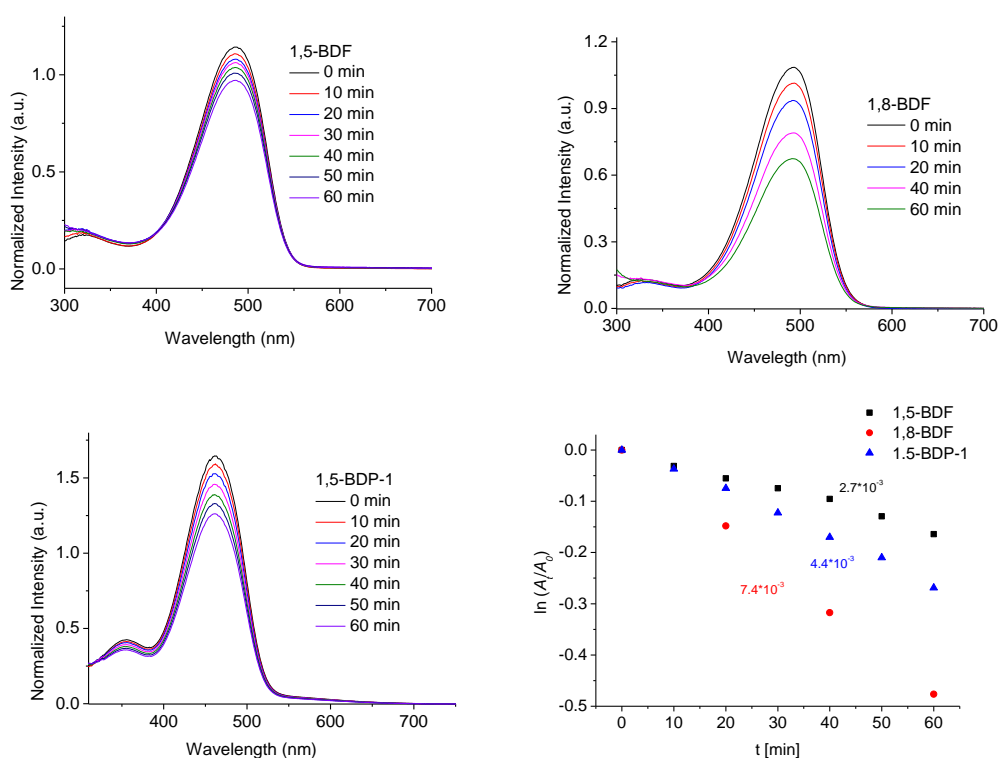
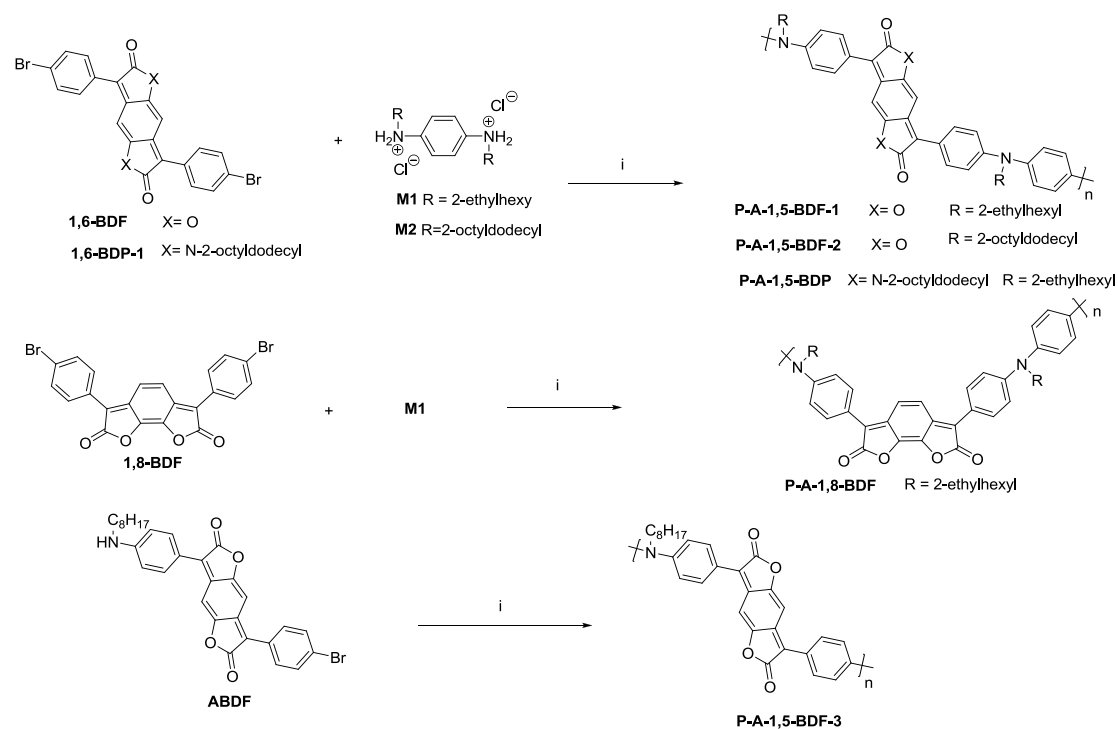


Figure 3.4. UV/Vis absorption spectra of the benzodione-based monomers before and after irradiation in toluene with a 200 W Hg-lamp and $\ln(A_t/A_0)$ vs. time for determination of rate constants k .

3.3.2 Preparation of polymers

The aminobenzodifuranon chromophore is a deeply blue colored dye with strong solvatochromism and a typical D-A system, in which aniline as an electron donor is combined with benzodifuranone as an electron acceptor. Five π -conjugated polymers based on ABDF were designed, synthesized and characterized. Monomeric benzodiones (**1,5-BDF**, **1,5-BDF-1** and **1,8-BDF**) were polymerized with *N,N'*-dialkylaminobenzene monomers **M1** and **M2** to yield four polymers (**P-A-1,5-BDF-1**, **P-1,5-BDF-2**, **P-A-1,5-BDP** and **P-A-1,8-BDF**). **1,5-ABDF** was reacted with itself to obtain polymer **P-A-1,5-BDF-3** upon Buchwald-Hartwig amination using $\text{Pd}_2(\text{dba})_3$ as catalyst and X-Phos as the ligand (Scheme 3.2) ⁹⁶.



Scheme 3.2. Synthetic route of aminobenzodione-based polymers. (i): $\text{Pd}_2(\text{dba})_3$, X-Phos, Cs_2CO_3 (*t*-BuOK for **P-A-1,5-BDP**), DMF/toluene (2/1) (dioxane for **P-A-1,5-BDF-3** and **P-A-1,5-BDP**), N_2 .

The weight-average molecular weights (M_w) of the polymers are between 4.6 and 10.1 kDa. The polymers were dark solids, and well soluble in hot common organic solvents such as dichloromethane, chloroform and toluene. The $^1\text{H-NMR}$ spectra showed broad signals for aromatic protons from 0.8-1.9 ppm, which are typical for the protons of alkyl units, and the chemical shifts at 3.0-3.2 and 3.6-3.7 ppm are typical for the protons from the $-\text{CH}_2-$ unit attached to the amino group (see Chapter 5, Experimental Part). The chemical shifts at 6.5-6.9 ppm and 7.6-7.7 ppm are typical for the protons of the phenyl group in the backbone, and the singles at 6.9-7.1 ppm are typical for the protons of the benzodione core.

UV/vis absorption of the polymers based on ABDF

The polymers based on ABDF show a strong absorption in the visible light in dichloromethane solution and in thin films. The UV/vis absorption spectra are shown in Figure 3.5, and the optical data are listed in Table 3.1. The polymers based on ABDF show a very broad absorption from 400 to 1000 nm, which matches the solar photon flux, which is mostly is in the 600-800 nm range.^{92,93}

The structures of **P-A-1,5-BDP-1** and **-2** are similar except that the alkyl chain substituent is different. From Figure 3.3.a and b, we can see that the UV/vis absorption spectra of these two polymers are similar. The UV/vis absorption maximum of **P-A-1,5-BDF-2** (725 nm) is 16 nm red-shifted compared with **P-A-1,5-BDF-1** (709 nm), since **P-A-1,5-BDF-2** has a higher molecular weight with more strongly extended π -system. The polymers are deeply green colored, the

extinction coefficients of the strongest bands being 16721 (**P-A-1,5-BDF-1**) and 23911 L mol⁻¹ cm⁻¹ (**P-A-1,5-BDF-2**) respectively (see Table 3.1). The UV/vis absorption maxima of thin films of **P-A-1,5-BDF-1** and **-2** are red-shifted by 15 and 16 nm compared to the solution, respectively, and the long-wavelength tails of the absorption bands extend to the infrared. This indicates a more planar conformation and/or the presence of π - π interchain association in the solid state. From the absorption onset of 947 and 1033 nm, optical band gaps of 1.31 (**P-A-1,5-BDF-1**) and 1.20 eV (**P-A-1,5-BDF-2**) can be calculated, respectively.

Figure 3.5.c shows that **P-A-1,5-BDF-3** in dichloromethane exhibits strong UV/vis absorption maxima at 645 nm and in thin films at 708 nm. Compared with **P-A-1,5-BDF-1-2**, the maximum of **P-A-1,5-BDF-3** is blue-shifted, because of a weaker D-A interaction between the alkylamino groups and the benzodifuranone core. In **P-A-1,5-BDF-1-2** enhanced intramolecular charge transfer (ICT) occurs due to the presence of the *N,N*-bis-alkyl-phenylene-1,4-diamine unit with more its powerful donor ability, which leads to a red shifted absorption.

The structures of **P-A-1,5-BDP** and **P-A-1,5-BDF** are similar except for the O-atom instead of the N-atom in the backbone. As show in Figure 3.5.a and 3.5.d, the UV/vis absorption spectra of the two polymers in dichloromethane solution and in thin film are much more different. The UV/vis absorption maximum of **P-A-1,5-BDP** (623 nm) is 86 nm blue-shifted in dichloromethane and in thin film compared with **P-A-1,5-BDF-1**. It seems that N-atom in the backbone of the polymer is not as advantageous as O-atom in order to contribute to a bathochromic shift, even if it enhance the polymer solubility. This indicates that the BDP monomer is a weaker

acceptor than BDF. **P-A-1,5-BDP** exhibits a blue color with a high extinction coefficient of $26762 \text{ L mol}^{-1} \text{ cm}^{-1}$ at λ_{max} being 623 nm in DCM. From the absorption onset at 843 nm, an optical band gap of 1.47 eV can be calculated.

Table 3.1. Optical data of the polymers based on ABDF.

Polymers	λ_{max} [nm]		Extinct coeff ϵ (λ_{max}) [$\text{L mol}^{-1} \text{ cm}^{-1}$]	$E_{\text{g}}^{\text{opt}}$ [eV] ^a
	in DCM	as thin film		
P-A-1,5-BDF-1	709	724	16721	1.31
P-A-1,5-BDF-2	725	741	23911	1.20
P-A-1,5-BDF-3	645	708	30600	1.19
P-A-1,5-BDP	623	638	26762	1.47
P-A-1,8-BDF	682	696	12500	1.25

^aOptical band gap $E_{\text{g}}^{\text{opt}}$ was measured at the onset of absorption of polymer film

($E_{\text{g}}^{\text{opt}} = 1240/\lambda_{\text{abs,onset}}$ eV).

From Figure 3.5.e, we can see that the UV/vis absorption maximum of **P-A-1,8-BDF** is at 682 nm in dichloromethane and at 696 nm in thin film. The absorption spectrum of **P-A-1,8-BDF** is much broader in thin film than in dichloromethane solution. **P-A-1,5-BDP** exhibits a blue color with high extinction coefficient at λ_{max} being $12500 \text{ L mol}^{-1} \text{ cm}^{-1}$. From the absorption onset at 992 nm, an optical band gap 1.25 eV can be calculated (Table 3.1).

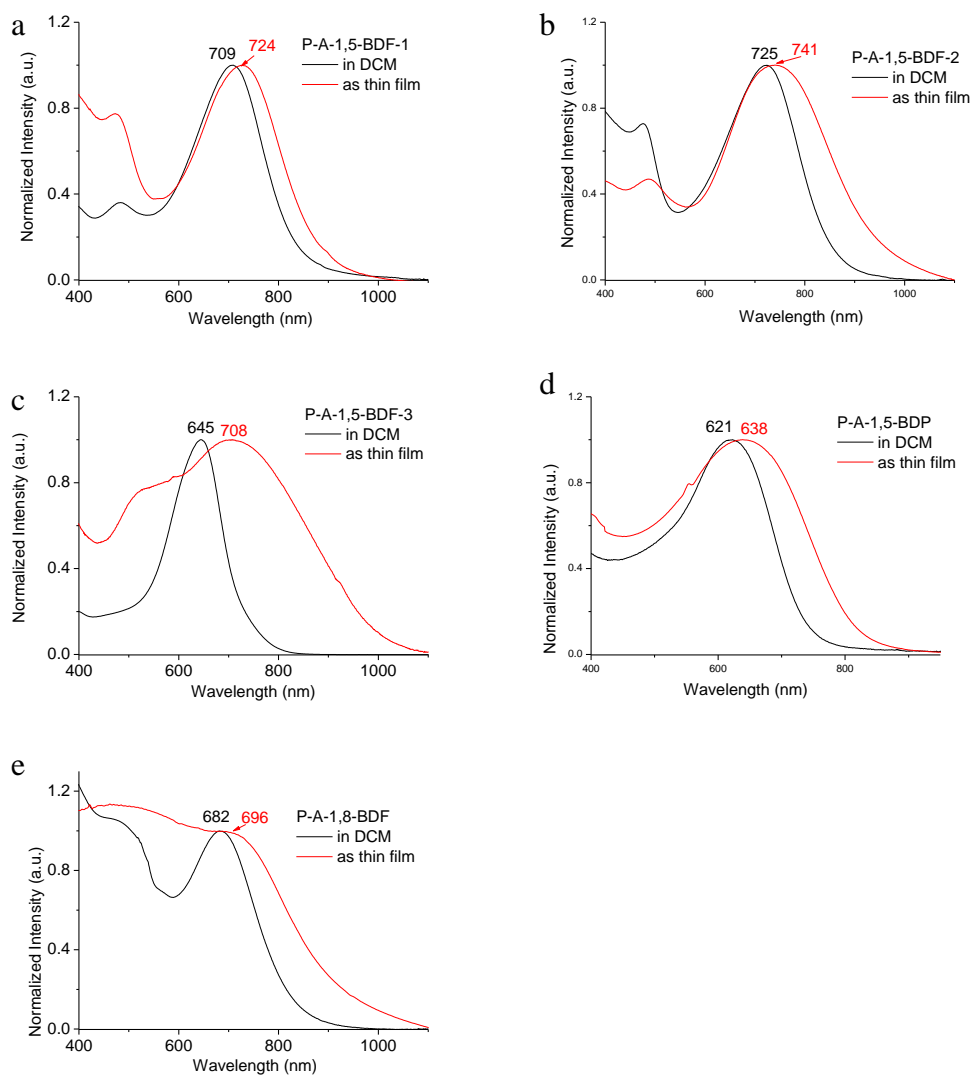


Figure 3.5. UV/Vis absorption spectra of polymers based on ABDF in dichloromethane and as thin film.

Solvatochromic properties of polymers

The monomer **ABDF** and the polymers **P-A-1,5-BDF-1**, **-3** were chosen to study the solvatochromic behaviour. Positive solvatochromic behaviour can be attributed to a number of specific and non-specific solute/solvent interactions as summarized in the simplified Kamlet– Taft equation (eqn (1))^{97,98} where s , a , and

b are solvent independent coefficients, and π^* ⁹⁹, α ¹⁰⁰ and β ¹⁰¹ reflect the general solvent dipolarity/polarizability, its specific H-bond donating (HBD) ability, and its specific H-bond accepting (HBA) ability, respectively, which may or may not oppose one another in terms of solvatochromic contributions. $\lambda_{\max,0}$ is the wavenumber of the UV/vis absorption maximum of the compound measured in a particular solvent, where $\pi^* = \alpha = \beta = 0$ (e.g. cyclohexane).⁵⁵

$$\lambda_{\max} = \lambda_{\max,0} + a\alpha + b\beta + s\pi^* \quad (1)$$

Until now, empirical polarity scales have always described the polarizability and dipolarity of the solvent together in one parameter. The first and only successful attempt to separate polarizability and dipolarity was suggested by Catalán with the introduction of the solvent acidity (*SA*),¹⁰²⁻¹⁰⁴ solvent basicity (*SB*),^{105,106} solvent polarizability (*SP*)¹⁰⁷ and solvent dipolarity (*SdP*)¹⁰⁸ (eqn (2)).

$$\lambda_{\max} = \lambda_{\max,0} + aSA + bSB + dSP + eSdP \quad (2)$$

The three compounds show the shortest wavelength UV/vis absorption band in *n*-hexane, and exhibit the strongest bathochromic shift in DMSO (For **ABDF**, **P-A-1,5-BDF-1** and, **-3**, $\Delta (\lambda_{\max, \text{pol}} - \lambda_{\max, \text{nonpol}})$ of 1700 cm^{-1} , 2400 cm^{-1} , and 1180 cm^{-1} , respectively).

The three compounds possess extended aromatic push-pull systems. Both equations show good accuracy for **ABDF** with $r > 0.9$ (parameters listed in Table 3.2 and 3.3). It is shown that especially the HBA ability of the solvents (β or *SB*) causes a strong

bathochromic shift ($b < 0$). This can be easily explained by H-bonding of the acid H-atom at the amino group with HBA-solvents. The influence of the β term on the bathochromic shift of **ABDF** represents the interactions of the HBA capacity of the solvents with the proton of the N-H group, which increases the +M-effect, and therefore a strengthening of the aromatic push-pull system occurs. HBD- solvents only exhibit a small effect typical for benzodifuranone-based dyes.⁵⁷ A weak bathochromic shift can be recognized due to interaction with the carbonyl groups ($a < 0$). Polarizability and dipolarity show a bathochromic shift (π^* , SP and $SdP < 0$), respectively. The solvatochromic extent of **ABDF** is 1700 cm^{-1} from *n*-hexane to DMSO. Hexamethylphosphortrisamide has not been included in the correlation, since it causes an unexpectedly high bathochromic shift of the UV/vis absorption maximum.

Table 3.2. Solvent-independent correlation coefficients a, b, d and e of the Catalán parameters SA , SB , SP and SdP , solute property of the reference system $_{\text{max},0}$ cyclohexane, number of solvents (n), correlation coefficient (r), standard deviation (sd), and significance (f) of the calculated solvatochromism of the model compounds **ABDF** and polymers **P-A-1,5-BDF-1, -3**

Compound	Catalán Equation					Correlation Data			
	$_{\text{max},0}$	a	b	d	e	n	r	sd	f
ABDF	18.537	-0.582	-1.158	-2.726	-0.570	32	0.95	0.156	<0.0001
P-A-1,5-BDF-3	20.284	-0.534	-1.191	-5.009	-1.246	33	0.93	0.284	<0.0001
P-A-1,5-BDF-1	16.629	0.137	-0.428	-2.452	-0.541	33	0.88	0.168	<0.0001

Table 3.3. Solvent-independent correlation coefficients a, b and s of the Kamlet–Taft parameters α , β and π^* , solute property of the reference system $\pi_{\text{max},0}$ cyclohexane, number of solvents (n), correlation coefficient (r), standard deviation (sd), and significance (f) of the calculated solvatochromism of the model compounds **ABDF** and polymers **P-A-1,5-BDF-1**, and **-3**.

Compound	Kamlet-Taft-Equation				Correlation Data			
	$\pi_{\text{max},0}$	a	b	s	n	r	sd	f
ABDF	16.623	-0.295	-0.951	-0.843	34	0.93	0.185	<0.0001
P-A-1,5-BDF-3	16.912	-0.143	-0.756	-1.949	35	0.86	0.393	<0.0001
P-A-1,5-BDF-1	14.985	-0.058	-0.290	-0.858	35	0.80	0.207	<0.0001

Since in **P-A-1,5-BDF-3** the N-H function is substituted, the effect of HBA-ability (b) should be decreased, but this was not observed. The remaining influence of the HBA- ability of the solvent on the polymeric dye might be ascribed to an N-H end group, for example. Especially for short-chain polymers a visible influence of end groups is conceivable. The influences of H-bonding (a+b) are almost unchanged. The most dominant effect on the solvatochromic behavior is caused by interaction with solvents of different dipolarity/polarizability, which is reflected in the large coefficient s for eq. 1, or coefficients d and e for eq.2.¹⁰⁹ Dyes with enlarged π - system usually are stabilized in the own molecule rather than by a solvent molecule. To our surprise, the effect of polarizability and dipolarity of **P-A-1,5-BDF-3** increases significantly compared with **ABDF** (the rate SP/SdP remains unchanged). This could firstly be ascribed to the fact that **P1** exhibits poor solubility in some solvents, if the chain length is getting larger. In those solvents only very short chains, probably dimers or

trimers, are measured by UV/vis spectroscopy. Secondly, the presence of N-H end groups found by the unchanged high influence of *SB*, speaks for such short chains. The solvatochromic shift of **P-A-1,5-BDF-3** from *n*-hexane to HMPA is 3140 cm⁻¹, and from *n*-hexane to DMSO is 2400 cm⁻¹, which is much larger than for **ABDF**

For **P-A-1,5-BDF-1**, the influence of HBA-solvents is smaller, since the N-H-functionality is not present anymore. The residual effect may point to an N-H-end group again. The influence of polarizability and dipolarity remains unchanged compared with **ABDF**. The solvatochromic shift is decreased compared with **ABDF** and **P-A-1,5-BDF-1**. From *n*-hexane to HMPA it is 1200 cm⁻¹, and from *n*-hexane to DMSO 1180 cm⁻¹.

Table 3.4: Kamlett-Taft and Catalán parameter sets and UV/vis absorption maxima of **ABDF**, **P-A-1,6-BDF-3** and **P-A-1,6-BDF-1** in different solvents.

Solvents	Catalán-Parameters ⁴				Kamlett-Taft-Parameters ⁵			λ_{\max} ABDF	λ_{\max} P-A-1,6-BDF-3	λ_{\max} P-A-1,6-BDF-1
	<i>SA</i>	<i>SB</i>	<i>SP</i>	<i>SdP</i>	α	β	π^*	[nm]	[nm]	[nm]
1,1,2,2-tetrachloroethane	0	0.017	0.845	0.792	0	0	0.95	640	682	722
1-butanol	0.341	0.809	0.674	0.655	0.84	0.84	0.47	662	659	705
1-propanol	0.367	0.782	0.658	0.748	0.84	0.9	0.52	660	661	708
1-decyl alcohol	0.259	0.912	0.722	0.383	0.7	0.82	0.45	-- a)	--	--
2,2,2,-trifluoroethanol	0.893	0.107	0.543	0.922	1.51	0	0.73	-- a)	--	--
acetone	0	0.475	0.651	0.907	0.08	0.43	0.71	638	664	691
acetonitrile	0.044	0.286	0.645	0.974	0.19	0.4	0.75	626	627	693
anisole	0.084	0.299	0.82	0.543	0	0.32	0.73	630	640	696
benzene	0	0.124	0.793	0.27	0	0.1	0.59	621	634	689
benzonitrile	0.047	0.281	0.851	0.852	0	0.37	0.9	649	685	714
8-butyrolactone	0.057	0.399	0.775	0.945	0	0.49	0.87	631	662	705
chloroform	0.047	0.071	0.783	0.614	0.2	0.1	0.58	622	661	703

cyclohexane	0	0.073	0.683	0	0	0	0	608	602	678
1,2-dichlorethane	0.030	0.126	0.771	0.742	0	0.1	0.81	625	641	705
dichloromethane	0.04	0.178	0.761	0.769	0.13	0.1	0.82	628	645	709
dioxane	0	0.444	0.737	0.312	0	0.37	0.55	616	630	674
1,2-dimethoxyethane	0	0.636	0.68	0.636	0	0.41	0.53	639	662	689
dimethyl sulfoxide	0.072	0.647	0.83	1	0	0.76	1	670	690	730
diethyl ether	0	0.562	0.617	0.385	0	0.47	0.27	625	614	682
ethanol	0.4	0.658	0.633	0.783	0.86	0.75	0.54	655	650	698
ethyl acetate	0	0.542	0.656	0.603	0	0.45	0.55	632	633	691
ethylene glycol	0.717	0.534	0.777	0.91	0.9	0.52	0.92	--	--	-- a)
formamide	0.549	0.414	0.814	1.006	0.71	0.48	0.97	--	--	-- a)
hexane	0	0.056	0.616	0	0	0	-0.04	602	592	672
hexafluorisopropanole	1.011	0.014	--	--	1.96	0	0.65	656	683	711
HMPA	0	0.813	0.744	1.1	0	1.05	0.87	706 b)	727	731
methanol	0.605	0.545	0.608	0.904	0.98	0.66	0.6	644	640	675
N,N-dimethylacetamide	0.028	0.65	0.763	0.987	0	0.76	0.88	669	703	717
N,N-dimethylformamide	0.031	0.613	0.759	0.977	0	0.69	0.88	665	689	721
nitromethane	0.078	0.236	0.71	0.954	0.22	0.06	0.85	630	634	694
N-methylformamide	--	--	--	--	0.62	0.8	0.9	662	679	712
pyridine	0.033	0.581	0.842	0.761	0	0.64	0.87	664	690	713
triethylamine	0	0.885	0.66	0.108	0	0.71	0.14	631	619	684
tetramethylurea	0	0.624	0.778	0.878	0	0.8	0.83	669	693	721
carbontetrachloride	0	0.044	0.768	0	0	0.1	0.28	618	611	674
tetrahydrofuran	0	0.591	0.714	0.634	0	0.55	0.58	644	671	692
toluene	0	0.128	0.782	0.284	0	0.11	0.54	621	639	689
water	1.062	0.025	0.681	0.997	1.17	0.47	1.09	--	--	--
p-xylene	0	0.16	0.778	0.175	0	0.12	0.43	620	620	692

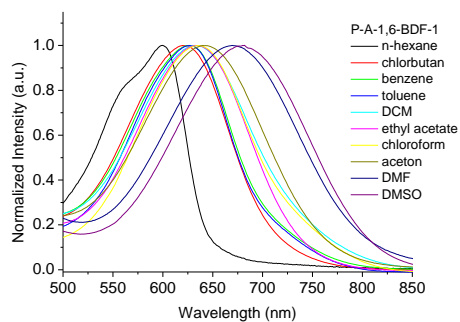


Figure 3.6. UV/Vis absorption spectra of **P-A-1,6-BDF-3** in different solvents.

Electrochemical Properties.

The electrochemical properties of the polymers were investigated using cyclic voltammetry. (Figure 3.7). The experimental conditions are described in Chapter 5, Experimental Part. The electrochemical data of the polymers are listed in Table 3.5.

Figure 3.7 shows the reductive cycles of all polymers. They exhibit two reversible cathodic waves, which originate from the reduction of the quinonoid to a benzoic structure, and also indicate a high stability of the anion radical. This can possibly be explained with a stabilizing negative charge of the oxygen atoms in the carbonyl groups of both the lacton groups in the benzodione units. On increasing the potential, two to three anodic waves with maxima between 0.5 and 1.2 V occur. This can be ascribed to the formation of cation radicals and dications. The oxidation of the polymers sets in at low potentials between 0.09 and 0.44 V, a low HOMO energy level between -4.91 and -5.32 eV can be calculated (Table 3.5). From the onset of cathodic waves the LUMO energy level between -3.8 and -4.25 eV can be calculated as shown in Table 3.5. Due to the low LUMO energy level of the polymers, good electron injection and ambient stabilities of OFET devices can be expected.

The polymers exhibit quite low HOMO-LUMO band gaps (1.01 to 1.37 eV, see Table 3.5). The electrochemical band gap of **P-A-1,5-BDF-1** is 0.17 eV larger than **P-A-1,5-BDF-1**. This can be ascribed to **P-A-1,5-BDF-2**, which has a higher molecular weight with more strongly extended π -system compared with **P-A-1,5-BDF-1**. The electrochemical band gaps are larger than the optical ones due to

the interfacial barrier for charge injection.

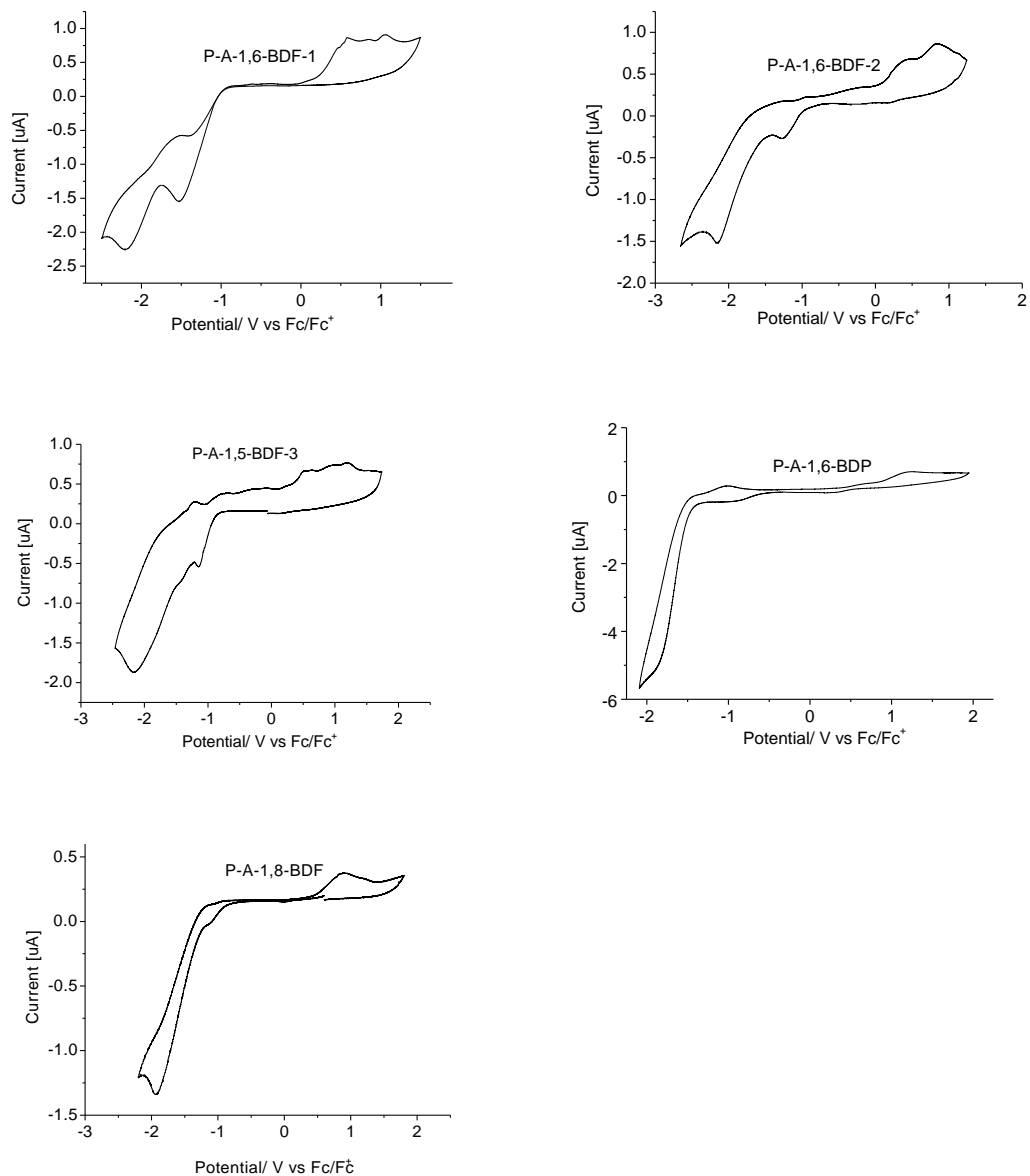


Figure 3.7. Cyclic voltammograms of polymers based ABDF as thin films deposited on ITO. Solution: 0.1 M TBAPF₆/acetonitrile. Potential calculated versus ferrocene. Scan rate: 100 mV s⁻¹; $T= 20\text{ }^{\circ}\text{C}$.

Table 3.5. Band Gap Data of Polymers^a.

Polymers	Oxidation Onset [V] {HOMO [eV]}	Reduction Onset [V] {LUMO [eV]}	Electrochem Band Gap [eV] ^a
P-A-1,5-BDF-1	0.18/-4.98	-1.00/-3.80	1.18
P-A-1,5-BDF-2	0.11/-4.91	-0.91/-3.89	1.01
P-A-1,5-BDF-3	0.32/-5.12	-0.81/-3.99	1.13
P-A-1,5-BDP	0.52/-5.32	-0.55/-4.25	1.07
P-A-1,8-BDF	0.49/-5.29	-0.88/-3.92	1.37

^aHOMO-LUMO gap was calculated according to the equations $-E_{\text{LUMO}} = E_{\text{onset(red)}} + 4.8 \text{ eV}$, and $-E_{\text{HOMO}} = E_{\text{onset(ox)}} + 4.8 \text{ eV}$. $E_{\text{onset(ox)}}$ and $E_{\text{onset(red)}}$ are onset potentials for oxidation and reduction processes vs Fc/Fc⁺ couple.

Photostability of polymers

The photostability was studied in the same way as described previously. The plots of $\ln(A_t/A_0)$ ($A_{t,0}$ = absorbance at time t and time $t=0$) vs. time for irradiation of polymers lead to nearly straight lines (Figure 3.8). From the initial slope the rate constants k of the photoreaction of 0.35 h^{-1} (**P-A-1,5-BDF-1**), 0.25 h^{-1} (**P-A-1,5-BDF-2**), 0.39 h^{-1} (**P-A-1,5-BDF-3**) and 0.99 h^{-1} (**P-A-1,5-BDP**) were derived (Figure 3.8.e).

Figure 3.8.a and b indicate that **P-A-1,5-BDF-2** is more stable than **P-A-1,5-BDF-1**, even though the structures of **P-A-1,5-BDP-1** and **-2** are similar except that the alkyl chain substitutes are different. This may be ascribed to the fact that **P-A-1,5-BDF-2** has a higher molecular weight and **P-A-1,5-BDF-1** contains some oligomeres and small molecules in side.

Though structures of **P-A-1,5-BDP** and **P-A-1,5-BDF** are similar except for the O-atom, which is replaced by the N-atom in the backbone, we can see from Figure 3.8.a and Figure 3.8.d, that **P-A-1,5-BDP** is less stable compared with **P-A-1,5-BDF-1**. This can be explained by the fact that the monomeric BDP chromophore is less stable than BDF in UV-light (Figure 3.4). Still, BDF and BDP based polymers exhibit a higher photostability than DPP based polymers.

In Figure 3.8.a, b and c, it is shown that **P-A-1,5-BDF-3** is less stable than **P-A-1,5-BDF-1**, or **-2** in UV-light since the *N,N'*-dialkyl-1,4-phenylenediamine unit exhibits a more powerful donor ability than the alkylamino unit. Probably the strong donor–acceptor character of these polymers prevents energy transfer from the amino groups to the BDF core and thus contributes to a higher photostability.

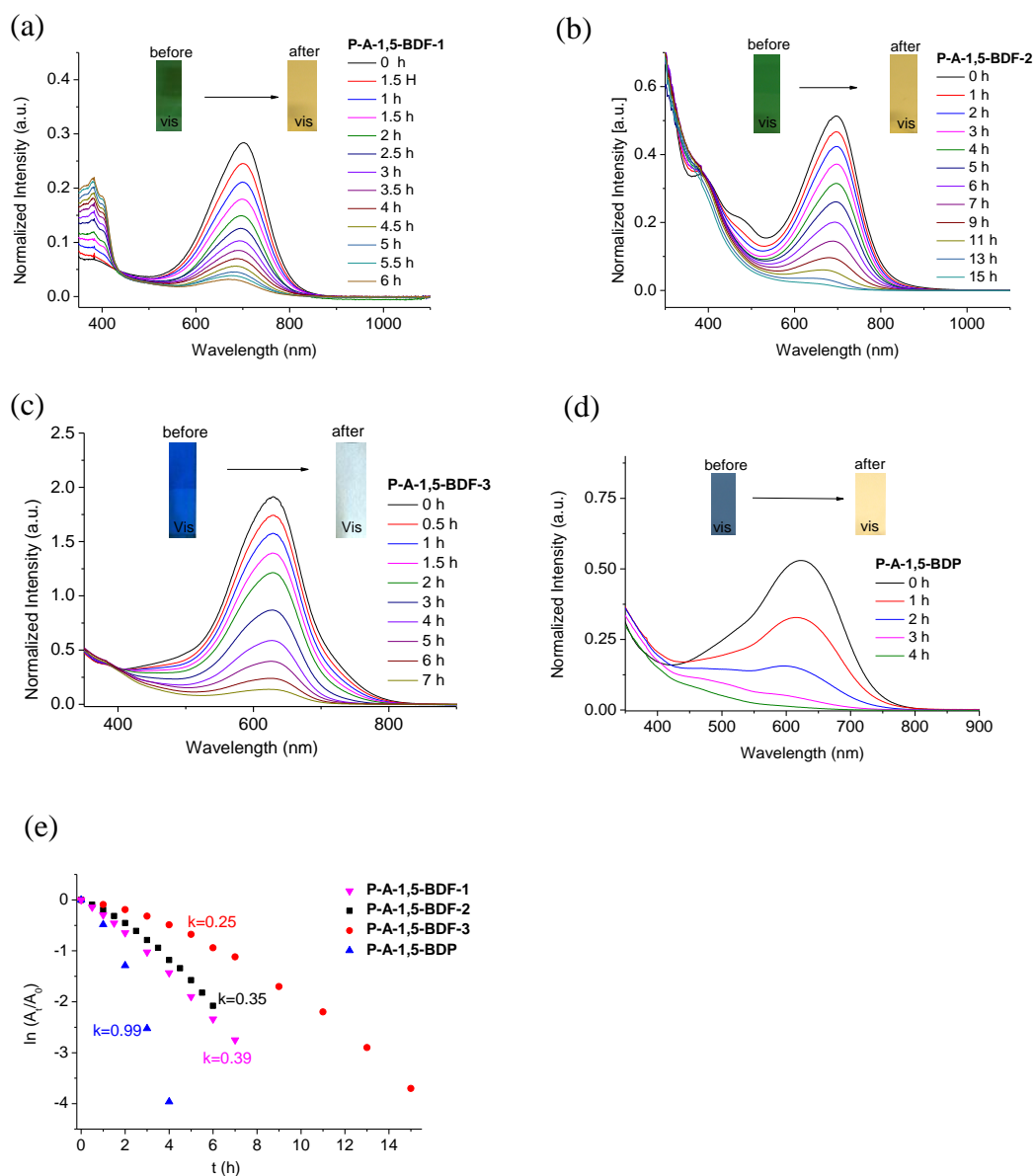
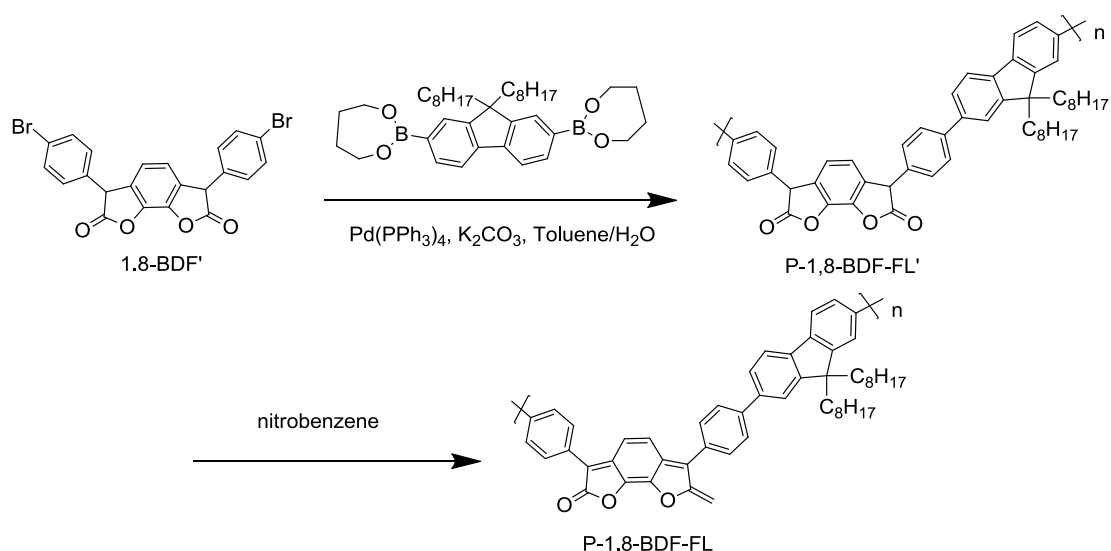


Figure 3.8. UV/vis absorption spectra of the polymers before and after irradiation in toluene with a 200 W Hg-lamp, and plot of $\ln(A_t/A_0)$ vs. time for determination of rate constants k for polymers.

3.3 Polymers based on 1,8-BDF via Suzuki and Stille coupling

1,8-BDF is a deep orange dye comparable with 1,5-BDF, which both are not well soluble in common organic solvents. In recent publications of our group, two

polymers based on 1,8-BDF were reported, which were synthesized electrochemically.^{62,63} Due to the poor solubility of this monomer, it is not easy to use it for polymerization directly.



Scheme 3.3. Synthetic route to Polymer **P-1,8-BDF-FL**.

Since the reduced form of the monomer 3,6-bis(4-bromophenyl)benzo[1,2-*b*:6,5-*b'*]1,2,3,5,6,7-hexahydrodifuran-2,7-dione (**1,8-BDF'**) is more soluble, it was used for polymerization with 2,2-(9,9-dioctyl-9H-fluorene-2,7-diyl)-bis(4,4,5,5-tetramethyl-1,3,2-dioxaborolane) upon Suzuki coupling in toluene (Scheme 3.3). The reduced polymer **P-1,8-BDF-FL'** was obtained. Subsequently **P-1,8-BDF-FL'** was oxidized with nitrobenzene to yield the conjugated polymer **P-1,8-BDF-FL** in a yield of 62%. The weight-average molecular weights (M_w) of the polymer is 17.5 kDa and the polydispersity (PDI) is 2.1. The polymer is a dark solid, which is well soluble in

common organic solvents such as dichloromethane, chloroform and toluene.

The molecular structures were analyzed using $^1\text{H-NMR}$ spectroscopy (see Chapter 5, Experimental Part). The signals around 0.8-2.6 ppm originate from the alkyl groups, while the broad signals at about 7.8-7.95 ppm can be ascribed to the protons of the fluorene moiety in the main chain. The broad signals from 8.10-8.25 ppm are typical for the protons of the core of BDF, while the broad signals with chemical shifts at about 7.58-7.76 ppm originate from the protons of the phenyl groups attached to the core of BDF. **P-1,8-NDF-FL**, differs from **P-1,8-NDF-FL'**, because the signal at about 5.3 ppm has disappeared due to the oxidization.

Theoretical computation

For a better understanding of the structures of the polymer, quantum chemical calculations were carried out at the B3LYP/6-31+G(d,p) level. In order to make computation possible, we choose repeating units with methyl instead of n-octyl substituents as simplified models. The structures and molecular orbital surfaces of the HOMO and LUMO of **P-1,8-NDF-FL** are shown in Figure 3.9.

Figure 3.9.a shows that the torsional angle between the phenyl ring and the fluorene unit is 36.8° , and the dihedral angle between the phenyl units and the BDF core is 30.1° . The calculated HOMO-LUMO gap of **P-1,10-NDF-FL** is found to be 1.96 eV. From Figure 3.9.b and c, we can see that if the polymer **P-1,10-NDF-FL** is excited,

electron transfer from the conjugated backbone to the BDF core will take place. The HOMO energy level of **P-1,8-BDF-FL** is -5.84 eV, and the LUMO energy level is -3.90 eV.

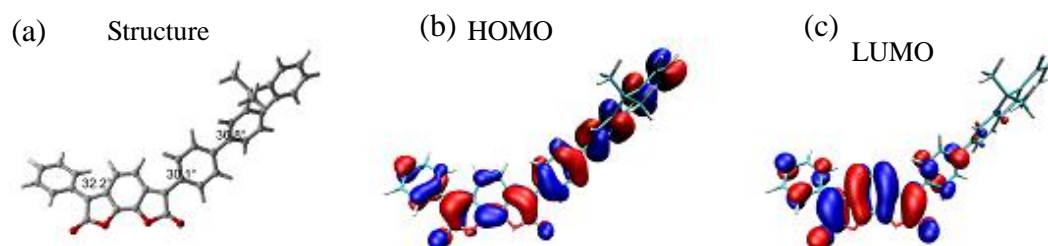


Figure 3.9. Structure (a) and molecular orbital surfaces of the HOMO (b) and LUMO(c) of **P-1,8-BDF-FL** obtained at the B3LYP/6-31G+(d,p) level.

UV/vis absorption of **P-1,8-BDF-FL**

The UV/vis absorption spectra of polymer **P-1,8-BDF-FL** and monomer **1,8-BDF**, in dichloromethane solution are shown in Figure 3.10, and the optical data are listed in Table 3.6.

P-1,8-BDF-FL exhibits a deep purple color in dichloromethane with an absorption maximum at 555 nm, the extinction coefficients of the strongest bands being 5.4×10^4 L mol⁻¹ cm⁻¹. Another two absorption bands appear at 340 nm and 405 nm, which can be ascribed to the absorption of the fluorene unit and the BDF core. The UV/vis absorption maximum of **P-1,8-BDF-FL** in dichloromethane is red-shifted by 68 nm

and the long-wavelength tail of the absorption bands is extended to the infrared compared with monomer **1,8-BDF** (Figure 3.4). This can be ascribed to the extension of the π -conjugated system due to the polymerization.

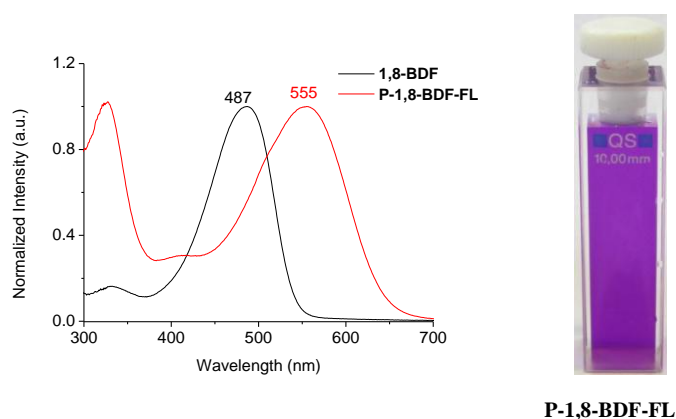


Figure 3.10. UV/Vis absorption spectra of **P-1,8-BDF-FL** and **1,8-BDF** in dichloromethane.

Table 3.6.. Optical data of polymer **P-1,8-BDF-FL**.

Polymers	λ_{\max} [nm]	Extinct Coeff ϵ (λ_{\max}) [L mol ⁻¹ cm ⁻¹]	Electrochem Band Gap [eV]
P-1,8-BDF-FL	324, 555	54643 (555 nm)	1.31

Electrochemical Properties

The electrochemical properties of the polymer **P-1,8-BDF-FL** were investigated using cyclic voltammetry. The experimental conditions are described in Chapter 5, Experimental Part. The electrochemical spectrum of **P-1,8-BDF-FL** is shown in Figure 3.11, and the electrochemical data of the polymer are listed in Table 3.7.

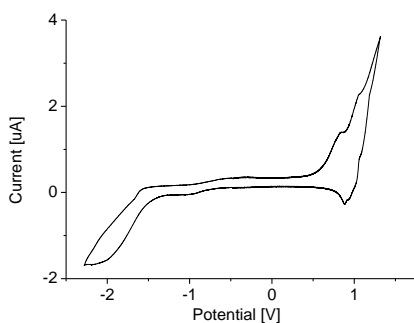


Figure 3.11. Cyclic voltammogram of **P-1,8-BDF-FL** as thin film deposited on ITO.

Solution: 0.1 M TBAPF₆/acetonitrile. Potential calculated versus ferrocene. Scan rate:

100 mV s⁻¹; T= 20 °C.

Table 3.7. Band gap data of polymer **P-1,8-BDF-FL**^a.

Polymer	Oxidation Onset [V] {HOMO [eV]}	Reduction Onset [V] {LUMO [eV]}	Electrochem. Band Gap [eV]
P-1,8-BDF-FL	0.47 {-5.37}	-0.84{-4.06}	1.31

^aHOMO-LUMO gap was calculated according to the equation $-E_{\text{LUMO}} = E_{\text{onset}(\text{red})} + 4.8 \text{ eV}$, and $-E_{\text{HOMO}} = E_{\text{onset}(\text{ox})} + 4.8 \text{ eV}$. $E_{\text{onset}(\text{ox})}$ and $E_{\text{onset}(\text{red})}$ are onset potentials for oxidation and reduction processes vs Fc/Fc⁺ couple.

Figure 3.11 shows that the reduction behaviour of **P-1,8-BDF-FL** is reversible, while the oxidation behaviour is irreversible. Anodic oxidation of **P-1,8-BDF-FL** sets in at potentials of 0.47 V. On increasing the potential, **P-1,8-BDF-FL** exhibits two anodic waves at 0.84 and 1.07 V. This can be ascribed to the formation of cation radicals and dications. Decreasing the potential again, the oxidation is reverted at 0.98 V. The reductive cycle shows two reversible cathodic waves at -1.03/ -0.66 V and -2.01/

-1.54 V, which originate from the reduction of the quinonoid to a benzoic structure, and also indicate a high stability of the anion radical.

From the onset of anodic and cathodic waves the HOMO and LUMO values as well as the electrochemical band gaps were calculated. As shown in Table 3.8, the HOMO energy levels of the polymer (-5.37 eV) is lower than the air oxidation (ca. -5.27 eV) indicating good air stability.^{110,111} The electrochemical band gap value of **P-1,8-BDF-FL** is 1.31 eV, which is 2.56 eV smaller than the calculated band gap value. This can be ascribed to the fact that the calculation is restricted to a single repeat unit, but does not include the full polymer backbone.

3.4 Conclusion

In this chapter, five π -conjugated polymers based on aminobenzodione units with low band gaps were designed and prepared. The polymers exhibit quite low band gaps (1.07–1.18 eV), high photostability and a large solvatochromic shift up to 3140 cm^{-1} . Furthermore, the polymers show broad UV/vis absorption bands in a range from 400 to 900 nm with high extinction coefficients of 1.7 to $3.1 \times 10^4 \text{ L mol}^{-1} \text{ cm}^{-1}$. This well matches the solar photon most intense flux. The broad absorption in the visible region of the spectra, combined with high color depth, high photostability and a low band gap render aminobenzodione-based polymers interesting as building blocks for optoelectronic materials, especially for solar cell.

Furthermore, we used a new method to obtain a 1,8-BDF-based polymer. The method based on Suzuki coupling of the non-oxidized, better soluble monomer **1.8-BDF'** in toluene, followed by oxidation of the polymer with nitrobenzene to obtain **P-1.8-BDF-FL**. This method might also be useful for polymerization of other monomers, which are not well soluble in organic solvents, but can be subsequently oxidized. The polymer based on 1,8-BDF exhibits a broad absorption and a low band gap, and might also be useful for optoelectronic materials.

4 Conjugated polymers based on naphthodiones

4.1 Introduction

Naphthodifuroanones (NDF) NDFs belong to a kind of electron-deficient chromophores, which have been developed in the last 30 years, and are prepared upon condensation of 1,2- or 1,5-dihydroxynaphthalene with derivatives of mandelic acid.⁷⁰⁻⁷³ Monomeric 1,10-naphthodifuranone (1,10-NDF), 1,6-naphthodifuranone (1,6-NDF) are deeply yellow to purple to blue colored dyes. The deep color originates from the quinonoid structure of the central core unit, which is obtained upon oxidation of the naphthalene unit with nitrobenzene. To our knowledge, only few articles reported on derivatives of NDF, while the properties of the monomers and polymers based on 1,6-NDF and polymers based on NDF are completely unknown. In this chapter, some new structure based on NDF and NDP were designed and synthesized.

4.2 Monomers and polymers based on NDF

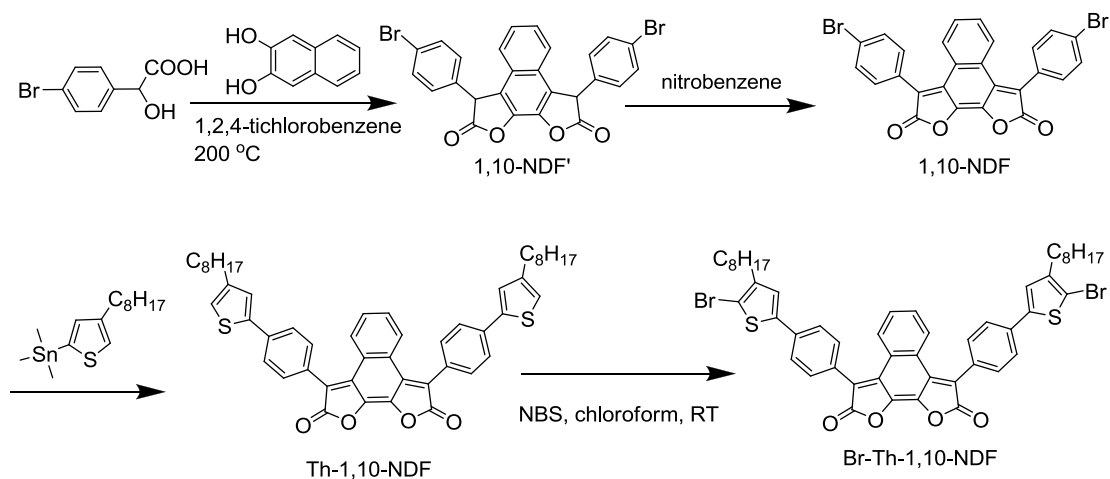
4.2.1 Monomers and polymers based on 1,10-NDF

4.2.1.1 Preparation of symmetrical monomers and polymers based on 1,10-NDF

4.2.1.1.1 Monomers

The synthetic route to new 1,10-NDF based monomers is described in Scheme 4.1. In general, the synthesis of the symmetrical monomer **1,10-NDF** required the condensation of 1 eq. 2,3-dihydroxynaphthalene and 2 eq. 4-bromo-mandelic acid,

respectively, leading to a double cyclization with formation of **1,10-NDF'**. Finally the conjugated naphthodifuranone **1,10-NDF** was obtained upon oxidation of **1,10-NDF'** in a yield of 70 %. The structure of **1,10-NDF** is similar to the monomer **1,8-BDF** (see Figure 4.1). **1,10-NDF** is well soluble in hot common organic solvents such as toluene and DMF. The solutions exhibit a deep yellow color, while the monomer **1,8-BDF** is not well soluble in common organic solvents. It seems the additional benzene ring in the NDF core enhances the solubility of this compound. The $^1\text{H-NMR}$ spectra of **1,10-NDF** displayed all the expected resonances with no discernible peaks corresponding to impurities. The signals with chemical shift at 7.35-7.38 and 8.07-8.01 ppm are typical for the naphthodifuranone core (see Chapter 5, Experimental Part).



Scheme 4.1. Synthesis of naphthodifuranone monomers **1,10-NDF** and **Br-Th-1,10-NDF**.

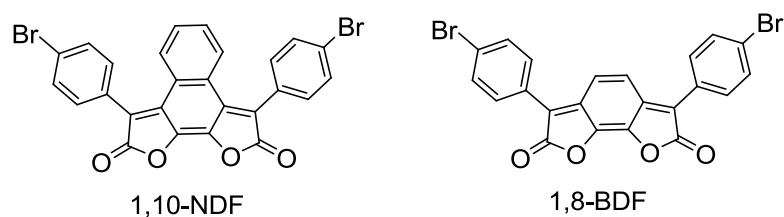


Figure 4.1. Structure of **1,10-NDF** and **1,10-BDF** .

Br-Th-1,10-NDF was prepared according Scheme 4.1. 4-N-octylthien-2-yl-trimethylstannane was reacted with **1,10-NDF** in order to obtain **Th-1,10-NDF** in a yield 85 % **Th-1,10-NDF** was subsequently brominated with NBS to yield monomer **Br-Th-1,10-NDF**. This monomer is well soluble in common organic solvents such as toluene and DMF. The solutions exhibit a deep red color. The $^1\text{H-NMR}$ spectra displayed all the expected resonances. The signals with a chemical shift at 6.98 and 7.31 ppm are typical for thiophene protons of **Th-1,10-NDF**. The spectrum of **Br-Th-1,10-NDF** differs from **Th-1,10-NDF**, because the signal at 6.98 ppm is missing due to the bromination. The signals with a chemical shift at 0.91-2.67 ppm are typical for the alkyl groups attached to the thiophene unit. The monomers **1,10-NDF** and **Br-Th-1,10-NDF** are suitable for Suzuki and Stille coupling due to the bromine end groups.

Molecular orbital computation of **1,10-NDF**

In order to better understand the electronic structure of **1,10-NDF**, quantum chemistry calculations by the density functional theory (B3LYP/6-31G^{*}) method were performed. From Figure 4.2, we can see that upon excitation of monomer **1,10-NDF**,

an electron transfer from the phenyl-NDF-core-phenyl part to the NDF core takes place. The HOMO energy level of this monomer is -6.28 eV and the LUMO energy level is -3.71 eV. From these levels a HOMO-LUMO gap of 2.56 eV. Can be calculated for **1,10-NDF**. The torsional angle between the lactam phenyl ring and the NDF core is 47° , which indicates that the phenyl groups are not coplanar with the NDF core units.

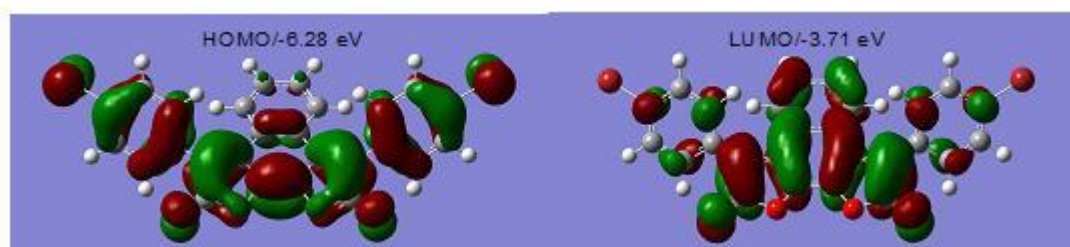


Figure 4.2. Structures and molecular orbital surfaces of the HOMO and LUMO of **1,10-NDF**, obtained at the B3LYP/6-31G* level.

Single crystal analysis of monomer **1,10-NDF**.

Crystals of **1,10-NDF** in a size of $0.1 \times 0.1 \times 0.03 \text{ mm}^3$ were prepared upon slow diffusion of dichloromethane into a mesitylene solution. The crystal structure and the packing are depicted in Figure 4.3. From Figure 4.3.a, we can see that an intramolecular hydrogen bonding exists of 2.545 \AA (C—H---O) between the C=O of the NDF core and the hydrogen atom of the phenyl ring of the neighboring molecule. The torsional angle of $\text{C}_{17}\text{—H}_{17}\text{---O}_4$ is 142.6° . From Figure 4.3.b, we can see that the unit cell with two molecules is triclinic with space group P-1. The crystal packing shows that the molecules adopt weak intermolecularly slipped π - π stacking separated

by a distance of 3.36 Å. Figure 4.3.c shows that the crystallographic center of symmetry is located at the midpoint of C₁₂ and C₁₃. The bond lengths were found to be 1.327 (C₈-C₇), 1.376(C₇-O₁), 1.398(O₁-C₆), 1.417(C₆-C₅), 1.376(C₅- C₁₄), 1.466(C₁₄- C₁₃), 1.385(C₁₃-C₁₅), 1.387(C₁₅- C₁₆), and 1.391 Å (C₁₆- C₁₇). Figure 4.3.d indicates that the core of 1,10-NDF is fully coplanar, just as in DPP and BDP, which ensures full conjugation. There is a torsional angle between 42° and 45° between the side benzene ring and the NDF core, which is similar to the angle of 47° obtained by computer calculation. This indicates that the phenyl groups are not coplanar with the NDF core units, and only cause weak π - π interactions.

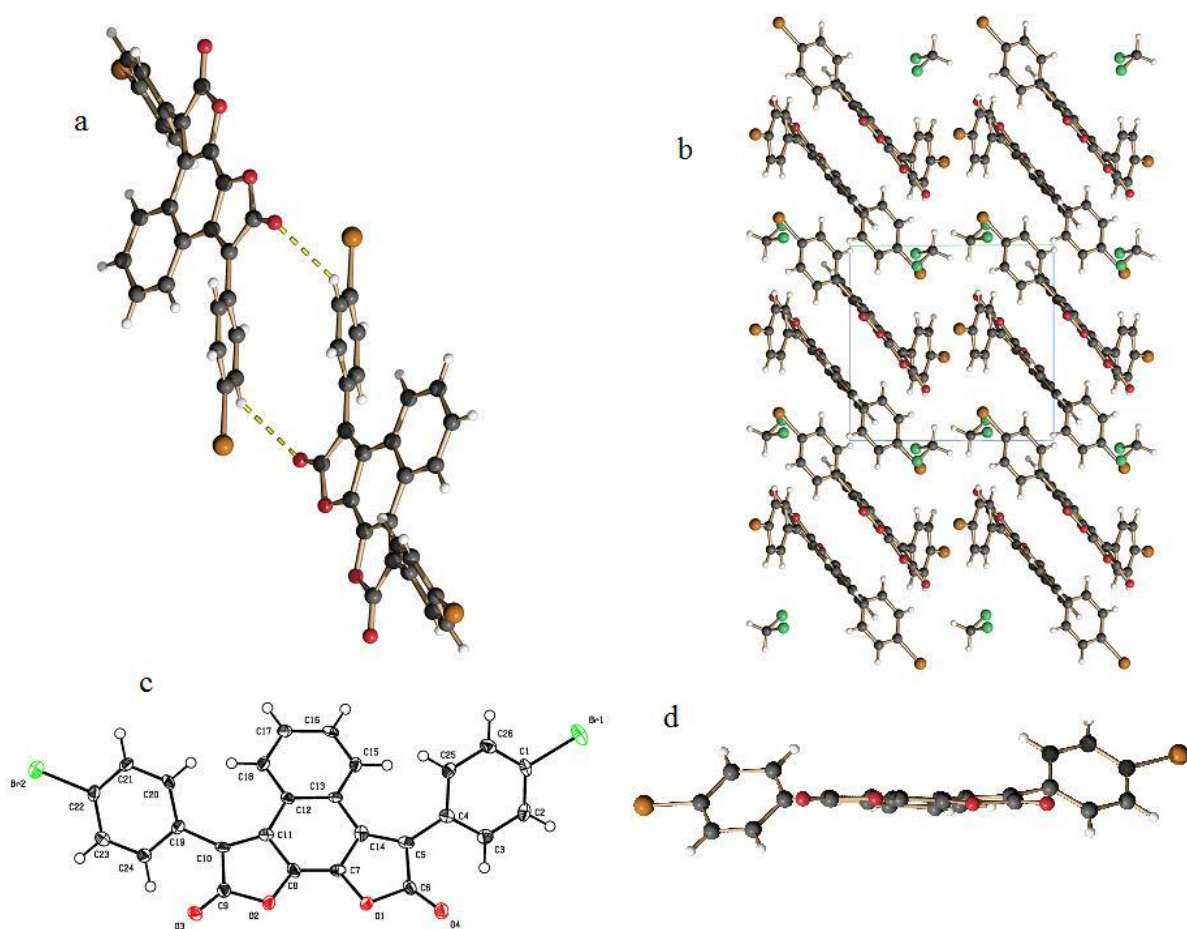


Figure 4.3. Single crystal structure of **1,10-NDF**.

Optical properties

UV/vis absorption and fluorescence spectra of **1,10-NDF**, **Th-1,10-NDF** and **Br-Th-1,10-NDF** in dichloromethane are shown in Figure 4.4. The excitation wavelength was 400 nm. The monomers based on 1,10-BDF exhibit a strong UV/vis absorption and weak emission in the visible range with large Stokes shifts from 80 to 130 nm. The optical data are listed in Table 4.1. The UV/vis absorption maxima of **Th-1,10-NDF** and **Br-Th-1,10-NDF** are at 505 and 487 nm, which are 78 and 60 nm red-shifted compared with **1,10-NDF** (427 nm), respectively. This can be ascribed to the fact that in **Th-1,10-NDF** and **Br-Th-1,10-NDF** theniyl units are donor units and the 1,10-NDF unit is a acceptor units, and that D-A interactions lead to the bathochromic shift of the UV/vis absorption maximum. The monomers exhibit yellow to red colors with high extinction coefficients at λ_{max} being 36620 (**1,10-NDF**), 24877 (**Th-1,10-NDF**) and 36412 L mol⁻¹ cm⁻¹ (**Br-Th-1,10-NDF**), respectively. From the absorption onset of the monomers in the range from 493 to 619 nm, optical HOMO-LUMO gaps between 2.52 and 2.00 eV can be calculated. The photographs of the monomer solutions are shown in Figure 4.5.

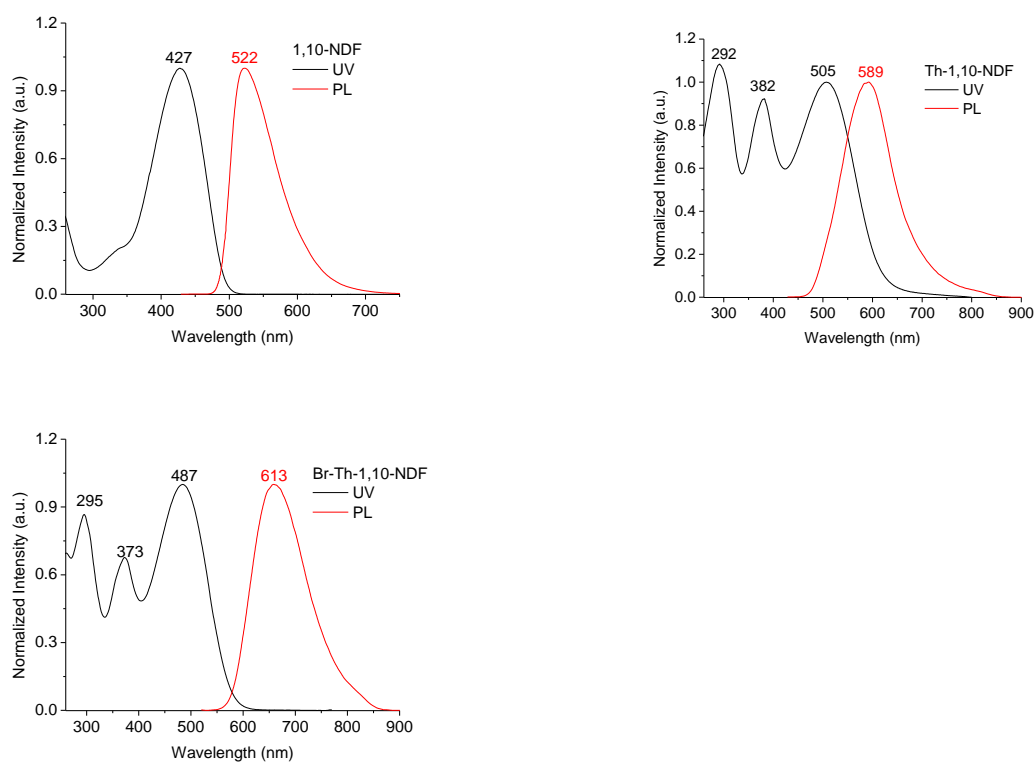


Figure 4.4. UV/Vis absorption and fluorescence spectra of **1,10-NDF**, **Th-1,10-NDF** and **Br-Th-1,10-NDF** in dichloromethane (excitation wavelength 400 nm).

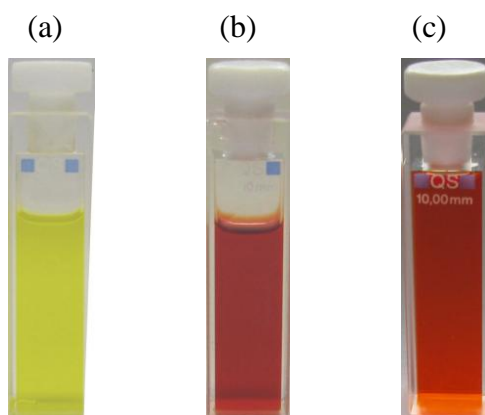


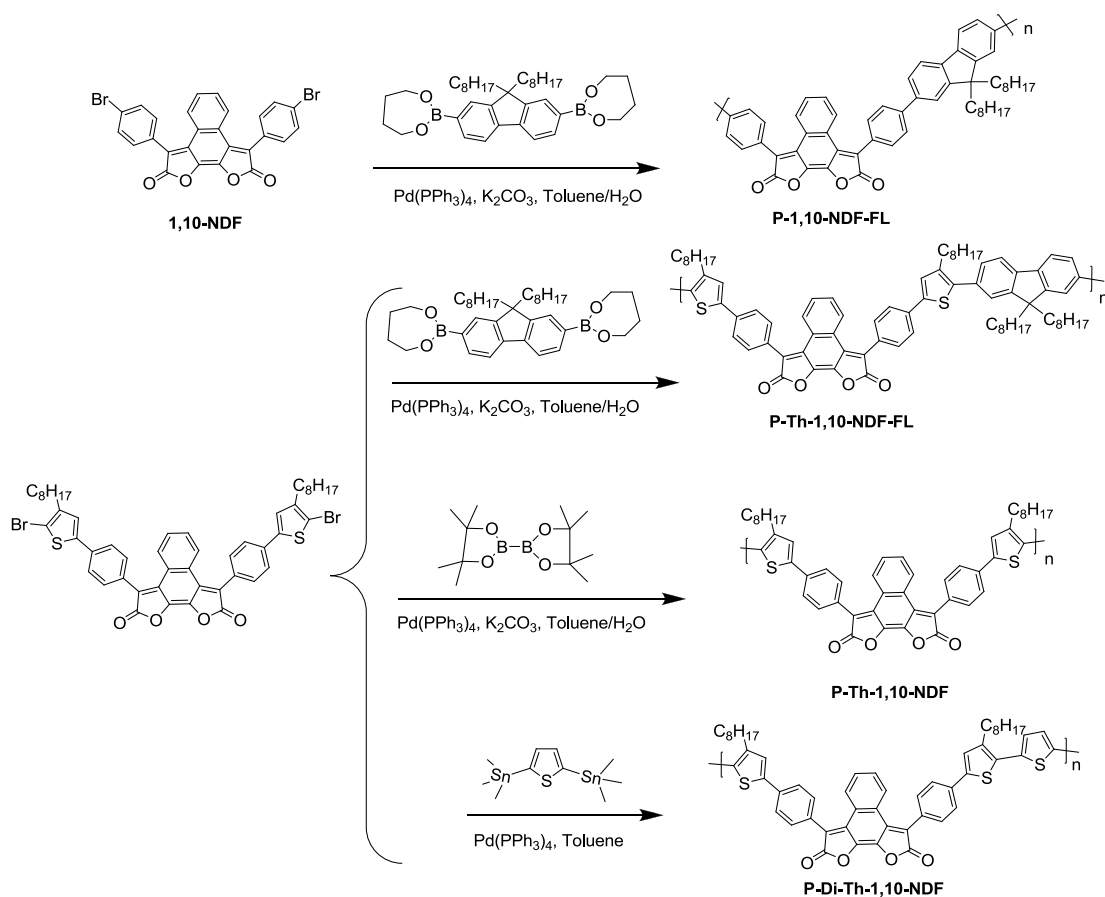
Figure 4.5. Photographs of solutions of **1,10-NDF** (a), **Th-1,10-NDF** (b) and **Br-Th-1,10-NDF** (c) in dichloromethane.

Table 4.1. Optical data of monomers **1,10-NDF**, **Th-1,10-NDF** and **Br-Th-1,10-NDF** in dichloromethane.

Monomers	$\lambda_{\text{abs,max}}/\text{nm}$	$\lambda_{\text{abs,onset}}/\text{nm}$	Optical band gap/eV	$\varepsilon(\lambda_{\text{abs,max}}) / \text{L mol}^{-1}\text{cm}^{-1}$	$\lambda_{\text{PL,max}}/\text{nm}$
1,10-NDF	427	493	2.52	36620	522
Th-1,10-NDF	292, 362,505	619	2.00	24877	589
Br-Th-1,10-NDF	295,303,487	575	2.16	36412	613

4.2.1.1.2 Polymers

Four π -conjugated polymers based on 1,10-NDF were designed, synthesized and characterized. **1,10-NDF** and **Br-Th-1,10-NDF** were polymerized with 9,9-di-n-octylfluorene-2,7-bis(trimethyleneborate), bis(pinacolato)diboron and 2,5-bis-(tributylstannyl)thiophene upon Suzuki and Stille coupling using tetrakis(triphenylphosphine)palladium as catalyst. The synthetic route is described in Scheme 4.2. The weight-average molecular weights (M_w) of the polymers are between 5.6 and 30.9 kDa. The polymers are dark solids, and well soluble in common organic solvents such as dichloromethane, chloroform and toluene.



Scheme 4.2. Synthesis of naphthodifuranone polymers **P-1,10-NDF-FL**, **P-Th-1,10-NDF-FL**, **P-Th-1,10-NDF** and **P-Di-Th-1,10-NDF**.

The $^1\text{H-NMR}$ spectra showed broad signals for aromatic protons, and the signals from 0.8-2.6 ppm are typical for the protons of the alkyl units (see Chapter 5, Experiment Part). The chemical shifts at 7.77-7.81 ppm are typical for the protons of the thienyl unit in polymers **P-Th-1,10-NDF-FL**, **P-Th-1,10-NDF** and **P-Di-Th-1,10-NDF**, and the signals at 7.76-7.93 ppm are typical for the protons of the fluorene moiety in the main chain of **P-1,10-NDF-FL** and **P-Th-1,10-NDF-FL**. The broad signals of **P-NDF-Th** with chemical shifts at about 7.38-7.44 ppm and 8.17-8.23 ppm are

typical for the protons of the 1,10-NDF core.

Theoretical calculation

Polymer **P-1,10-NDF-FL** was chosen to study quantum chemical HOMO/LUMO calculations. In order to make computation possible, we choose repeating units with methyl instead of n-octyl substituents as simplified models. The structures and molecular orbital surfaces of HOMO and LUMO of **P-1,10-NDF-FL** are shown in Figure 4.6. One can see that if the polymer **P-1,10-NDF-FL** is excited, electron transfer from the conjugated backbone to the NDF core takes place.

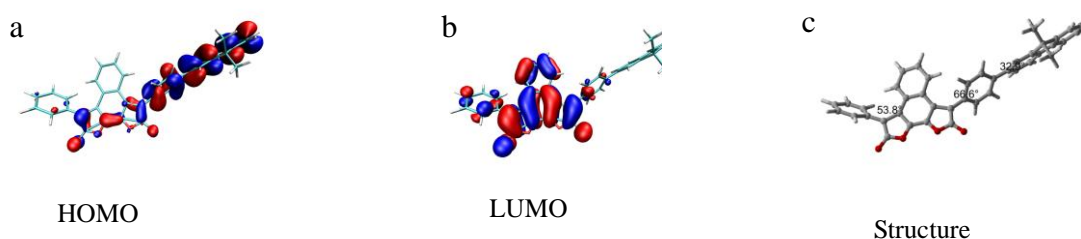


Figure 4.6. Structures and molecular orbital surfaces of HOMO and LUMO of **P-1,10-NDF-FL** obtained at the B3LYP/6-31G+(d,p) level.

From Figure 4.6.c, it can be derived that the torsional angle between the phenyl ring and the fluorene units is 32.9° , and that the dihedral angle between the phenyl units and the NDF core is 66.6° . The structure of the repeat unit of **P-1,10-NDF-FL** is similar to **P-1,8-BDF-FL**, but the backbone of **P-1,8-BDF-FL** is more planar than **P-1,10-NDF-FL** (Chapter 3). The HOMO energy level of **P-1,10-NDF-FL** is -5.90 eV

and the LUMO energy level is -3.85 eV. From these levels the HOMO-LUMO gap of **P-1,10-NDF-FL** was calculated to be 2.05 eV.

Optical properties

The polymers based on 1,10-NDF show strong absorption and weak emission in the visible with large Stokes shifts in a range from 150 to 200 nm. The UV/vis absorption and emission spectra of polymers in dichloromethane solution and UV/vis absorption spectra of polymers in thin films are shown in Figure 4.7. The optical data are listed in Table 4.2.

From Figure 4.7.a, we can see that **P-1,10-NDF-FL** in dichloromethane exhibits strong UV/vis absorption maxima at 331, 396 and 482 nm, and a weak red fluorescence with maximum at 686 nm. The quantum yield is very low, only 0.17 %. The polymer exhibits a red color with a high extinction coefficient of $38748 \text{ L mol}^{-1} \text{ cm}^{-1}$ at $\lambda_{\text{max}} = 480 \text{ nm}$. The absorption spectrum of **P-1,10-NDF-FL** as thin film is red-shifted by 26 nm compared to the solution, and the long-wavelength tail of the absorption is extended to the infrared. This indicates a gain of planar conformation and/or the presence of π - π interchain association in the solid state. From the absorption onset of the polymer at 800 nm, an optical HOMO-LUMO gap of 1.55 eV can be calculated.

Figure 4.7.b, shows that **P-Th-1,10-NDF-FL** in dichloromethane exhibits a strong

UV/vis absorption with a shoulder at around 370 nm, which can be ascribed to the main absorption of fluorene, and an absorption band with maximum at 522 nm, which belongs to the NDF core. The absorption of **P-Th-1,10-NDF-FL** is red-shifted by 35nm compared with **Br-Th-1,10-NDF**. This can be ascribed to the extension of the π -conjugated system due to polymerization. **P-Th-1,10-NDF-FL** exhibits a weak fluorescence with maximum at 686 nm. The quantum yield is quite low, only 0.02 %, resulting in a rather unsmooth fluorescence spectrum. The polymer exhibits a purple color (Figure 4.8.) with high extinction coefficient of $24877 \text{ L mol}^{-1} \text{ cm}^{-1}$ at $\lambda_{\text{max}} = 522\text{nm}$. The UV/vis absorption maxima of **P-Th-1,10-NDF-FL** as thin film are at 383 and 552 nm. They are about 30 nm red-shifted compared to the solution. From the onset of absorption at 898 nm, an optical HOMO-LUMO gap of 1.38 eV can be calculated, which is 0.17 eV smaller than for **P-1,10-NDF-FL**. This can be ascribed to the thienyl unit and the 1,10-NDF core in the backbone of **P-Th-1,10-NDF-FL** leading to D-A interactions, which reduce the optical HOMO-LUMO gap.

The molecular structures of **P-Th-1,10-NDF** and **P-Di-Th-1,10-NDF** are similar. They only differ in the additional thienyl unit in the backbone of **P-Di-Th-1,10-NDF**. From Figure 4.4.b and c, one can see that the UV/vis absorption and emission spectra of the two polymers are nearly identical. The absorption spectra of **P-Th-1,10-NDF** and **P-Di-Th-1,10-NDF** in dichloromethane exhibit strong absorption maxima at 303, 371 and 482 nm, and at 300, 375 and 483 nm, respectively. They also resemble the absorption spectrum of the monomer **Br-Th-1,10-NDF**, the absorption maxima of

which are at 295, 373 and 487 nm. This indicates that the thienyl unit does not favour for the planarity of the conjugated polymer chains in solution. The two polymers exhibit a weak fluorescence with maxima at 663 and 667 nm, respectively. The quantum yields are 4.7 and 4.8 %, respectively. The UV/vis absorption maximum of **P-Di-Th-1,10-NDF** at 564 nm, i.e., gnm blue-shifted compared with **P-Th-1,10-NDF** at 573 nm. This can be ascribed to the molecular weight of **P-Th-1,10-NDF** compared with **P-Di-Th-1,10-NDF**. From the absorption onset of the polymers at 900 and 890 nm, optical HOMO-LUMO gaps 1.37 and 1.39 eV can be calculated, respectively.

Table 4.2. Optical properties of polymers based on 1,10-NDF

Polymers	λ_{\max} [nm]		λ_{em} [nm]	Stokes shift	Φ_f [%]	ϵ (λ_{\max}) [L mol ⁻¹ cm ⁻¹]
	in DCM	in thin film				
P-1,10-NDF-FL	331,396,482	334,416,508	686	204	0.17	38748 (482 nm)
P-Th-1,10-NDF-FL	371, 522	383, 552	680	158	0.02	24887 (522 nm)
P-Th-1,10-NDF	303,371,482	448,573	663	181	4.7	25617 (482 nm)
P-Di-Th-1,10-NDF	300,375,483	437, 564	667	184	4.8	10736 (483 nm)

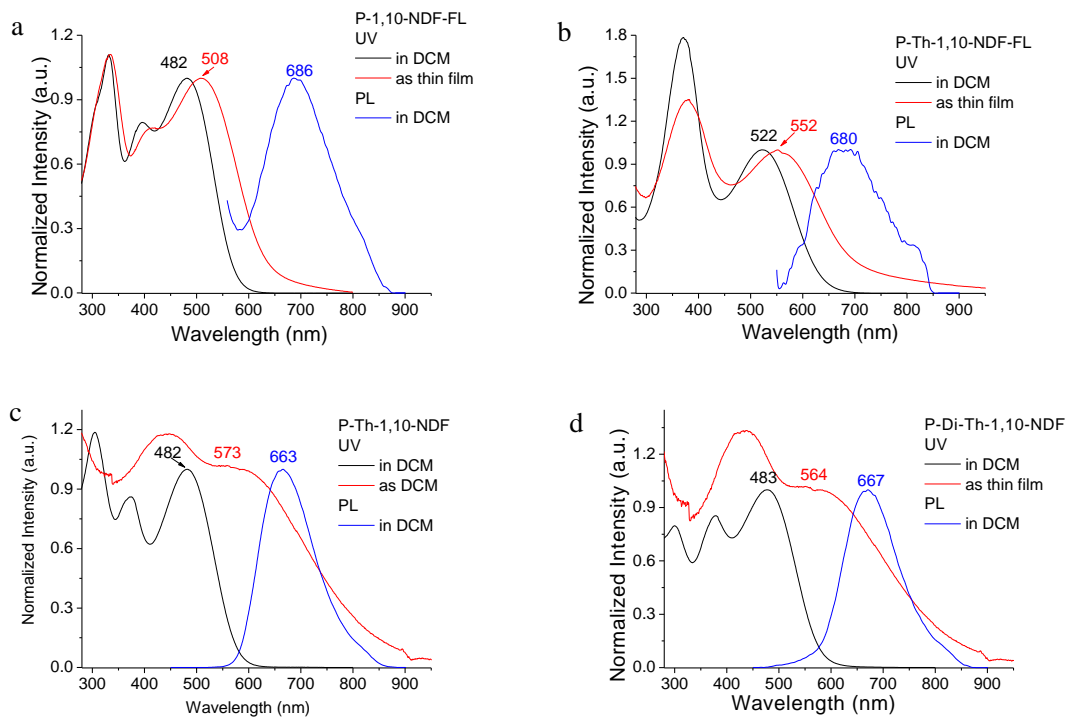


Figure 4.7. UV/vis absorption and emission spectra of polymers based on 1,10-NDF in dichloromethane solution, and UV/vis absorption spectra of polymers based on 1,10-NDF in thin films.

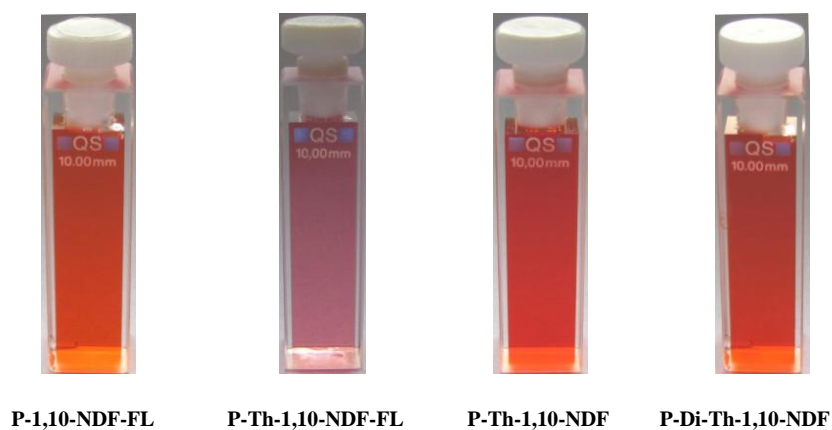


Figure 4.8. Photographs of the solutions of polymers based on 1,10-NDF in dichloromethane.

Electrochemical Properties.

The electrochemical response of polymers based on 1,10-NDF was studied using cyclic voltammetry (Figure 4.9.). The experimental conditions are described in Chapter 5, Experiment Part. The electrochemical data of the polymers are listed in Table 4.3.

In Figure 4.9.a, it is shown that the oxidation and reduction behaviour of **P-1,10-NDF-FL** is reversible. On increasing the potential, **P-1,10-NDF-FL** exhibits an anodic wave at +1.24 V. Decreasing the potential again, the oxidation is reverted at +1.23 V. The reductive cycle shows two reversible cathodic waves at -0.48/ -0.92 V and -1.02/ -2.03 V, which originate from the reduction of the quinonoid to a benzoic structure and also indicate a high stability of the anion radical. This can possibly be explained with a stabilizing negative charge of the oxygen atoms in the carbonyl groups of the two the lacton groups in the benzodione chromophore. The electrochemical band gap of **P-1,10-NDF-FL** is 1.53 eV, which is similar to the optical ones.

As shown in Figure 4.9.b, the oxidation and reduction behavior of **P-Th-1,10-NDF-FL** is irreversible. The anodic oxidation of **P-Th-1,10-NDF-FL** sets in at a low potential of 0.54 V. Two anodic waves with maxima at 0.77 and 1.29 V occur. This can be ascribed to formation of cation radicals and dications. The electrochemical band gap of for **P-Th-1,10-NDF-FL** is 1.45 eV which is 0.08 eV

smaller than **P-1,10-NDF-FL**. This can be ascribed to the thienyl unit and the 1,10-NDF core in the backbone of **P-Th-1,10-NDF-FL**, which lead to D-A interactions reducing the electrochemical band gap.

Although the molecular structures of **P-Th-1,10-NDF** and **P-Di-Th-1,10-NDF** are similar, the electrochemical behavior appears to be different. From Figure 4.9.c and d, one can see that the oxidation and reduction behaviour of **P-Th-1,10-NDF** is reversible, while the oxidation behaviour of **P-Di-Th-1,10-NDF** is irreversible. This can be ascribed to the lower molecular weight of **P-Di-Th-1,10-NDF**. The anodic oxidation of the two polymers sets in at low potentials of 0.81 (**P-Th-1,10-NDF**) and 1.16 V (**P-Di-Th-1,10-NDF**), respectively. The HOMO energy levels of the polymers are -5.61 and -5.96 eV, respectively. They are lower than the air oxidation (ca. -5.27 eV) indicating good air stability. Moreover, due to the low HOMO energy level of the polymers (Table 4.4.), a higher V_{oc} could be potentially obtained for solar cells. The electrochemical band gap of **P-Di-Th-1,10-NDF** is 0.23 eV larger than for **P-Th-1,10-NDF**. This can be ascribed to the lower molecular weight of **P-Di-Th-1,10-NDF**, which goes along with a less extended π -system.

Table 4.3. Bandgap data of polymers^a based on 1.10-NDF.

Polymer	$\lambda_{\text{abs,onset}}$ of Film [nm]	Oxidation Onset [V] {HOMO [eV]}	Reduction Onset [V] {LUMO [eV]}	Opt/Electrochem Band Gap [eV]
P-1,10-NDF-FL	800	0.93 {-5.73}	-0.60{-4.20}	1.55/1.53
P-Th-1,10-NDF-FL	898	0.54 {-5.34}	-0.91 {-3.89}	1.38/1.45
P-Th-1,10-NDF	900	0.81{-5.61}	-0.59{-4.21}	1.37/1.40
P-Di-Th-1,10-NDF	890	1.16 {-5.96}	-0.47 {-4.43}	1.39/1.63

^aOptical band gap E_{opt} was measured at the onset of absorption of polymer film ($E_{\text{opt}} = 1240/\lambda_{\text{abs,onset}}$ eV). HOMO-LUMO gap was calculated according to the equation $-E_{\text{LUMO}} = E_{\text{onset(red)}} + 4.8$ eV, and $-E_{\text{HOMO}} = E_{\text{onset(ox)}} + 4.8$ eV. $E_{\text{onset(ox)}}$ and $E_{\text{onset(red)}}$ are onset potentials for oxidation and reduction processes vs Fc/Fc⁺ couple.

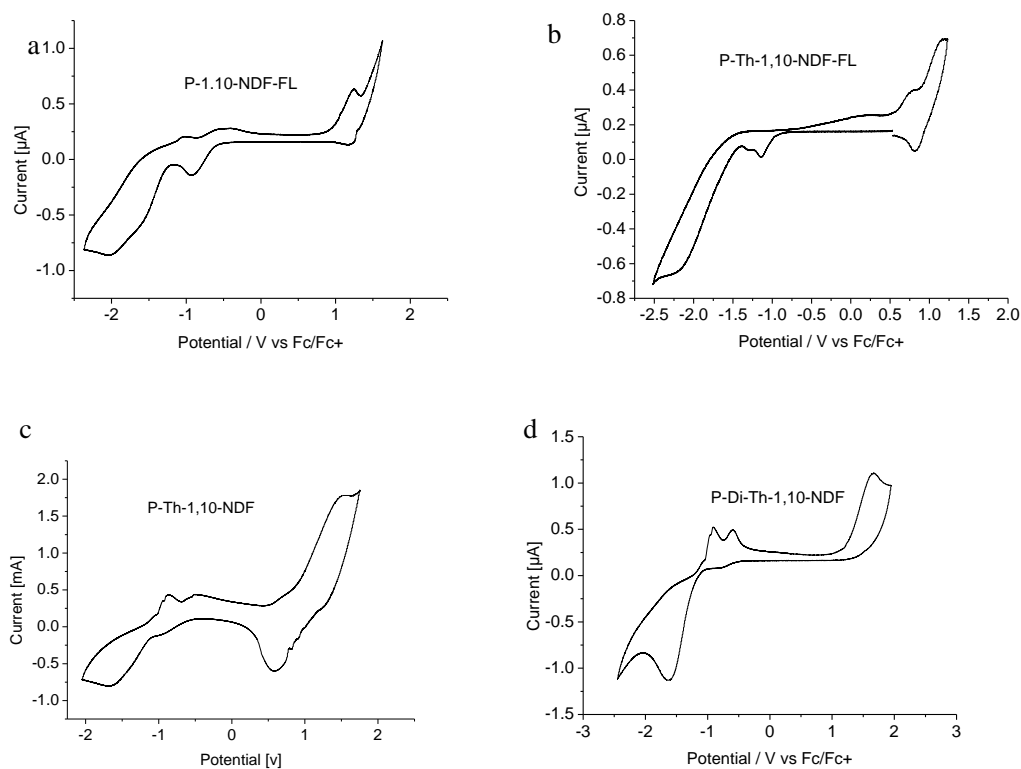


Figure 4.9. Cyclic voltammograms of polymers based on 1.10-NDF as thin films deposited on ITO. Solution: 0.1 M TBAPF₆/acetonitrile. Potential calculated versus ferrocene. Scan rate: 100 mV s⁻¹; T= 20 °C.

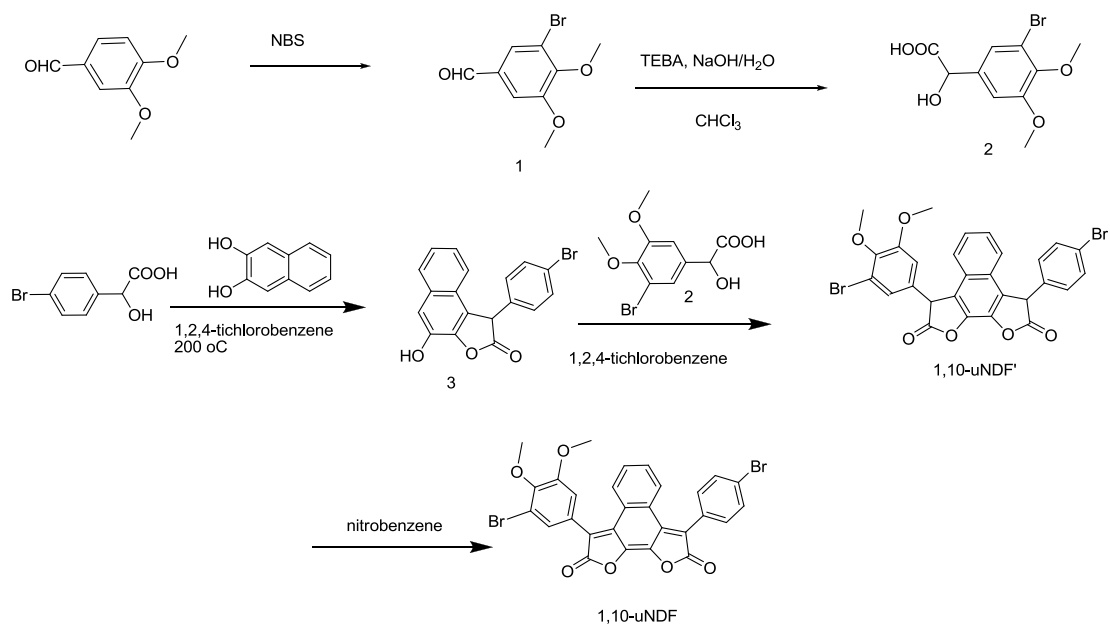
4.2.1.2 Preparation of asymmetric monomers and polymers based on 1,10-NDF

In Chapter 4.2.1.1, the monomers and polymers based on symmetrical 1,10-NDF have been described. For comparison, monomer and polymers based on an unsymmetrical 1,10-NDF was also designed, synthesized and characterized.

4.2.1.2.1 Monomer

The synthetic route to the new asymmetric monomer **1,10-uNDF** is described in Scheme 4.3. The starting compound **2** was prepared according to literature procedures (see Chapter 5, Experiment Part). 1 eq. 2,3-dihydroxynaphthalene was reacted with 1 eq. 4-bromo-mandelic acid, which led to single cyclization with formation of derivative **3**. In the following, 1 eq. of **3** is followed reacted with 1.2 eq. **2** leading to double cyclization with formation of **1,10-uNDF'**. **1,10-uNDF'** was oxidized with nitrobenzene to result in the conjugated monomer **1,10-uNDF** in a yield of 63 %.

The ¹H-NMR spectrum of **1,10-uNDF** displayed all the expected resonances with no discernible peaks corresponding to impurities. The signals with a chemical shift at 3.88-4.01 ppm are typical for protons of the methoxy groups attached to the phenyl unit, and the chemical shifts at 7.31-7.52 ppm are typical for the naphthodifuranone core. (see Chapter 5, Experimental Part)



Scheme 4.3. Synthetic route to unsymmetrical monomer **1,10-uNDF**.

Molecular orbital computation

In order to better understand the electronic structure of monomer **1,10-uNDF**, quantum chemistry calculations by the density functional theory (B3LYP/6-31G^{*}) method were performed. As shown in Figure 4.10, the LUMO orbitals of **1,10-uNDF** are mainly localized at the NDF core, while the HOMO orbitals are delocalized nearly along the phenyl-NDF-core-phenyl axis. If **1,10-uNDF** is excited, an electron transfer from the phenyl-NDF-core-phenyl part to the NDF core takes place, which is similar to monomer 1,10-NDF (Figure 4.2). The core of NDF is nearly fully coplanar, which ensures full conjugation. The torsional angle between the lactam phenyl ring and the NDF core is between 53.5° and 55.3°, which indicates that the phenyl groups are less coplanar with the NDF core, and only cause weak π - π interactions. The HOMO-LUMO gap of **1,10-uNDF** was calculated to be 2.68 eV.

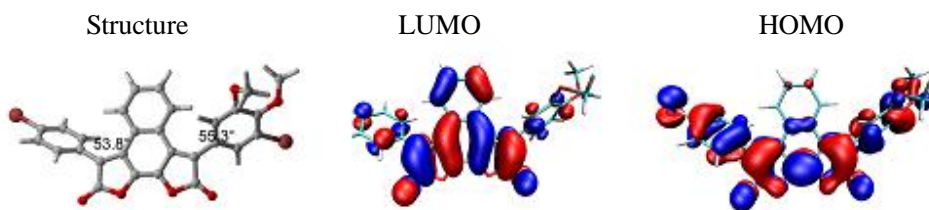


Figure 4.10. Structures and molecular orbital surfaces of the HOMO and LUMO of **1,10-uNDF**, obtained at the B3LYP/6-31G* level.

UV/vis absorption of **1,10-uNDF**

The UV/vis absorption spectrum of **1,10-uNDF** in dichloromethane is shown in Figure 4.11. **1,10-uNDF** shows a strong UV/vis absorption with maximum at 400 nm which is around 27 nm blue shifted compared with **1,10-NDF**. This is surprising, since **1,10-uNDF** has two methoxy units attached to the phenyl ring favoring a bathochromic shift compared with **1,10-NDF** due to an increased donor-acceptor character. Compared with Figure 4.2. and Figure 4.10, we can see that the structure of **1,10-uNDF** is less planar than **1,10-NDF**. It seems the planarity of the molecule plays a decisive role for the bathochromic shift. **1,10-uNDF** is highly soluble in common organic solvents and exhibits a high extinction coefficient of $4.2 \cdot 10^4 \text{ L mol}^{-1} \text{ cm}^{-1}$ in dichloromethane.

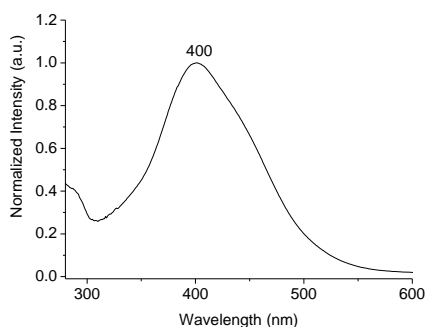
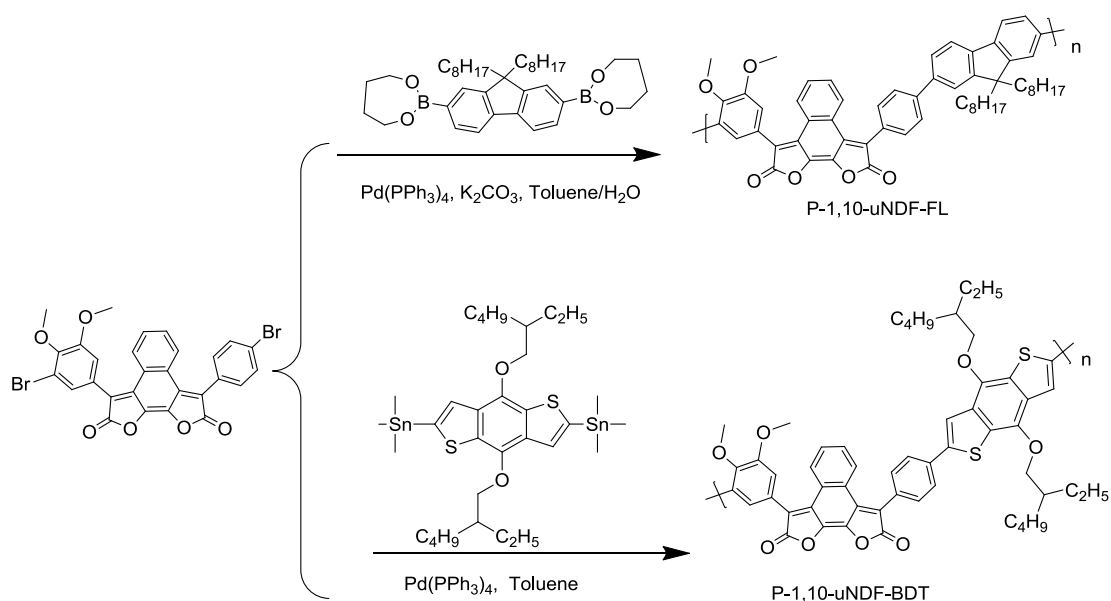


Figure 4.11. UV/vis absorption spectrum of **1,10-uNDF** in dichloromethane solution.

4.2.1.2.2 Polymers

The two polymers **P-1,10-uNDF-FL** and **P-1,10-uNDF-BDT** were prepared upon Suzuki and Stille coupling reactions of **1,10-uNDF** and 9,9-di-n-octylfluorene-2,7-bis(trimethyleneborate), or (4,8-bis(2-ethylhexyloxy)-benzo[1,2-*b*:4,5-*b'*]dithiophene-2,6-diyl)-bis(trimethyl-stannane), respectively, and the yields being 66 and 72 % (Scheme 4.4.). The polymers show excellent solubility in common organic solvents such as toluene, dichlorobenzene and tetrahydrofuran. The weight-average molecular weights (M_w) of the polymers are 17.5 kDa (**P-1,10-uNDF-FL**), and 9.6 kDa (**P-1,10-uNDF-BDT**), and the polydispersities (PDI) are 2.1 and 1.8, respectively.



Scheme 4.4. Synthesis of naphthodifuranone polymers **P-1,10-uNDF-FL** and **P-1,10-uNDF-BDT**.

Optical properties

In Figure 4.12., the UV/vis absorption spectra of the polymers **P-1,10-uNDF-FL** and **P-1,10-uNDF-BDT** in dichloromethane solution are shown. The two polymers are deeply colored, the extinction coefficients of the strongest bands being $39257 \text{ L mol}^{-1} \text{ cm}^{-1}$ for **P-1,10-uNDF-FL**, and $40254 \text{ L mol}^{-1} \text{ cm}^{-1}$ for **P-1,10-uNDF-BDT**, respectively. The absorption spectrum of **P-1,10-uNDF-BDT** in dichloromethane exhibits strong absorption maxima at 487 nm. **P-1,10-uNDF-FL** exhibits a shoulder at around 388 nm, which can be ascribed to the main absorption of fluorene, and a main absorption band at 464 nm, which belongs to the backbone. The absorption bands are very broad ranging from 300 to 520 nm for **P-1,10-uNDF-FL**, and from 420 to 530 nm for **P-1,10-uNDF-BDT**. The absorption maximum of

P-1,10-uNDF-BDT is 23 nm red shift compared with **P-1,10-uNDF-FL** due to the strong donor ability of the BDT unit. The absorption maxima of the polymers are red-shifted by 64 nm (**P-1,10-uNDF-FL**) and 87 nm (**P-1,10-uNDF-BDT**) compared with monomer **1,10-uNDF**, Broadening and red-shift of the absorption bands originate from the extension of the π -conjugated system due to polymerization.

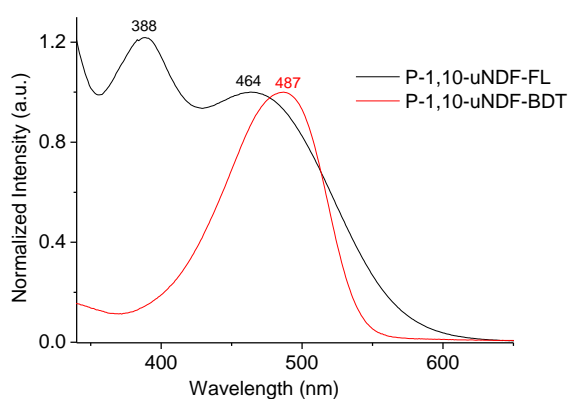


Figure 4.12. UV/vis absorption spectra of **P-1,10-uNDF-FL** and **P-1,10-uNDF-BDT** in dichloromethane solution.

Electrochemical Properties

The electrochemical properties of the polymers were investigated using the same method as described previously. From Figure 4.13, it can be seen that anodic oxidation of **P-1,10-uNDF-FL** and **P-1,10-uNDF-BDT** sets in at potentials of 1.01 and 0.31 V, respectively. Two anodic waves with maxima at 1.07 and 1.36 V (**P-1,10-uNDF-FL**), and 0.64 and 1.44 V (**P-1,10-uNDF-BDT**) occur. This can be ascribed to formation of cation radicals and dication. The reductive cycle of **P-1,10-uNDF-FL** exhibits two reversible cathodic waves at -1.21 and -1.64 V, which

are reverted at -0.95 and -0.59 V. For **P-1,10-uNDF-BDT** two cathodic waves at -0.88 and -1.60 V occur, which are reverted at -1.27 and -0.76 V. They originate from the reduction of the quinonoid to a benzoic structure and also indicate a high stability of the anion radical.

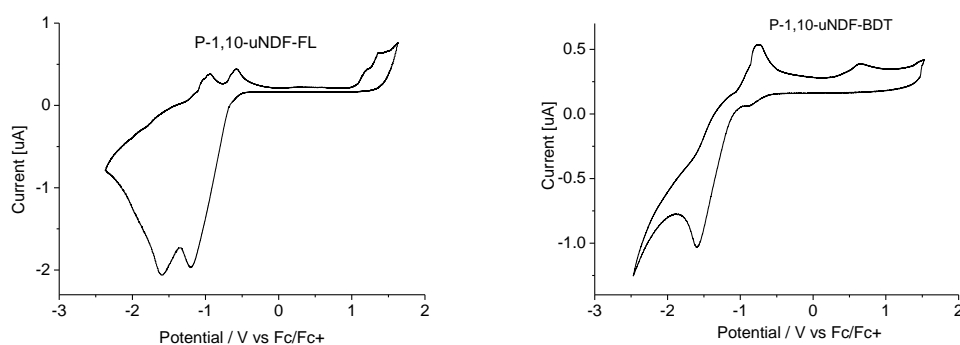


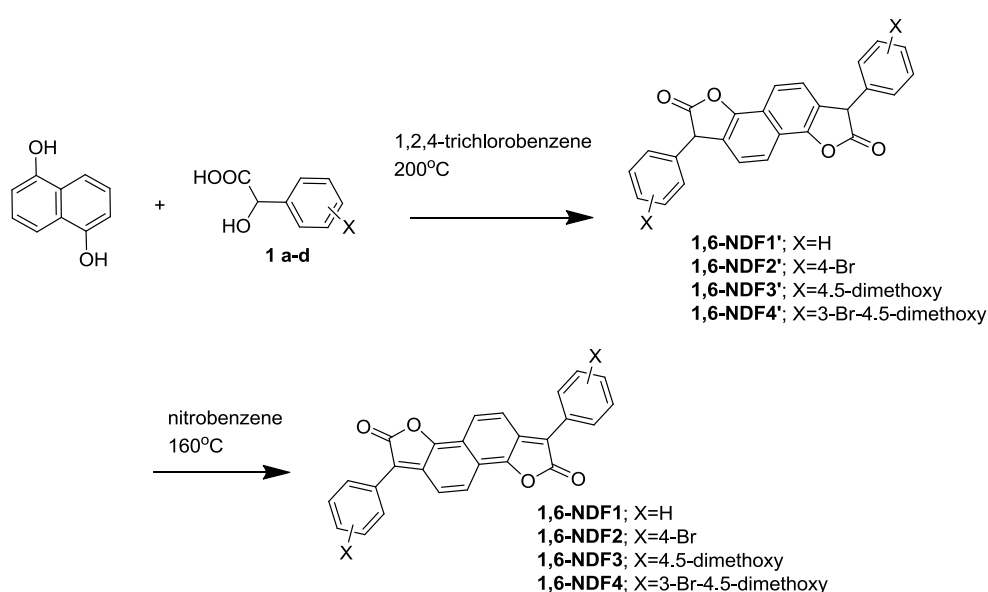
Figure 4.13. Cyclic voltammograms of polymers **P-1,10-uNDF-FL** and **P-1,10-uNDF-BDT** as thin films deposited on ITO. Solution: 0.1 M TBAPF₆/acetonitrile. Potential calculated versus ferrocene. Scan rate: 100 mV s⁻¹; T= 20 °C.

From the onset of anodic and cathodic waves the HOMO and LUMO values as well as the electrochemical band gaps were calculated. The electrochemical band gap values are 1.66 eV for **P-1,10-uNDF-FL**, and 1.01 eV for **P-1,10-uNDF-BDT**, respectively. The electrochemical band gap value of **P-1,10-uNDF-BDT** is 0.65 eV smaller than **P-1,10-uNDF-FL**, since the BDT unit is a more powerful donor unit than the fluorene unit.

4.2.2 Monomers and polymers based on 1,6-NDF

4.2.2.1 Monomers

Monomeric 1,6-naphthodifuranone (1,6-NDF) is a deeply bluish purple dyes. The structure of 1,6-NDF is similar to 1,5-benzodifuranone (1,5-BDF) and 1,10-NDF. 1,6-NDFs belong to a kind of electron-deficient chromophores, which have been developed in the last 30 years, and are prepared upon condensation of 1,5-dihydroxynaphthalene with derivatives of mandelic acid. The final deep color originates from the quinonoid structure of the central core unit, which is obtained upon oxidation of the naphthalene unit with nitrobenzene. The synthetic route to new 1,6-NDF-based monomers **1,6-NDF1-4** is described in Scheme 4.5. The starting compounds were prepared according to literature procedures (see Chapter 5, Experimental part). Monomer **1,6-NDF2** is not well soluble in common organic solvents, while the other monomers are well soluble in hot toluene.



Scheme 4.5. Synthetic route to monomer based on 1,6-NDF.

UV/vis absorption of monomers

The monomers **1,6-NDF1-4** show strong and broad absorption in the visible and exhibit purple to blue color. The optical data are listed in Table 4.5 and the UV/vis absorption spectra and photographs of the solutions are displayed in Figure s4.14 and Figure 4.15, respectively.

The absorption spectra of 1,6-NDF-based monomers in dichloromethane indicate strong bands with maxima between 550 and 635 nm, and extinction coefficients up to $102626 \text{ L mol}^{-1} \text{ cm}^{-1}$. **1,5-NDF-3** and **-4** exhibit a blue colour, and the absorption maxima are red shifted compared with **1,6-NDF1** and **-2**, because the methoxy groups attached to phenyl rings increase the donor-acceptor character, and thus favor a bathochromic shift.

From the absorption edges of the monomers between 607 and 711 nm, optical HOMO-LUMO gaps of 1.75 to 2.05 eV can be calculated. Monomer **1,6-BDF3** with additional π -electrons from the methoxy-groups shows the smallest HOMO-LUMO gap of 1.75 eV. In comparison, monomer **1,6-NDF1** with no substituent shows the largest HOMO-LUMO gap of 2.05 eV among the four monomers.

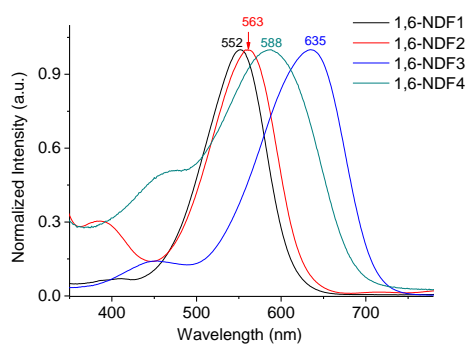


Figure 4.14. UV/vis absorption spectra of monomers **1,6-NDF1-4** in dichloromethane solution.

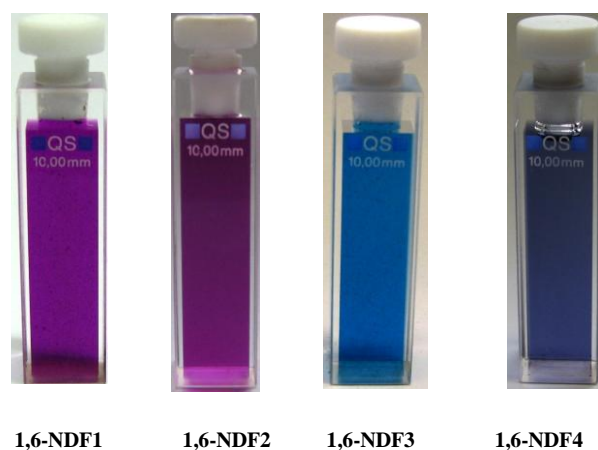


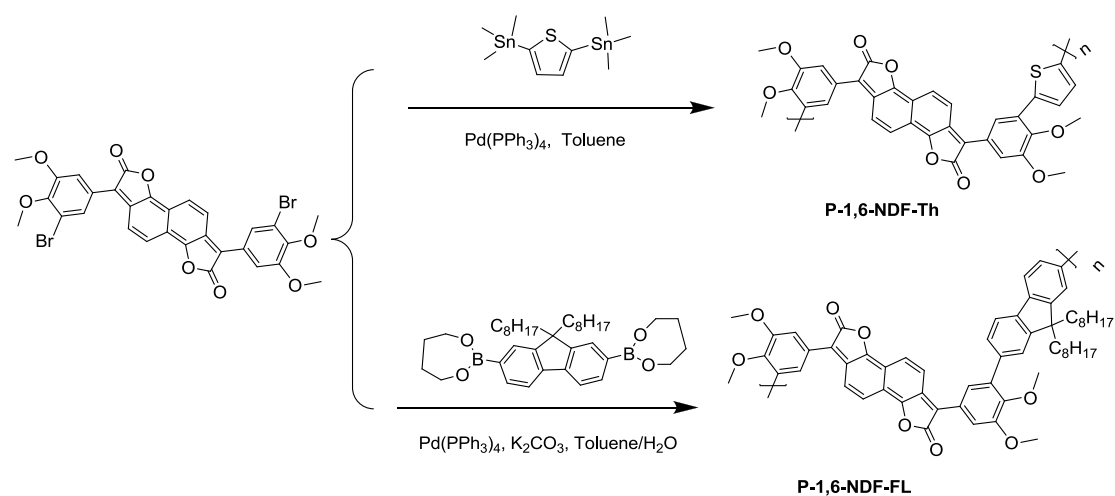
Figure 4.15. Photographs of the solutions of monomers **1,6-NDF1-4** in dichloromethane.

Table 4.4. Optical properties of monomers **1,6-NDF1-4**.

Monomers	$\lambda_{\text{abs,max}}/\text{nm}$	$\lambda_{\text{abs,onset}}/\text{nm}$	Optical band gap /eV	$\epsilon/L \text{ mol}^{-1}\text{cm}^{-1}$
1,6-NDF1	552	607	2.05	54093
1,6-NDF2	563	630	1.97	--
1,6-NDF3	635	711	1.75	102626
1,6-NDF4	588	681	1.82	26208

4.2.2.2 Polymers

The two polymers were prepared upon Suzuki and Stille coupling reactions of **1,6-NDF** and 2,5-bis(trimethyl-stannane)thiophene (**P-1,6-NDF-Th**), or 9,9-di-n-octylfluorene-2,7-bis(trimethyleneborate) (**P-1,6-NDF-FL**), the yields being 45-64% (Scheme 4.6). Polymer **P-1,6-NDF-FL** shows excellent solubility in common organic solvents such as toluene, dichlorobenzene and tetrahydrofuran, while **P-1,6-NDF-Th** is only moderately soluble. The weight-average molecular weights (M_w) of the polymers are 7.9 kDa (**P-1,6-NDF-Th**), and 8.7 kDa (**P-1,6-NDF-FL**), and the polydispersities (PDI) are 1.5 and 2.2, respectively.



Scheme 4.6. Synthetic route to polymers **P-1,6-NDF-Th** and **P-1,6-NDF-FL**.

UV/vis absorption of **P-1,6-NDF-Th** and **P-1,6-NDF-FL**

The UV/vis absorption spectra of polymers **P-1,6-NDF-Th** and **P-1,6-NDF-FL** in solution and as thin film are displayed in Figure 4.16, and the optical data are listed in Table 4.5.

The two polymers exhibit a deep green (**P-1,6-NDF-Th**) and blue (**P-1,6-NDF-FL**) color with maxima in dichloromethane at 644 and 620 nm, respectively. **P-1,6-NDF-Th** is only moderately soluble in common organic solution, the extinction coefficient of the strongest band being $1.9 \times 10^4 \text{ L mol}^{-1} \text{ cm}^{-1}$ in 1,2,4-trichlorobenzene. **P-1,6-NDF-FL** is well soluble in common organic solvents such as dichloromethane with an extinction coefficient of $2.1 \times 10^4 \text{ L mol}^{-1} \text{ cm}^{-1}$. The absorption maxima of the polymers are 56 nm (**P-1,6-NDF-Th**) and 32 nm (**P-1,6-NDF-FL**) red-shifted compared with the related monomers. The strong shift of **P-1,6-NDF-Th** can be ascribed to D-A interactions between the 1,6-naphthodione and thienyl units giving rise to enhanced intramolecular charge transfer (ICT) and π -extension.

Polymer films were prepared upon spin coating from hot 1,2,4-trichlorobenzene (**P-1,6-NDF-Th**) and dichloromethane (**P-1,6-NDF-FL**) on a Si/SiO₂ substrate. The absorption spectra of films show maxima at 692 nm, and 638 nm, respectively. They are about 48 and 16 nm red-shifted compared with the solution spectra, and the long-wavelength tail of the absorption bands is extended to the infrared. This indicates a gain of planar conformation and/or the presence of π - π interchain association in the solid state.

From the absorption edges of the polymers at 1050 (**P-1,6-NDF-Th**) and 791 nm (**P-1,6-NDF-FL**), optical HOMO-LUMO gaps between 1.18 and 1.56 eV can be calculated. In comparison, the optical band gap of **P-1,6-NDF-Th** is around 0.38 eV smaller than of **P-1,6-NDF-FL**. This can be ascribed to the thienyl units with more powerful donor ability compared with the fluorene unit.

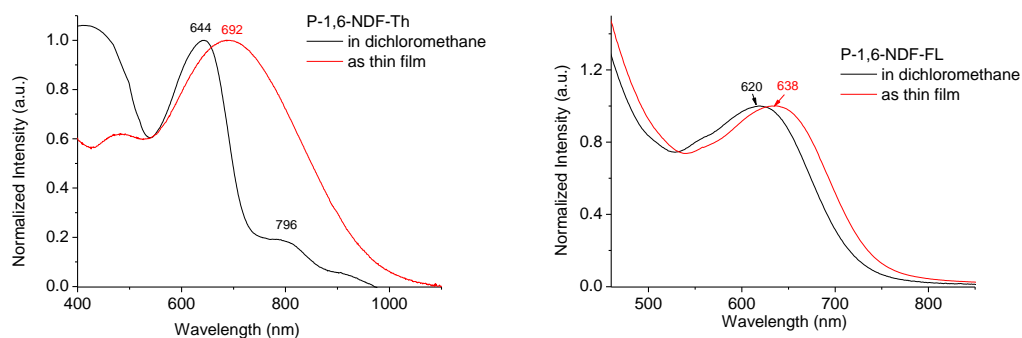


Figure 4.16. UV/vis absorption spectra of polymers **P-1,6-NDF-Th** and **P-1,6-NDF-FL** in solution and as thin film.

Table 4.5. Optical properties of polymers **P-1,6-NDF-Th** and **P-1,6-NDF-FL**.

Polymers	$\lambda_{\text{abs,max}}/\text{nm}$		$\lambda_{\text{abs,onset}}/\text{nm}$	Optical band gap /eV	Extinct coeff ϵ (λ_{max}) [L mol ⁻¹ cm ⁻¹]
	solution	film			
P-1,6-NDF-Th	644	692	1050	1.18	19425
P-1,6-NDF-FL	620	638	791	1.56	21364

Electrochemical Properties

The electrochemical properties of the polymers were investigated using the same method as described previously. From Figure 4.17, it can be seen that anodic oxidation of polymers sets in at low potentials of 0.33 V (**P-1,6-NDF-Th**) and 0.78 V (**P-1,6-NDF-FL**). One anodic wave occurs with maximum at 1.38 and 0.98 V, respectively. This can be ascribed to formation of cation radicals and dications. The reductive cycle of **P-1,6-NDF-Th** exhibits two reversible cathodic waves at -1.12 and -2.07 eV, which are reverted at -1.29 and -0.71 eV. This originates from the reduction of the quinonoid to a benzoic structure and also indicates a high stability of the anion

radical, which can possibly be explained with a stabilizing negative charge at the oxygen atoms of the two carbonyl groups in the naphthodione units. For **P-1,6-NDF-FL** two cathodic waves at -0.44 and -1.92 eV occur, which are reverted at -1.21 and -0.35 eV.

From the onset of anodic and cathodic waves the HOMO and LUMO values as well as the electrochemical band gaps were calculated. The electrochemical band gap values are 1.08 eV for **P-1,6-NDF-Th**, and 1.17 eV for **P-1,6-NDF-FL**, respectively.

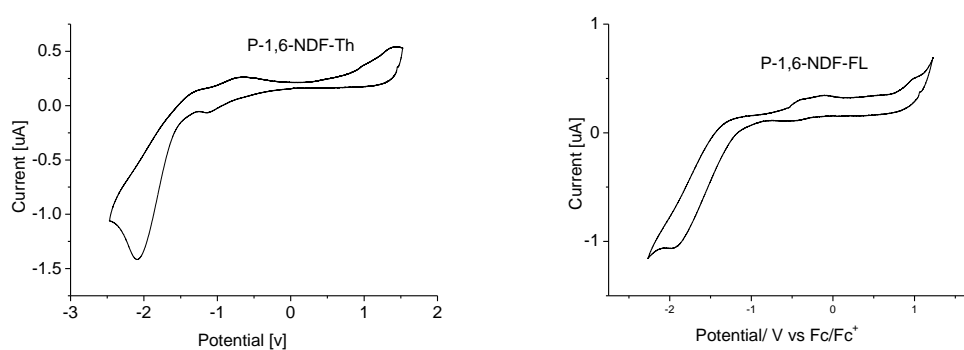


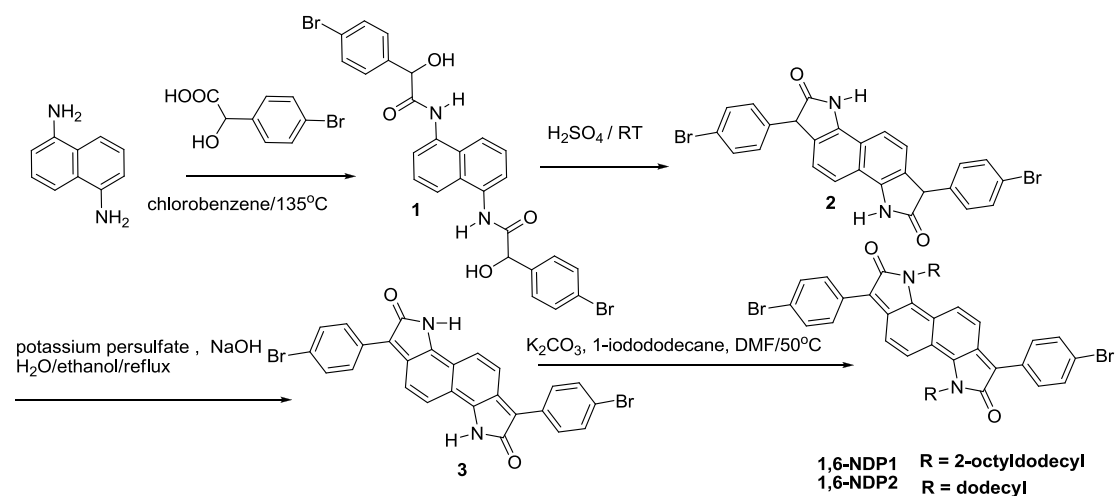
Figure 4.17. Cyclic voltammograms of polymers **P-1,6-NDF-Th** and **P-1,6-NDF-FL** as thin films deposited on ITO. Solution: 0.1 M TBAPF₆/acetonitrile. Potential calculated versus ferrocene. Scan rate: 100 mV s⁻¹; T= 20 °C.

4.3 Monomers and polymers based on 1,6-NDP

4.3.1 Monomers

The synthetic route to monomers **1,6-NDP1** and **-2** is described in Scheme 4.7. The structures of **1,6-NDP1** and **-2** are similar to **1,5-BDP1** and **-2**, except that an

additional benzene ring is present in the core of NDP, similar to 1,6-NDF. **1,6-NDP1** and **-2** were obtained from 1,5-diaminonaphthalene with 4-bromo mandelic acid in chlorobenzene and followed by ring closure in sulfuric acid at room temperature. The final deep color originates from the quinonoid structure of the central core unit, which is obtained upon oxidation of the phenylene unit with potassium persulfate.



Scheme 4.7. Synthetic route to monomers **1,6-NDP1-2**.

Single crystal structure of **1,6-NDP2**

Single crystals of **1,6-NDP2** of 0.3*0.04*0.02 mm in size were grown upon slow evaporation of the solvent dichloromethane. The solid state packing, molecular structure and interactions were investigated using X-ray diffraction (Figure 4.18). The unit cell with one molecule (Figure 4.18.c) was found to be triclinic with space group P-1, the crystallographic center of symmetry being located at the midpoint of C11 and C11a (Figure 4.18.b). The core of **1,6-NDP2** is nearly fully planar, which ensures full conjugation.

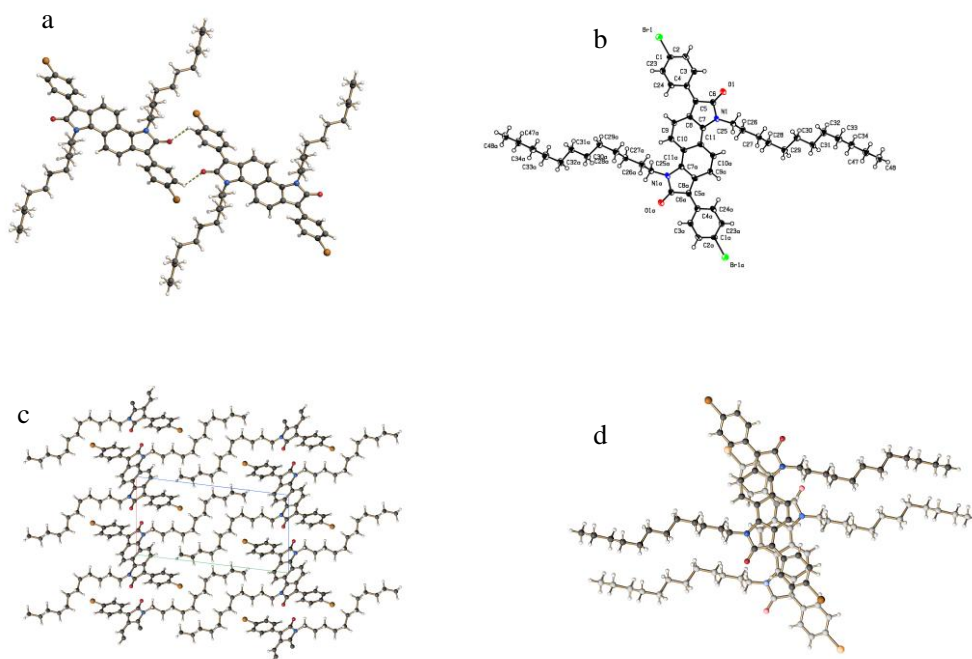


Figure 4.18. Single crystal structure of **1,6-NDP2**.

The torsional angle between the 4-bromophenyl ring and the 1,6-NDP core is 24.9° , which is 13.1° smaller than for 1,5-BDP (see Chapter 3.2). This indicates that **1,6-NDP2** is much more planar, which is advantageous for π -conjugation. The crystal packing shows that the molecules adopt a weak, intermolecularly slipped π - π stacking separated by the distance of 3.38 \AA (Figure 4.18.d), which is slightly shorter than for 1,5-BDP (3.56 \AA). There is an intramolecular hydrogen bonding between the C=O group of the 1,6-NDP core and the hydrogen atom of the phenyl ring of the neighboring molecule with a distance 2.545 \AA ($\text{C}_2\text{---H}_2\text{---O}_1$), and the torsional angle of $\text{C}_2\text{---H}_2\text{---O}_1$ (Figure 2a) is found to be 142.6° .

UV/vis absorption of monomers **1,6-NDP1-2**

The monomer **1,6-NDP1** and **-2** show strong and broad absorption bands in the visible and exhibit a purple color. The optical data are listed in Table 4.6. The UV/vis absorption spectra and photographs of solutions are displayed in Figures 4.19 and 4.20, respectively.

UV/vis absorption spectra of **1,6-NDP1** and **-2** in dichloromethane (Figure 4.19) indicate strong absorption maxima at 571 nm, the extinction coefficients being 48716 L mol⁻¹ cm⁻¹ and 46423 L mol⁻¹ cm⁻¹, respectively. The tails of the absorption bands reach to a wavelength of 670 nm. The absorption spectra of **1,6-NDP1** and **-2** are quite similar. The two monomers exhibit quite a weak fluorescence, which can hardly be detected. The monomer structure of 1,6-NDP is quite similar to 1,5-BDP, except that an additional benzene ring is present in 1,6-NDF core. However the UV/vis absorption spectra of the two kinds of monomers are quite different. The absorption maximum of 1,6-NDF is about 90 nm red-shifted compared with 1,5-BDP, since the additional benzene core of 1,6-NDP increases the size of the π -conjugated system of the monomer. The structure of 1,6-NDP is also similar to 1,6-NDF, and the UV/vis absorption spectra are also quite similar. From the absorption edges of the monomers at almost 705 nm, optical HOMO-LUMO gaps around 1.75 eV can be calculated.

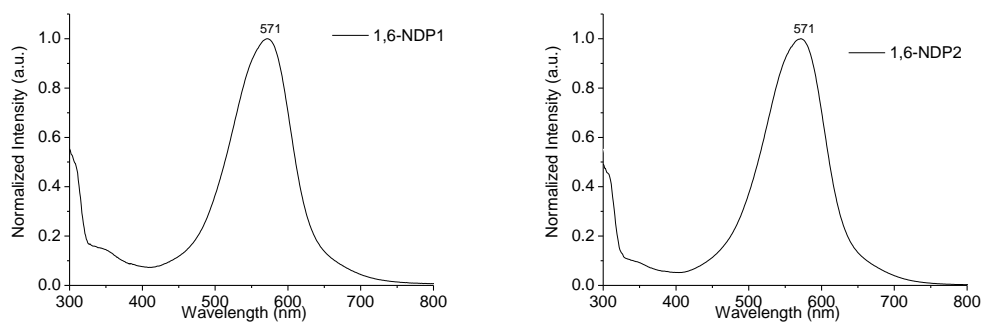


Figure 4.19. UV/vis absorption spectra of **1,6-NDP1** and **-2** in dichloromethane solution.



Figure 4.20. Photographs of the solutions of **1,6-NDP1** and **-2** in dichloromethane.

Table 4.6. Optical properties of monomers **1,6-NDP2**.

Monomers	$\lambda_{\text{abs,max}}/\text{nm}$	$\lambda_{\text{abs,onset}}/\text{nm}$	Optical band gap /eV	$\epsilon/\text{L mol}^{-1}\text{cm}^{-1}$
1,6-NDP1	571	701	1.75	48716
1,6-NDP2	571	701	1.75	46423

Photostability of monomers based on 1,6-NDP

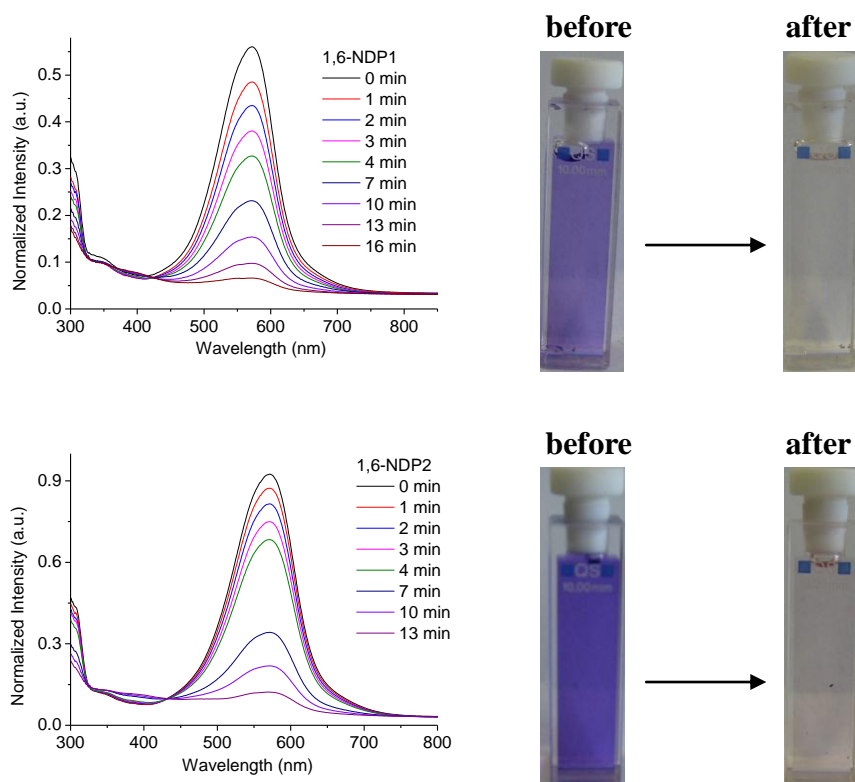


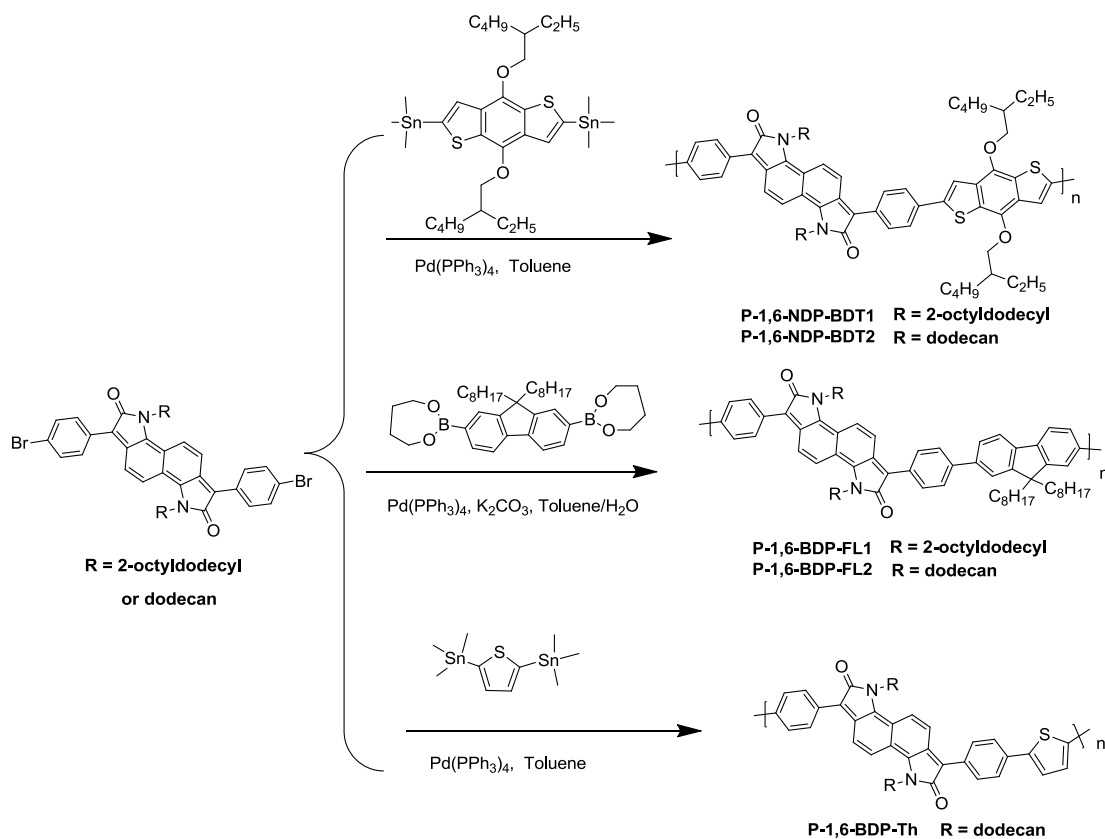
Figure 4.21. UV/Vis absorption spectra of the monomers **1,6-NDP1** and **-2** before and after irradiation in toluene with a 200 W Hg-lamp. Photographs of the solutions before and after irradiation are also shown.

The photostability of monomers **1,6-NDP1** and **-2** was measured using the same method as previously described. The monomer based on 1,6-NDP is similar to 1,5-BDP, except that an additional benzene ring is present in the 1,6-NDP core. However the photostability of the two kinds of monomers is quite different. It can be seen from Figure 4.21, the monomer based on 1,6-NDP is not stable in UV-light. After

16 min irradiation, the monomers exhibit no absorption anymore, while the solutions containing monomers based on 1,5-BDP still exhibit a strong absorption after 1 h of irradiation (see Chapter 3.2). It seems that the additional benzene ring of the 1,6-NDP core decreases the photostability of the 1,6-NDP monomer.

4.3.2 Polymers

Five polymers based on 1,6-NDP were prepared upon Suzuki and Stille coupling reactions in toluene, **1,6-NDP1** and **-2** were reacted with 9,9-di-n-octylfluorene-2,7-bis(trimethyleneborate) (**P-1,6-NDP-FL1** and **-2**), (4,8-bis(2-ethylhexyloxy)benzo[1,2-*b*:4,5-*b'*]dithiophene-2,6-diyl)-bis(trimethyl-stannane) (**P-1,6-NDF-BDT1** and **-2**), or 2,5-bis(trimethyl-stannane)thiophene (**P-1,6-NDP-Th**), the yields being 56-72 % (Scheme 4.8). Polymers show excellent solubility in common organic solvents such as toluene, dichlorobenzene and tetrahydrofuran. The weight-average molecular weights (M_w) of the polymers are between 9.6 and 25.6 kDa.



Scheme 4.8. Synthetic route to polymers based on 1,6-NDP.

UV/vis absorption of the polymers based on 1,6-NDP

The UV/vis absorption spectra of the polymers based on 1,6-NDP in solution and as thin film are displayed in Figure 4.22, and the optical data are listed in Table 4.7.

The five polymers exhibit a deep blue color in dichloromethane solution with maximum absorption between 603 and 666 nm. The absorption maxima of **P-1,6-NDP-BDT1** and **-2** in dichloromethane solution appear at 666 and 659 nm, respectively, the extinction coefficients of the strongest bands are $4.3 \cdot 10^4$ and $4.5 \cdot 10^4$ $\text{L mol}^{-1} \text{cm}^{-1}$ respectively. The absorption of the two polymers is red-shifted by around 90 nm compared with corresponding monomers. Broadening and red-shift of the

absorption bands originate from the extension of the π -conjugated system due to polymerization, and from D-A interactions between the 1,6-BDP and benzo[1,2-*b*:4,5-*b'*]dithiophene units enhancing intramolecular charge transfer (ICT). For **P-1,6-NDP-FL1** and **-2**, the absorption maxima in dichloromethane solution appear at 603 and 612 nm, respectively, which is about 50 nm blue shifted compared with **P-1,6-NDP1** and **-2**. This can be ascribed to the fluorene unit exhibiting a weak donor ability compared with the benzo[1,2-*b*:4,5-*b'*]dithiophene unit. The extinction coefficients of the strongest bands of **P-1,6-NDP-FL1** and **-2** are 8.6×10^4 and 8.8×10^4 L mol⁻¹ cm⁻¹, respectively. The absorptions of **P-1,6-NDP-FL1** and **-2** are red-shifted by about 30 nm compared with the polymers **1,6-NDP-BDT1** and **-2**. Broadening and red-shift of the absorption bands originate from the extension of the π -conjugated system due to polymerization. The absorption maximum of **P-1,6-NDP-Th** in dichloromethane solution appears at 615 nm, the extinction is 2.8×10^4 L mol⁻¹ cm⁻¹.

Table 4.7. Optical properties of polymers based on 1,6-NDP.

Polymers	$\lambda_{\text{abs,max}}/\text{nm}$		$\lambda_{\text{abs,onset}}/\text{nm}$	Optical band gap /eV	Extinct coeff ϵ (λ_{max}) [L mol ⁻¹ cm ⁻¹]
	solution	film			
P-1,6-NDP-BDT1	666	696	908	1.36	43521
P-1,6-NDP-BDT2	659	684	1100	1.13	45254
P-1,6-NDP-FL1	603	624	790	1.57	85625
P-1,6-NDP-FL2	612	639	805	1.54	87623
P-1,6-NDP-Th	615	678	1100	1.13	28456

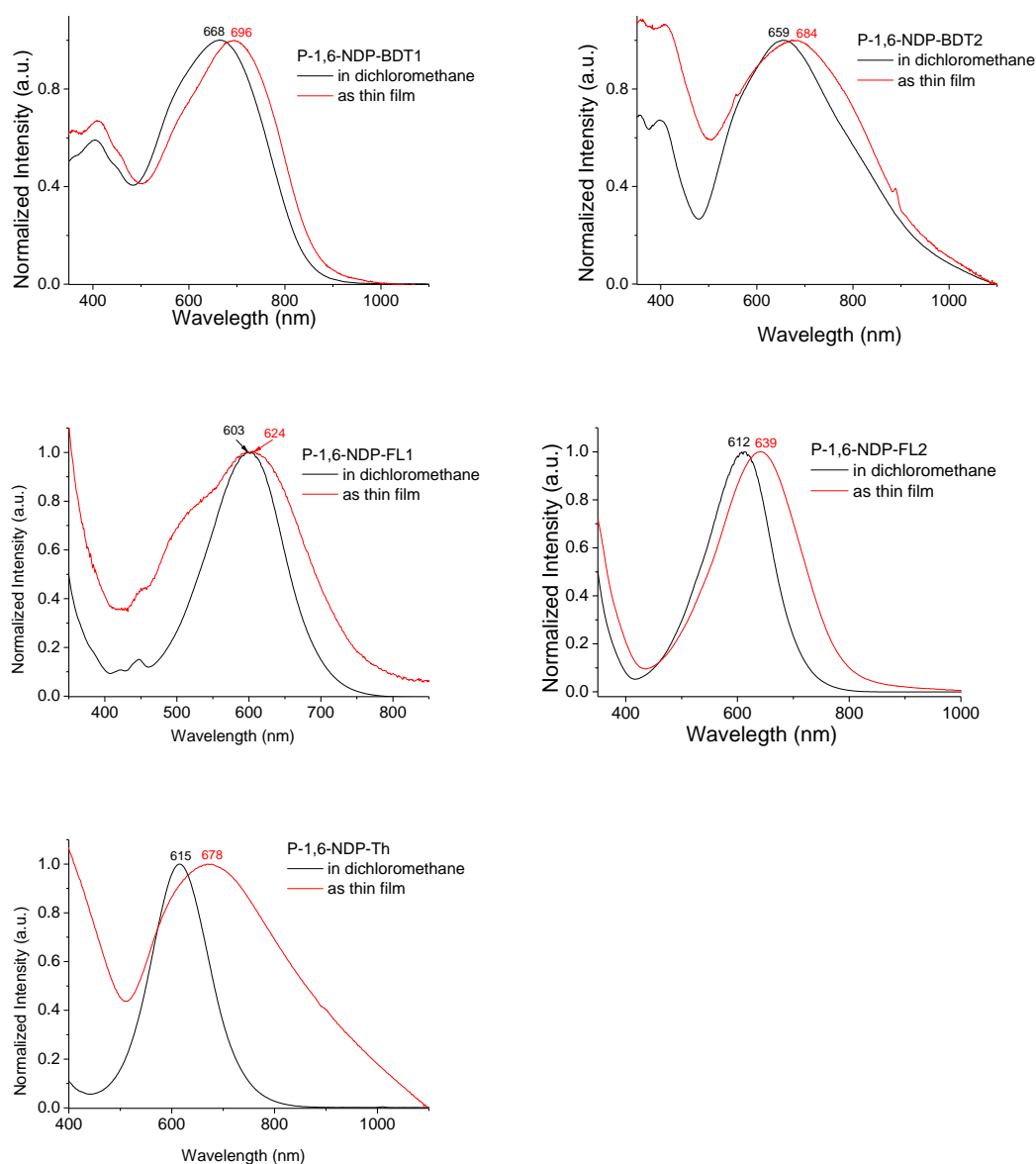


Figure 4.22. UV/vis absorption spectra of polymers based on 1,6-NDP in solution and as thin film.

The absorption maxima of the polymers as thin films are red-shifted compared to those in solution, the red-shift being 30 nm for **P-1,6-NDP-BDT1** and **-2**, 20 nm for **P-1,6-NDP-FL1** and **-2**, and 60 nm for **P-1,6-NDP-Th**, respectively, and the long-wavelength tail of the absorption bands is extended to the infrared. This

indicates a gain of planar conformation and/or the presence of π - π interchain association in the solid state. The absorption spectra of the polymers as thin films are quite broad and reach from 400 to 900 nm.

From the absorption edges of the polymers between 790 and 1100 nm, optical HOMO-LUMO gaps of 1.13 to 1.57 eV can be calculated. For comparison, the optical band gap of **P-1,6-NDP-BDT1** and **-2** and **P-1,6-NDP-Th** is smaller than for **P-1,6-NDP-FL1** and **-2**. This can be ascribed to the benzo[1,2-*b*:4,5-*b'*]dithiophene and thienyl units, which exhibit a more powerful donor ability than the fluorene unit.

Photostability of P-1,6-NDP-BDT2

The photostability of **P-1,6-NDP-BDT2** was measured using the same method as described previously. From Figure 4.23.a, one can see that **P-1,6-NDP-BDT2** is not very stable in toluene, if irradiated with UV light. The absorption spectrum decreases very quickly, and after 14 min the blue solution turns into colorless. Figure 4.23.c shows that **P-1,6-NDP-BDT2** is much more stable in the solid film state. We assume that the conjugated backbone of **P-1,6-NDP-BDT2** reacts with oxygen under formation of a colorless photoproduct. In densely packed films the photobleaching is much slower because the permeation of oxygen is strongly retarded. From Figure 4.23.b, one can see that the polymer is almost stable in the visible light. The absorption spectrum remains nearly unchanged after 3 h of irradiation through the 400nm edge-filter. We also compared the photostability of the polymer and relevant monomer. It seems that the polymer is more stable than the **1,6-NDP2**. This can be

ascribed to the extension of the π -system upon polymerization, and the D-A character of the system

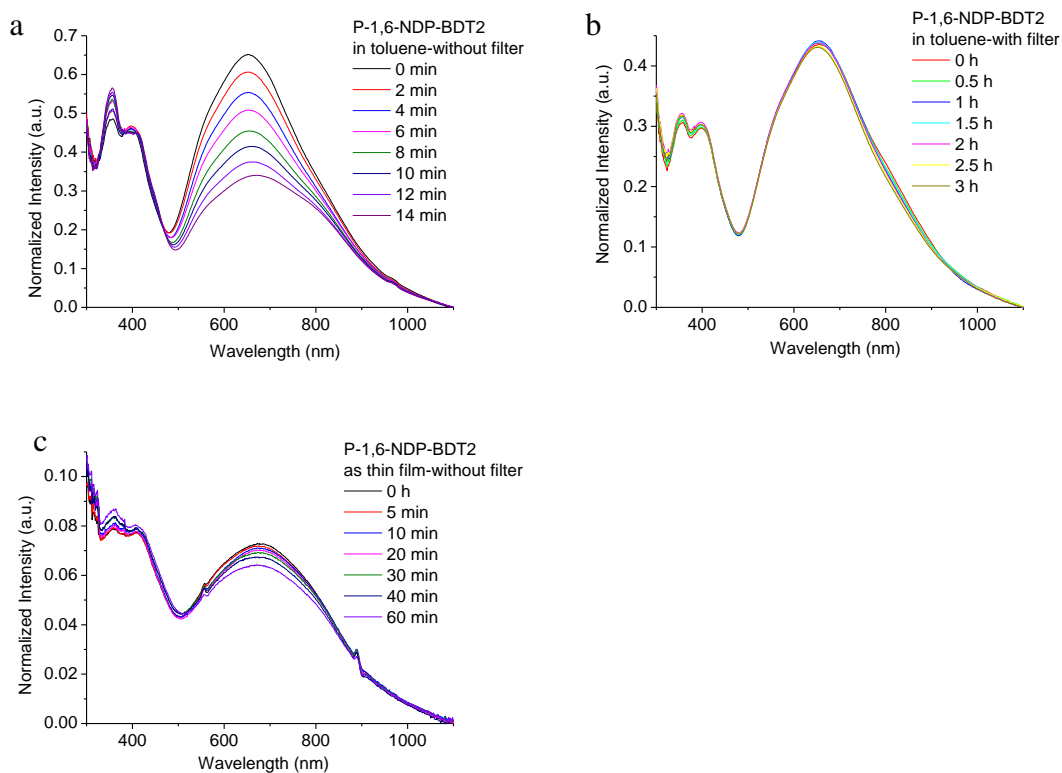


Figure 4.23. UV/Vis absorption spectra of **P-1,6-NDP-BDT2** before and after irradiation in toluene with a 200 W Hg-lamp with and without 400 nm edge filter, and as thin film without filter.

Electrochemical Properties

The electrochemical properties of the polymers based on 1,6-NDP were investigated using the same method as described previously. From Figure 4.24, it can be seen that the anodic oxidation of the polymers sets in at potentials between of 0.42 and 1.07 V.

For **P-1,6-NDP-BDT1** two anodic waves occur with maxima at 0.54 and 1.55 V, and for **P-1,6-NDP-BDT2** two waves occur at 0.74 and 1.31 V. This can be ascribed to formation of cation radicals and dications. The reductive cycles of **P-1,6-NDP-BDT1** and **-2** exhibit two reversible cathodic waves at -0.96 and -1.70 eV (**P-1,6-NDP-BDT1**), and -1.10, -2.36 eV (**P-1,6-NDP-BDT2**), which are reverted at -1.28, -0.76 eV (**P-1,6-NDP-BDT1**) and -1.63, -1.06 eV (**P-1,6-NDP-BDT2**). This originates from the reduction of the quinonoid to a benzoic structure, and also indicates a high stability of the anion radical, which can possibly be explained with a stabilizing negative charge at the oxygen atoms of the two carbonyl groups in the naphthodione units.

Table 4.8. Band gap data of polymers based on 1,6-NDP^a.

Polymer	Oxidation Onset [V] {HOMO [eV]}	Reduction Onset [V] {LUMO [eV]}	Electrochem Band Gap [eV]
P-1,6-NDP-BDT1	0.42 {-5.22}	-0.81 {-3.99}	1.23
P-1,6-NDP-BDT2	0.53 {-5.33}	-0.71 {-4.09}	1.24
P-1,6-NDP-FL1	0.96 {-5.76}	-0.29 {-4.51}	1.35
P-1,6-NDP-FL2	1.07 {-5.87}	-0.20 {-4.60}	1.27
P-1,6-NDP-Th	0.54 {-5.34}	-0.66 {-4.14}	1.20

^a HOMO-LUMO gap was calculated according to the equation $-E_{\text{LUMO}} = E_{\text{onset}(\text{red})} + 4.8 \text{ eV}$, and $-E_{\text{HOMO}} = E_{\text{onset}(\text{ox})} + 4.8 \text{ eV}$. $E_{\text{onset}(\text{ox})}$ and $E_{\text{onset}(\text{red})}$ are onset potentials for oxidation and reduction processes vs Fc/Fc⁺ couple.

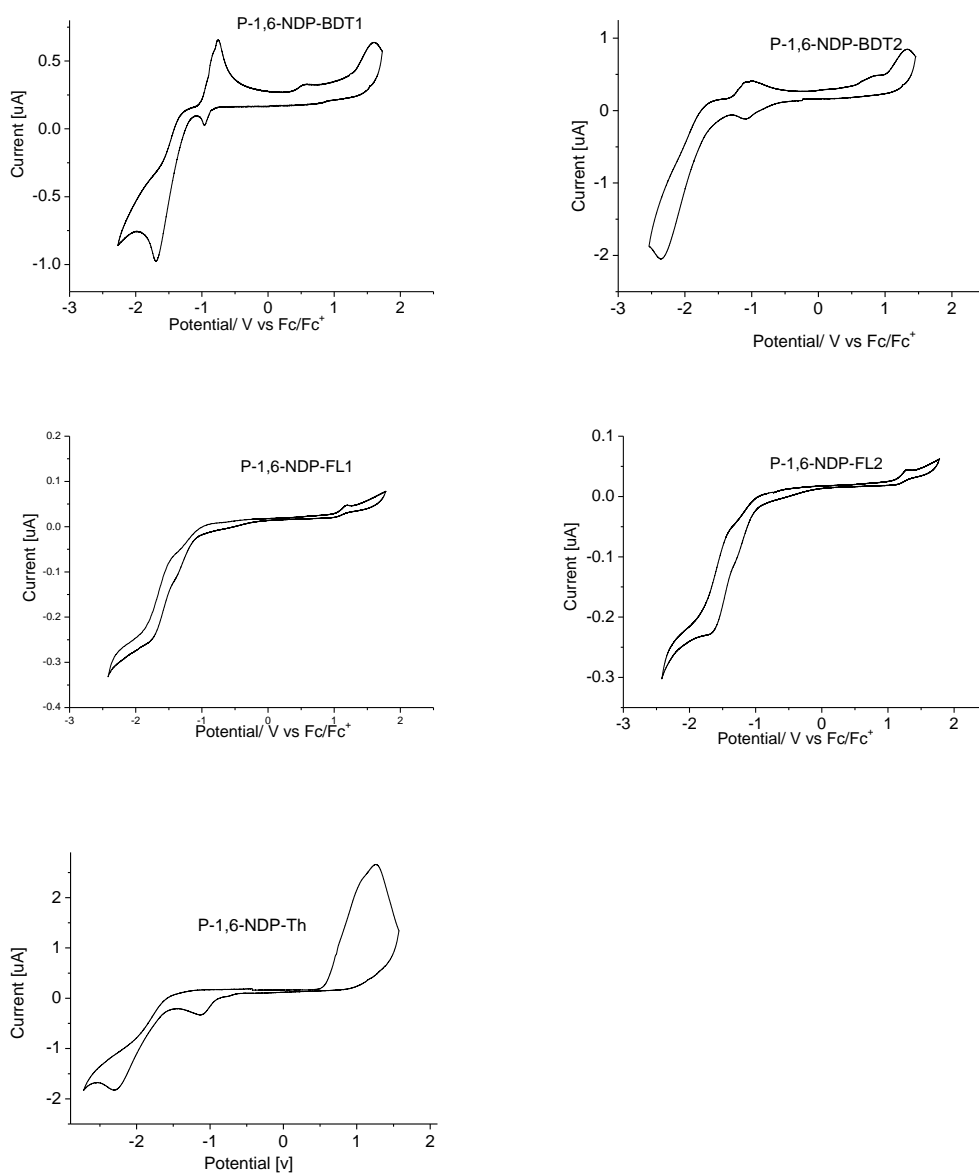


Figure 4.24. Cyclic voltammograms of polymers based on 1,6-NDP as thin films deposited on ITO. Solution: 0.1 M TBAPF₆/acetonitrile. Potential calculated versus ferrocene. Scan rate: 100 mV s⁻¹; T= 20 °C.

The oxidation and reduction behaviour of **P-1,6-NDF-FL1** and **-2** is reversible. **P-1,6-NDF-FL1** and **-2** show a quasi-reversible oxidation peak at 1.15 and 1.24 V, respectively, which can be ascribed to the formation of cation radicals and dications.

They are reverted at +1.44 V and 1.61 V. Significantly, the reductive cycle shows two reversible cathodic waves at -1.40/-1.02 V, -1.75/-1.02 V (**P-1,6-NDF-FL1**) and -1.29/-0.96 V, -1.66/-1.42 V (**P-1,6-NDF-FL2**) originating from the reduction of the quinonoid to a benzoid structure as described before.

For **P-1,6-NDP-Th**, one anodic wave with maximum at 1.25 V occurs, and two reversible cathodic waves at -1.13/-1.58 V and -2.28/-1.58 V. From the onset of the anodic and cathodic waves, the HOMO and LUMO values as well as the electrochemical band gaps were calculated (Table 4.8) The electrochemical band gap values of the polymers based on 1,6-NDP are between 1.20 and 1.35 eV. For **P-1,6-NDP-BDT1** and **-2** and **P-1,6-NDP-Th**, they are smaller than for **P-1,6-NDP-FL1** and **-2**. This can be ascribed to the benzo[1,2-*b*:4,5-*b'*]dithiophene and thienyl units, which exhibit a more powerful donor ability compared with the fluorene unit.

4.4 Conclusion

In this chapter new naphthodione monomers and relevant π -conjugated polymers have been designed, synthesized, and characterized. The first single crystal structures of a **1,10-NDF** and **1,6-NDP2** derivative are reported. The two monomers exhibit a weak π - π stacking with a distance of 3.36 Å and 3.38 Å between the NDF or NDP cores, respectively. The monomers based on naphthodione exhibit yellow to purple and blue colours with high extinction coefficients up to $1.0 \times 10^5 \text{ L mol}^{-1} \text{ cm}^{-1}$ (**1,6-NDF3**). This makes renders the naphthodione-based monomers useful as colourants, in dyes and inks.

The polymers were obtained upon Suzuki and Stille coupling and exhibit red to blue and green colours with high extinction coefficients up to $8.8 \times 10^4 \text{ L mol}^{-1} \text{ cm}^{-1}$ (**P-1,6-NDP-FL2**). The polymers exhibit low band gaps down to 1.20 eV, (**P-1,6-NDP-Th**) and broad absorption bands ranging from 400 to 1000 nm with high extinction coefficients. This well matches the solar photon most intense flux. Due to their interesting electronic and optical properties, in addition to the planar structure, naphthodiones are promising building blocks for the development of novel π -conjugated polymers for optoelectronic applications.

5 Experimental Part

5.1 Materials

Chemicals for preparative and analytical procedures were purchased from the chemical suppliers Sigma-Aldrich, Alfa Aesar, Acros and Zhongsheng Huateng and used without further purification. Monomeric isoDPP was kindly provided by Irina Welterlich. The purification of solvents such as DCM, chloroform, methanol, ethanol and so on was carried out according to literature procedures.¹¹²

5.2 Instrumentation and general procedures

UV/vis absorption spectra were recorded on a Perkin-Elmer Lambda 14 spectrometer using quartz cuvettes (thickness 1 cm) and solvents of spectroscopic grade. Samples in the solid state were measured on quartz substrates.

Photoluminescence spectra were recorded on a Perkin-Elmer LS50B spectrometer under the same conditions as for the UV/vis measurements.

The photostability was recorded using a 200 W Hg lamp with and without 400 nm edge filter (Oriel Instruments 6283) at a distance of 20 cm at room temperature.

¹H-NMR spectra were recorded using Bruker DPX 300 and 500 spectrometers, which operate at 300 MHz.

Molecular weights were determined upon size exclusion chromatography (SEC) using a Water/Millipore UV detector 481 and a mixed gel column (Latek/Styragel 50/1000nm pore size). All measurements were carried out in tetrahydrofuran at 45 °C. The column was calibrated using commercially available polystyrene standards.

Cyclic voltammograms were recorded using a potentiostat PG 390 from Heka Company. Thin films of the polymers were cast on an ITO electrode and cycled in acetonitrile (saturated with nitrogen) containing 0.1 M tetrabutylammonium hexafluorophosphate (TBAPF₆) as electrolyte salt. Reference and counter electrodes were platinum. The voltage data were calculated for the ferrocene/ferrocenium redox couple. The scan rate was 100 mV s⁻¹, the temperature was 20 °C.

Elemental analyses were obtained using a Perkin-Elmer 2400 elemental analyzer.

The single crystal structures were determined with a Nonius Kappa CCD-Diffractometer Mo-K_α ($\lambda=0.71073$ Å) controlled by COLLECT (Nonius). The structures were solved using Shelx197 and refined by Shelx197.

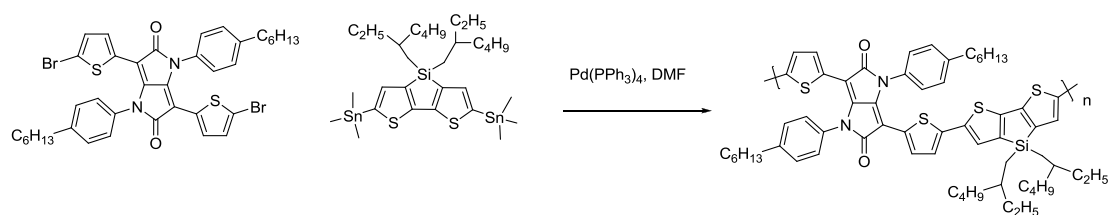
Differential scanning calorimetry (DSC) and thermogravimetric analysis (TGA) were performed under a nitrogen atmosphere (50 ml min⁻¹) using a NETZSCH 2041F1 and a NETZSCH 209F1. DSC and TGA traces were determined at heating rates of 10 °C min⁻¹ (DSC) and 20 °C min⁻¹ (TGA), respectively.

Electronic structures, HOMOs and LUMOs were calculated with Gaussian 03¹¹² using the density functional theory B3LYP/6-31+G(d,p).

5.3 Synthesis

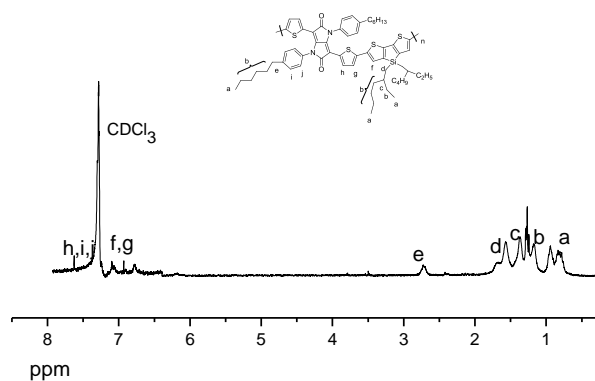
5.3.1 Conjugated polymers based on isoDPP

Polymer P-isoDPP-DTS

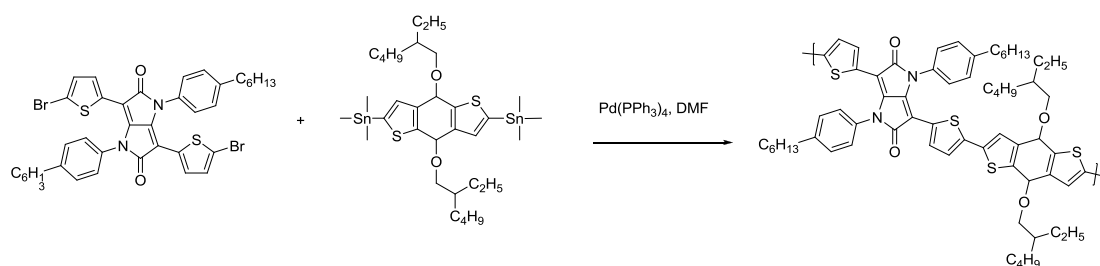


In a Schlenk flask, **isoDPP** (0.2 g, 0.26 mmol), 4,4'-bis(2-ethylhexyl)-5,5'-bis(trimethyltin)dithieno[3,2-b:2',3'-d]silole (0.19 g, 0.26 mmol) and tetrakis(triphenylphosphine)palladium(0) (12.3 mg, 0.01 mmol) were dissolved in dry DMF (10 ml). Then the mixture was heated and kept at 100 °C under nitrogen for 18 hours. Then the reactant was cooled to room temperature, and the polymer was precipitated by adding 50 ml methanol filtered, and subjected to Soxhlet extraction with methanol and hexane. The polymer was dried under vacuum for one day and was obtained as dark solid. (0.17 g, yield: 64 %). Molecular weight (GPC, THF): $M_w = 14.8$ kDa, $M_n = 8.5$ kDa, PD = 1.74. ¹H-NMR (300 MHz, d₁-CHCl₃) δ ppm:

7.25-7.41 (br, 6H), 6.63-7.17 (br, 4H), 2.65-2.76 (br, 4H), 1.69 (s, 4H), 1.35 (s, 2H), 1.15-1.20 (br, 16H), 0.70-0.98 (br, 18H). UV/Vis (DCM): 587 nm; ϵ (587) = 64887 L mol⁻¹ cm⁻¹. PL (DCM): 744 nm (excitation at 450 nm); PL quantum yield Φ_f : 0.13 %.

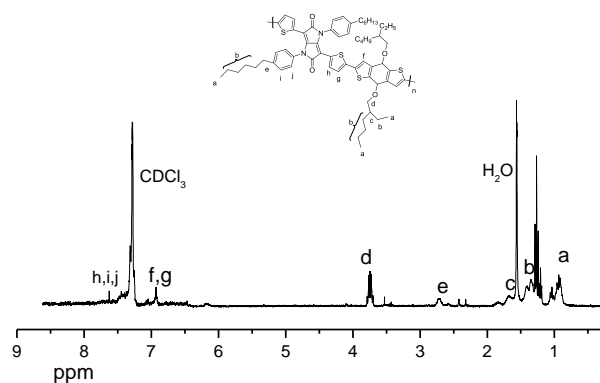


Polymer P-isoDPP-BDT



In a Schlenk flask, **isoDPP** (0.2 g, 0.26 mmol), (4,8-bis(2-ethylhexyloxy)benzo[1,2-*b*:4,5-*b*]dithiophene-2,6-diyl)bis(trimethylstannane) (0.19 g, 0.26 mmol) and tetrakis(triphenylphosphine)palladium(0) (12.3 mg,

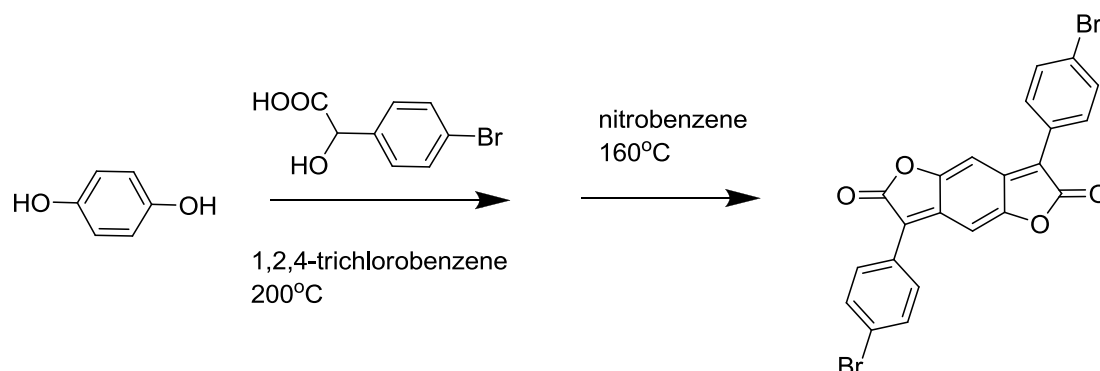
0.01 mmol) were dissolved in dry DMF (10 ml). Then the mixture was heated and kept at 100 °C under nitrogen for 18 hours. Then the reactant was cooled to room temperature, and the polymer was precipitated by adding 50 ml methanol, filtered, then subjected to Soxhlet extraction with methanol and hexane. The polymer was dried under vacuum for one day and was obtained as dark solid. (0.18 g, yield: 62 %). $M_w = 5.7$ kDa, $M_n = 3.8$ kD, PD = 1.50. $^1\text{H-NMR}$ (300 MHz, $\text{d}_1\text{-CHCl}_3$) δ ppm: 7.25-7.70 (br, 6H), 6.61-7.12 (br, 4H), 3.69-3.79 (m, 4H), 2.65-2.76 (br, 4H), 1.61-1.77 (br, 2H), 1.19-1.47 (br, 16H), 0.87-1.08 (br, 18H). UV/vis (DCM): 502 nm; ϵ (502) = 26485 $\text{L mol}^{-1} \text{cm}^{-1}$. PL (DCM): 680 nm (excitation at 450 nm); PL quantum yield Φ_f : 0.82 %.



5.3.2 Conjugated polymers based on benzodiones

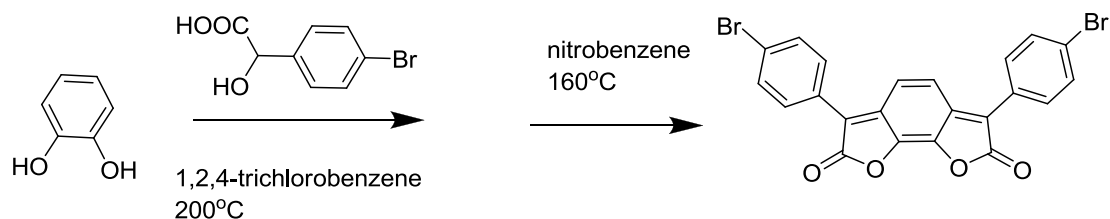
5.3.2.1 Conjugated polymers based on amino-benzodiones via Buchwald-Hartwig amination

3,7-Bis(4-bromophenyl)benzo[1,2-b:4,5-b']difuran-2,6-dione (1,5-BDF)



Using a Dean Stark apparatus, hydroquinone (1.0 g, 8.09 mmol) and 4-bromo-mandelic acid (4.1 g, 17.8 mmol) were dissolved in 1,2,4-trichlorobenzene (25 ml) and stirred for 6 h at 200 °C. After cooling to 100 °C, nitrobenzene (2.3 ml) was added and the mixture was stirred for another hour at 160 °C. After cooling to room temperature, 50 ml methanol were added. A precipitate formed, which was filtered off, washed with methanol and dried in air. The title compound was obtained as a dark greenish solid (2.75 g, yield: 68%), which was only little soluble in common solvents at room temperature. Microanalysis found C, 53.25 %, H, 1.92% (C, 53.05 %; H, 2.02 %). Solubility is not enough to measure NMR.

3,6-Bis(4-bromophenyl)benzo[1,2-b:6,5-b']difuran-2,7-dione (1,8-BDF)

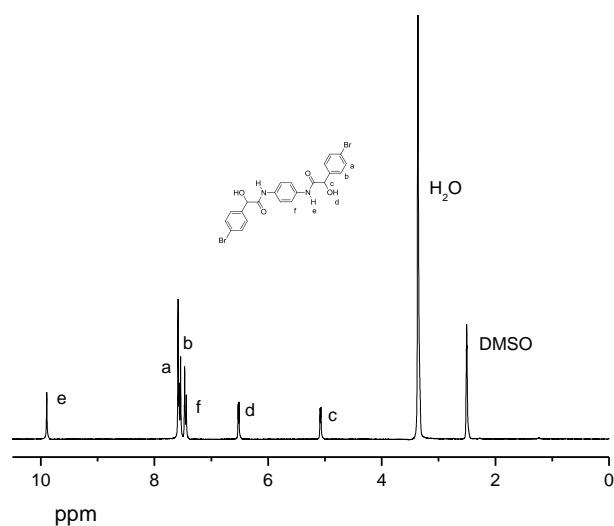


Using a Dean Stark apparatus, catechol (1.0 g, 8.09 mmol) and 4-bromo-mandelic acid (4.1 g, 17.8 mmol) were dissolved in 1,2,4-trichlorobenzene (25 ml) and stirred for 6 h at 200 °C. After cooling to 100 °C, nitrobenzene (2.3 ml) was added and the mixture was stirred for another hour at 160 °C. After cooling to room temperature, 50 ml methanol were added. A precipitate formed, which was filtered off, washed with methanol and dried in air. The title compound was obtained as a dark greenish solid (1.56 g, yield: 39%), which was only little soluble in common solvents at room temperature. Microanalysis found C, 52.98 %, H, 2.13% (C, 53.05 %; H, 2.02 %). Solubility is not enough to measure NMR.

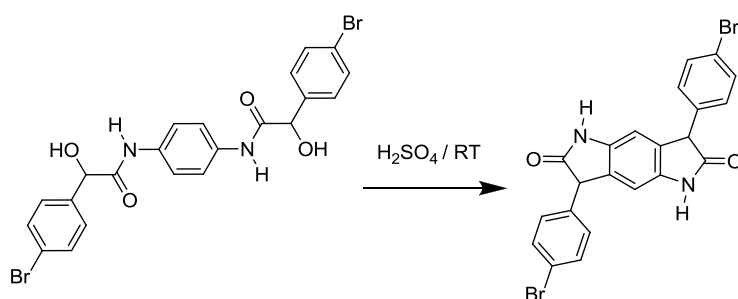
1,4-Bis(α -hydroxy(4-bromophenyl)acetyl)amino)benzene



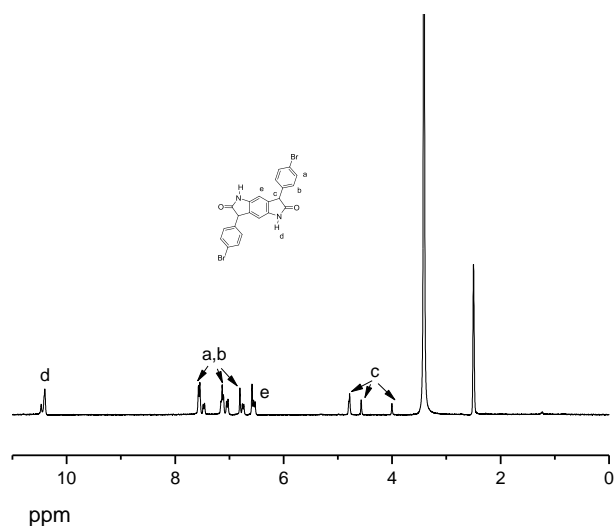
p-Phenylenediamine (0.94 g, 8.7 mmol) and 4-bromomandelic acid (6.00 g, 26.0 mmol) were dissolved in 16 mL chlorobenzene. The reaction mixture was heated at 130 °C for 20 h. After the reaction was complete, the milky suspension was filtered and washed several times with ethanol and dried in air. The title compound was obtained as a white powder (3.96 g, yield: 85.2 %). ¹H-NMR (300 MHz, DMSO) δ ppm: 9.89 (s, 2 H); 7.58 (s, 4 H); 7.55 (d, *J*= 8.5 Hz, 4 H); 7.45 (d, *J*= 8.5 Hz, 4 H); 6.52 (d, *J*= 4.7 Hz, 2 H); 5.07 (d, *J*= 4.6 Hz, 2 H).



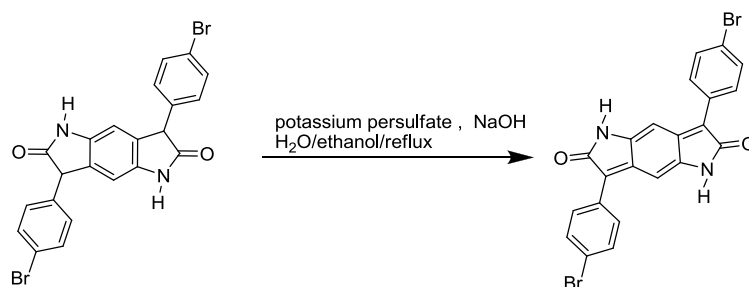
3,7-Di(4-bromophenyl)-2,6-dioxo-1,2,3,4,5,6,7-hexahydrobenzo-[1,2-*b*:4,5-*b'*]-dipyrrole



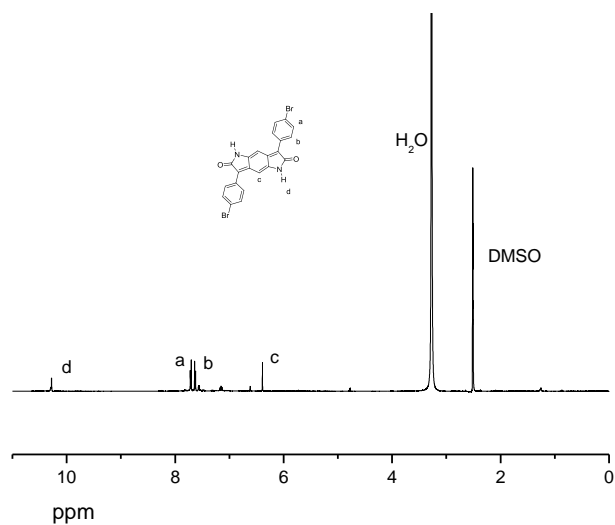
1,4-Bis(α -hydroxy(4-bromophenyl)acetyl-amino)benzene (3.96 g, 7.4 mmol) was added to concentrated sulfuric acid (32 ml). The resulting suspension was allowed to stir for 24 h at room temperature. After the reaction was completed, the mixture was poured into ice water (100 ml). The precipitate was filtered, washed with water and dried to yield the title compound as a light pink solid (3.59 g, yield: 97%). $^1\text{H-NMR}$ (300 MHz, DMSO) δ ppm: 10.33-10.57 (m, 2 H); 7.41-7.62 (m, 3 H); 7.00-7.19 (m, 3 H); 6.66-6.90 (m, 2 H); 6.46-6.64 (m, 2H); 4.74-4.83 (m, 1 H); 4.00-4.59 (m, 1 H).



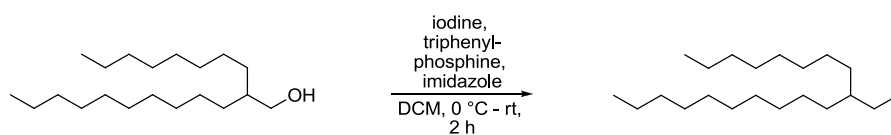
3,7-Di(4-bromophenyl)-2,6-dioxo-1,2,5,6-tetrahydrobenzo[1,2-*b*:4,5-*b'*]dipyrrole



3,7-Di(4-bromophenyl)-2,6-dioxo-1,2,3,4,5,6,7-hexahydrobenzo-[1,2-*b*:4,5-*b'*]-dipyrrole (3.59 g, 7.2 mmol) was suspended in ethanol (22 ml). Then 5 N sodium hydroxide solution (2.7 ml, 13.5 mmol) was dropwise added to the mixture. The colour of the light pink suspension turned to brown. After that potassium persulfate (5.26 g, 19.4 mmol) in water (18 ml) was added. The mixture was heated at reflux for 3 h. After the reaction was complete, the precipitate was filtered, and washed 5 times with water and ethanol. The product was obtained as a dark brown powder (2.39 g, yield: 66%) ¹H-NMR (500 MHz, DMSO, 70 °C) δ ppm: 10.18 (s, 2 H); 7.69 (d, *J*= 8.6 Hz, 4 H); 7.62 (d, *J*= 8.6 Hz, 4 H); 6.39 (s, 2 H).



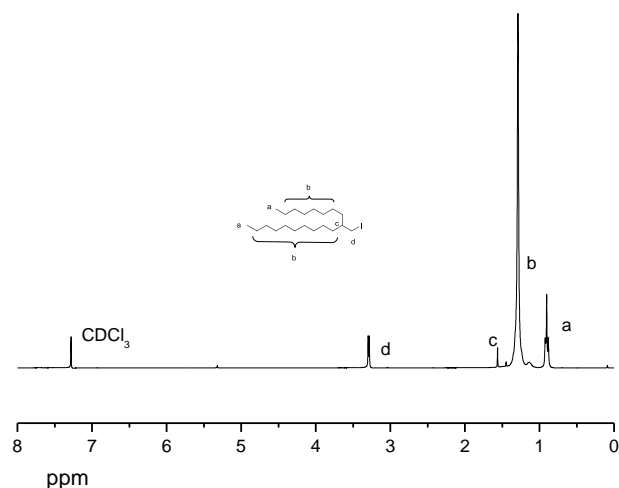
1-Iodo-2-octyldodecane



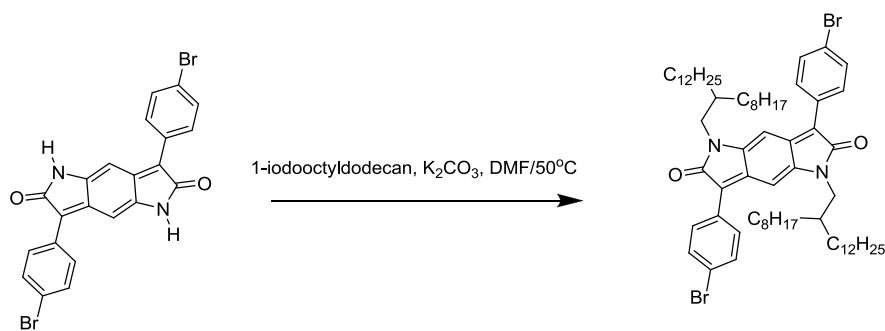
2-Octyl-1-dodecanol (6.2 g, 20.8 mmol), triphenylphosphine (6.53 g, 24.9 mmol) and imidazole (1.69 g, 24.9 mmol) were dissolved in dichloromethane (40 ml). The clear solution was cooled down to 0 °C and iodine (6.32 g, 24.9 mmol) was slowly added to the solution. After stirring for 15 min at this temperature, the reaction mixture was allowed to warm up to room temperature over 2 h. The reaction was quenched with 10 ml aqueous saturated sodium sulfite to reduce excess iodine. The solvent was removed by rotary evaporation. Then the mixture was dissolved in 200 mL *n*-hexane, washed three times with 100 mL of water and once with 70 mL of brine. The raw product was passed through a 3 cm silica gel plug and dried over anhydrous

magnesium sulfate. After filtration the solvent was removed by rotary evaporation.

The title product was obtained as colorless oil (8.01 g, yield: 94%). ¹H-NMR (300 MHz, d₁-CHCl₃) δ ppm: 3.27 (d, *J*= 4.5 Hz, 2 H); 1.17-1.38 (m, 33 H); 0.88 (t, 6 H).



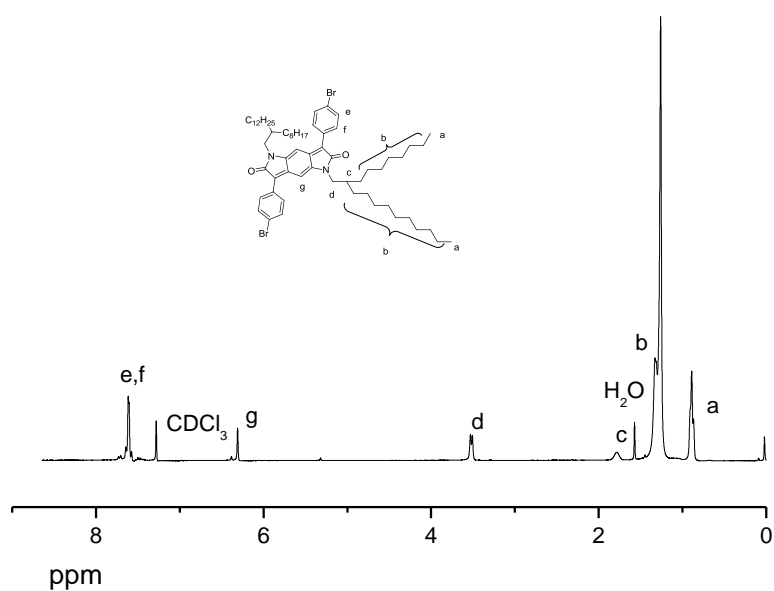
***N,N'*-Di(2-octyldodecyl)-3,7-di(4-bromophenyl)-2,6-dioxo-1,2,5,6-tetrahydrobenzo[1,2-*b*:4,5-*b'*]dipyrrole (1,5-BDP-1)**



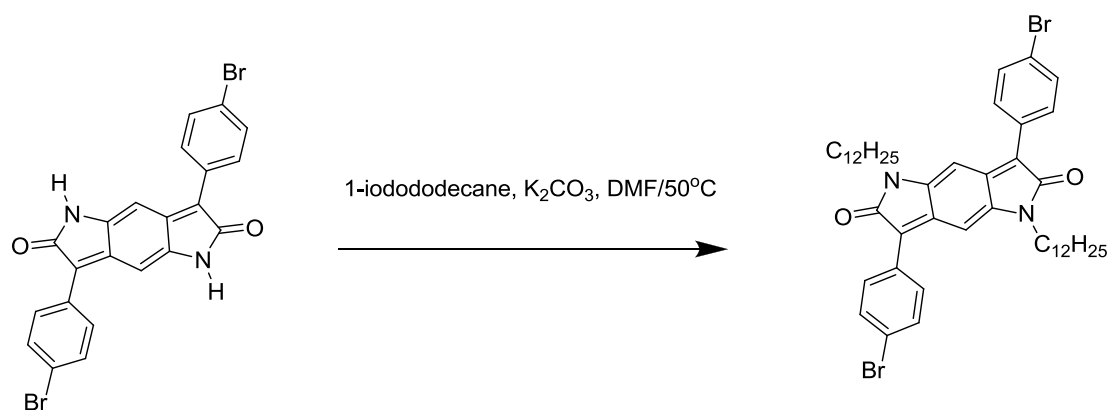
3,7-Di(4-bromophenyl)-2,6-dioxo-1,2,5,6-tetrahydrobenzo[1,2-*b*:4,5-*b'*]dipyrrole (1.5 g, 3.0 mmol) and K₂CO₃ (2.226 g, 21.0 mmol) were dissolved in dry DMF (15 ml).

Then 1-iodo-2-octyldodecane (4.9 g, 12.0 mol) was added. The mixture was stirred

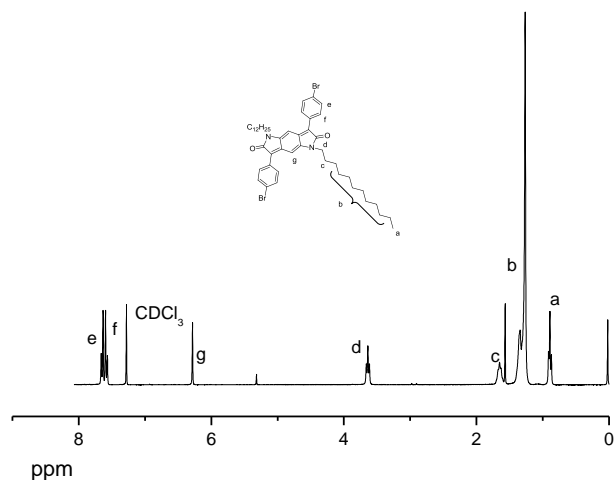
for 24 h at 80 °C. After the reaction was complete, the dark brown solution was treated with DCM, washed three times with water and once with brine. Then the organic layer was dried over anhydrous magnesium sulfate and the solvent was removed at reduced pressure. The raw product was obtained as a dark brown oil and purified by column chromatography (Hexane:DCM = 1:2) on silica gel. After that the crude product was precipitated in methanol. The monomer 1,5-BDP-1 was obtained as a dark brown solid (1.49 g, yield: 47 %). $^1\text{H-NMR}$ (300 MHz, $\text{d}_1\text{-CHCl}_3$) δ ppm: 7.43-7.75 (m, 8 H); 6.29 (s, 2 H); 3.61-3.66 (t, 4 H); 1.76 (s, 2 H); 1.16-1.31 (m, 64 H), 0.87 (t, $J= 6.3$ Hz, 12 H).



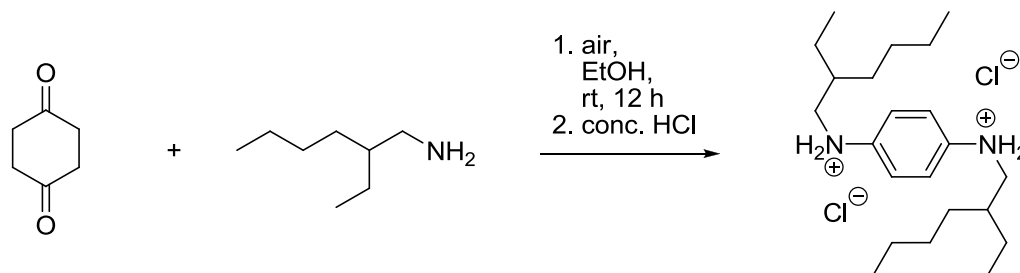
***N,N'*-Di(*n*-dodecyl)-3,7-di(4-bromophenyl)-2,6-dioxo-1,2,5,6-tetrahydrobenzo[1,2-*b*:4,5-*b'*]dipyrrole (1,5-BDP-1)**



3,7-Di(4-bromophenyl)-2,6-dioxo-1,2,5,6-tetrahydrobenzo[1,2-*b*:4,5-*b'*]dipyrrole (1.5 g, 3.0 mmol) and K_2CO_3 (2.226 g, 21.0 mmol) were dissolved in dry DMF (15 ml). Then 1-iodo-2-octyldodecane (3.55 g, 12.0 mol) was added. The mixture was stirred for 24 h at 80 °C. After the reaction was complete, the dark brown solution was treated with DCM, washed three times with water and once with brine. Then the organic layer was dried over anhydrous magnesium sulfate and the solvent was removed at reduced pressure. The raw product was obtained as a dark brown oil and was purified by column chromatography (Hexane:DCM = 1:2) on silica gel. After that the crude product was precipitated in methanol. The monomer **1,5-BDP-2** was obtained as a dark brown solid (1.62 g, yield: 64 %). 1H -NMR (300 MHz, d_1 - $CHCl_3$) δ ppm: 7.64 (d, $J=8.4$ Hz, 4 H); 7.57 (d, $J=8.7$ Hz, 4 H); 6.28 (s, 2 H); 3.61-3.66 (t, 4 H); 1.65 (s, 4 H), 1.21-1.28 (br, 28 H); 0.86-0.91 (t, $J= 6.3$ Hz, 6 H).

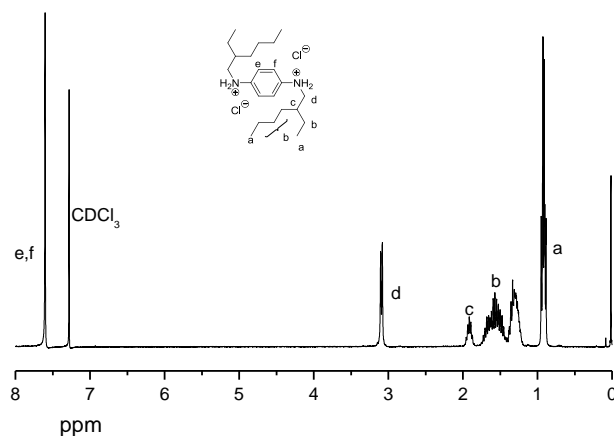


***N,N*-bis(2-ethylhexyl)benzene-1,4-diamine dihydrochloride salt**

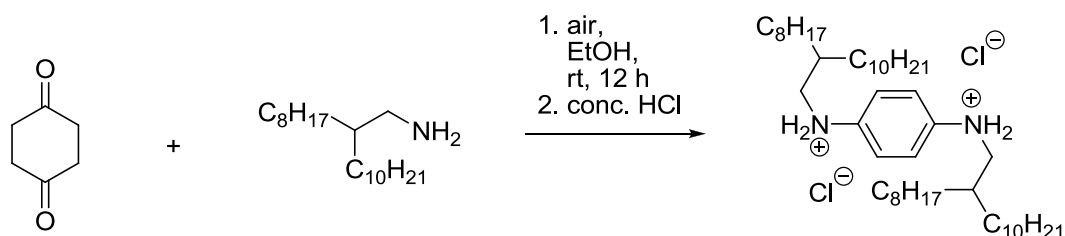


1,4-Cyclohexanedione (1.4 g, 12.5 mmol) and 2-ethylhexyl amine (5.98 ml, 37.5 mmol) were dissolved in ethanol (125 ml). The reaction mixture was stirred at room temperature with air bubbling through the solution for 4 h. After the reaction complete, the solvent was removed under reduced pressure. The raw product as a black oil was dissolved in acetone (12 ml) and concentrated hydrochloric acid (4 ml) was added to form the dihydrochloride salt. The salt was filtered and washed several times with acetone. The title product was obtained as white crystals (0.81 g, yield: 60%).

$^1\text{H-NMR}$ (500 MHz, $\text{d}_1\text{-CHCl}_3$) δ ppm: 7.58 (s, 4H); 3.03-3.12 (m, 4 H), 1.85-1.94 (m, 2 H); 1.41-1.67 (m, 16 H); 0.90 (t, 12 H).

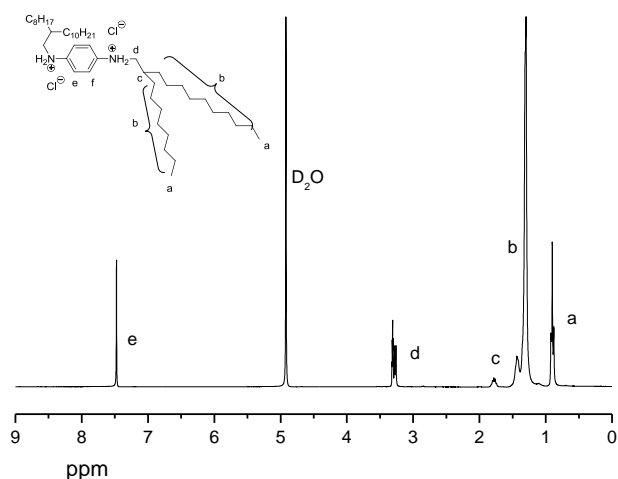


***N,N*-bis(2-ethylhexyl)benzene-1,4-diamine dihydrochloride salt**

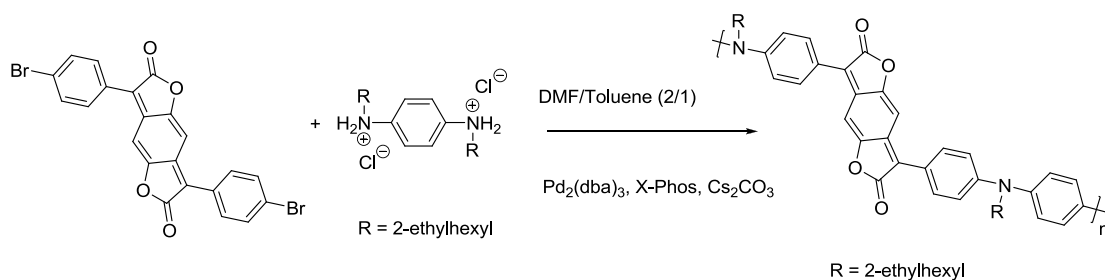


1,4-Cyclohexanedione (1.4 g, 12.5 mmol) and 2-ethylhexyl amine (11.2 g, 37.5 mmol) were dissolved in ethanol (125 ml). The reaction mixture was stirred at room temperature with air bubbling through the solution for 4 h. After the reaction complete, the solvent was removed under reduced pressure. The raw product was obtained as a black oil was dissolved in acetone (12 ml), and concentrated hydrochloric acid (4 ml) was added to form the dihydrochloride salt. The salt was filtered and washed several

times with acetone. The titled product was obtained as white crystals (2.32 g, yield: 25%). $^1\text{H-NMR}$ (300 MHz, D_2O) δ ppm: 7.48 (s, 4 H); 3.26-3.31 (m, 4 H), 1.76-1.80 (s, 2 H); 1.21-1.43 (m, 64 H); 0.87-0.92 (t, 12 H).

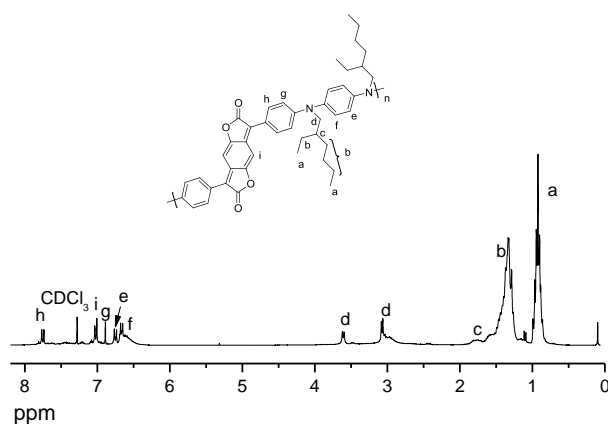


Polymer P-A-1,5-NDP-1

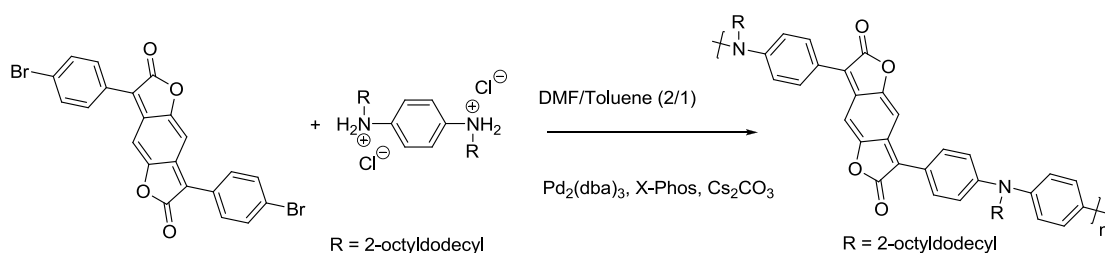


In a Schlenk flask, 3,7-bis(4-bromophenyl)benzo[1,2-b:4,5-b']difuran-2,6-dione (214 mg, 0.43 mmol), *N,N*-bis(2-ethylhexyl)benzene-1,4-diamine dihydrochloride salt (175 mg, 0.43 mmol), $\text{Pd}_2(\text{dba})_3$ (11.9 mg, 0.015 mmol) and X-Phos (39.2 mg, 0.082 mmol) were dissolved in a mixture of DMF/toluene (2:1) (6 ml) under nitrogen.

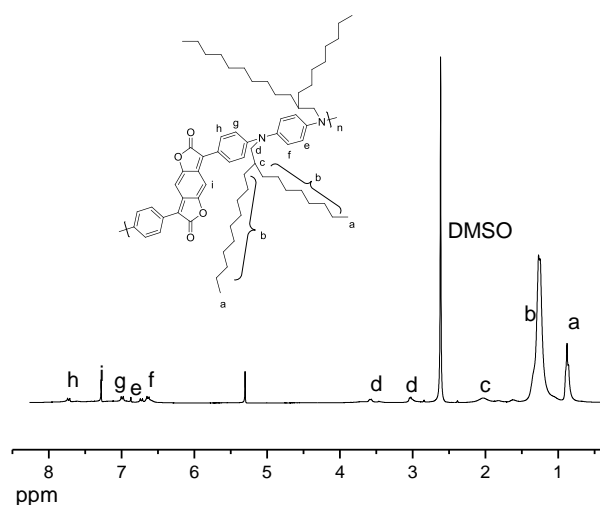
Then cesium carbonate (310 mg, 0.95 mmol) was added and the mixture was allowed to stir for 48 hours under nitrogen at 90 °C. After completion of the reaction, the dark blue solution was treated with DCM, washed three times with water and once with brine. Then the organic layer was dried over anhydrous magnesium sulfate, and the solvent was removed at reduced pressure. Subsequently the crude product is dissolved in a minimal amount of DCM and precipitated in methanol. The product was obtained as a dark solid (181.2 mg, yield: 63 %). Molecular weight (GPC, THF): $M_w = 5.7$ kDa, $M_n = 3.8$ kDa, PD = 1.5. UV/vis (DCM): 709 nm, UV/Vis (thin film): 724 nm;; ϵ (709) = 16721 L mol⁻¹ cm⁻¹.



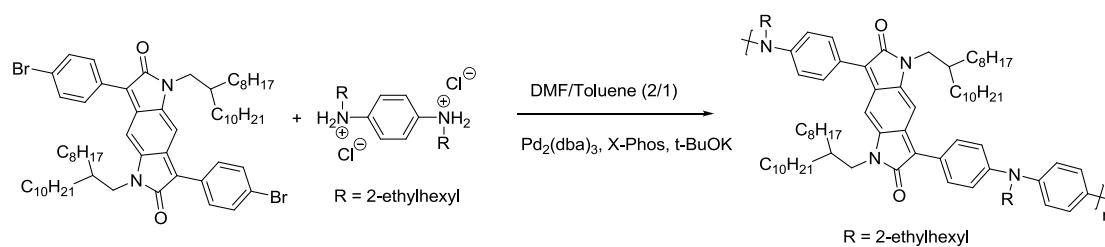
Polymer P-A-1,5-NDP-2



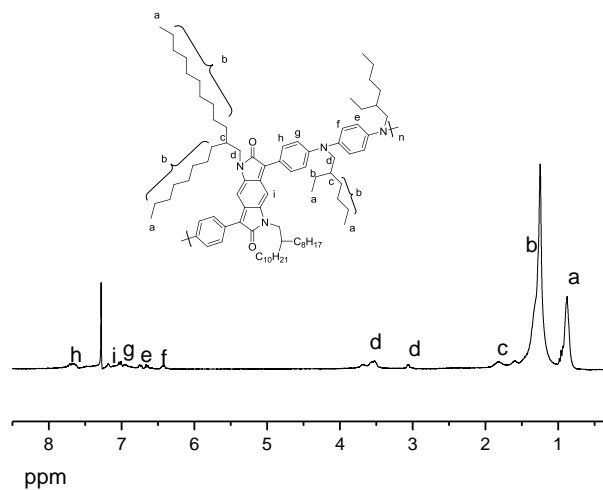
In a Schlenk flask, 3,7-bis(4-bromophenyl)benzo[1,2-b:4,5-b']difuran-2,6-dione (137.6 mg, 0.28 mmol), *N,N*-bis(2-octyldodecyl)benzene-1,4-diamine dihydrochloride salt (205 mg, 0.28 mmol), Pd₂(dba)₃ (7.6 mg, 0.008 mmol) and X-Phos (25 mg, 0.053 mmol) were dissolved in a mixture of DMF/toluene (2:1) (3.2 ml) under nitrogen. Then cesium carbonate (198 mg, 0.60 mmol) was added and the mixture was allowed to stir for 48 hours under nitrogen at 90 °C. After completion of the reaction, the dark solution was treated with DCM, washed three times with water and once with brine. Then the organic layer was dried over anhydrous magnesium sulfate and the solvent was removed at reduced pressure. Subsequently the crude product was dissolved in a minimal amount of DCM and precipitated in methanol. The product was obtained as a dark blue solid (156.5 mg, yield: 54 %). Molecular weight (GPC, THF): *M_w* = 9.7 kDa, *M_n* = 5.7 kDa, PD = 1.7 UV/Vis (DCM): 725 nm, UV/Vis (thin film): 741 nm; ε (725) = 23911 L mol⁻¹ cm⁻¹.



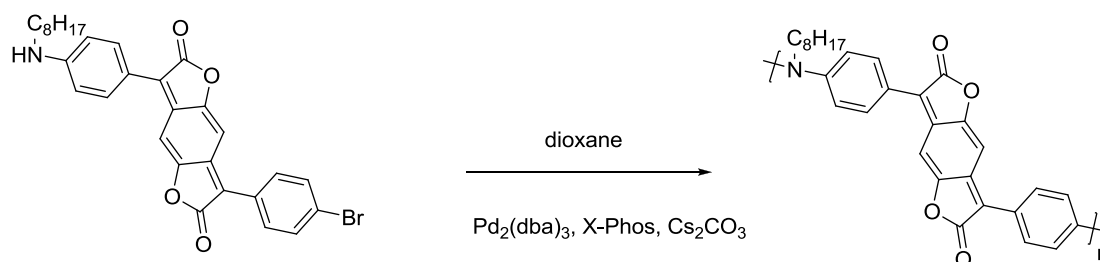
Polymer P-A-1,5-BDP



In a Schlenk flask, *N,N'*-di(2-octyldodecyl)-3,7-di(4-bromophenyl)-2,6-dioxo-1,2,5,6-tetrahydrobenzo[1,2-b:4,5-b']dipyrrole (100.0 mg, 0.095 mmol), *N,N*-bis(2-ethylhexyl)benzene-1,4-diamine dihydrochloride salt (38.4 mg, 0.095 mmol), Pd₂(dba)₃ (2.6 mg, 0.029 mmol) and X-Phos (8.2 mg, 0.017 mmol) were dissolved in dry toluene (3 ml) under nitrogen. Then *t*-BuOK (45 mg, 0.44 mmol) was added and the mixture is allowed to stir for 24 hours under nitrogen at 90 °C. After completion of the reaction, the dark blue solution is treated with DCM, washed three times with water and once with brine. Then the organic layer was dried over anhydrous magnesium sulfate and the solvent was removed at reduced pressure. After that, the crude product was dissolved in a minimal amount of DCM and precipitated in methanol. The product was obtained as a dark blue solid (65.7 mg, yield: 57 %). Molecular weight (GPC, THF): $M_w = 10.1$ kDa, $M_n = 6.8$ kDa, PD = 1.5 UV/Vis (DCM): 623 nm, UV/Vis (thin film): 638 nm;; ϵ (623) = 26762 L mol⁻¹ cm⁻¹.



Polymer P-A-1,5-BDF

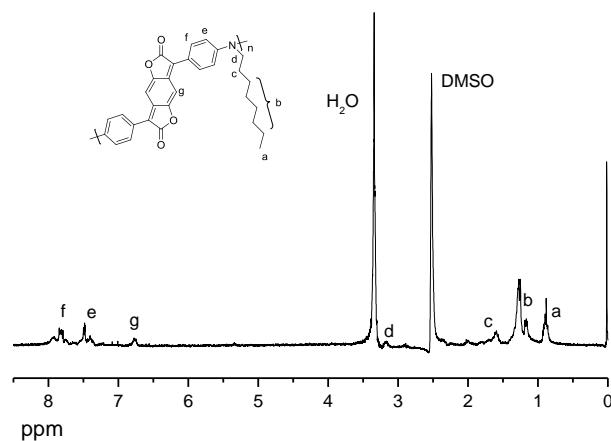


In a Schlenk flask, 3-(4-bromophenyl)-7-(*N*-octylaminophenyl)-benzo[1,2-*b*:4,5-*b'*]-difuran-2,6-dione (**ABDF**, 300 mg, 0.55 mmol), *N,N'*-dioctyl-*p*-phenylenediamine dihydrochloride salt (350 mg, 0.86 mmol), potassium phosphate (584 mg, 2.75 mmol), Pd₂(dba)₃ (15.1 mg, 0.016 mmol) and X-Phos (50 mg, 0.11 mmol) were dissolved in dioxane (6 ml) under nitrogen. The mixture was heated to 100 °C and stirred for 40 hours under nitrogen. After cooling to room temperature, water was added in order to precipitate the product. The precipitate was filtered off and washed with methanol.

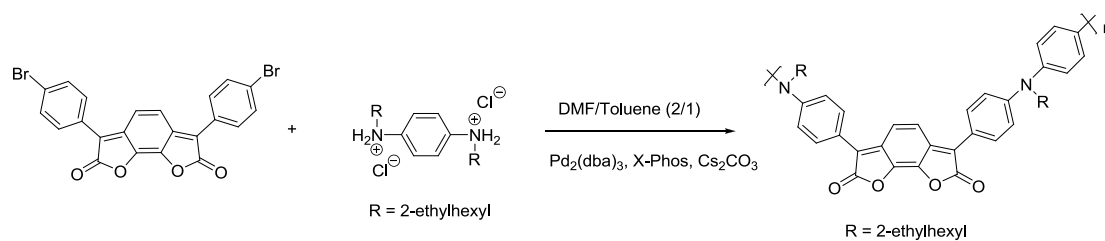
After extraction with toluene, a black solid was obtained (95 mg, yield: 37 %).

Molecular weight (GPC, THF): $M_w = 5.9$ kDa, PD = 2.2. UV/vis (DCM): 645 nm,

UV/Vis (thin film): 708 nm; ϵ (645) /L mol⁻¹cm⁻¹: 30600.



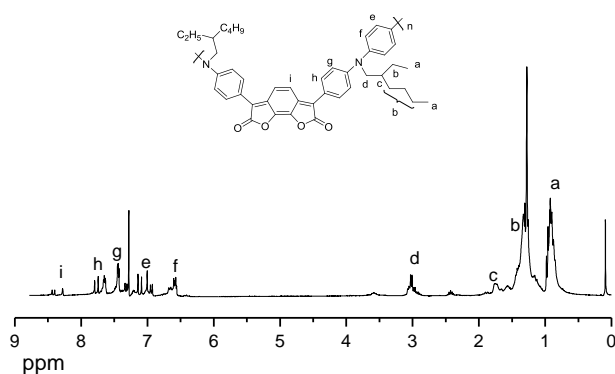
Polymer P-A-1,8-BDF



In a Schlenk flask, 3,7-bis(4-bromophenyl)benzo[1,2-b:4,5-b']difuran-2,6-dione (214 mg, 0.43 mmol), *N,N*-bis(2-ethylhexyl)benzene-1,4-diamine dihydrochloride salt (175 mg, 0.43 mmol), Pd₂(dba)₃ (11.9 mg, 0.015 mmol) and X-Phos (39.2 mg, 0.082 mmol) were dissolved in a mixture of DMF/toluene (2:1) (6 ml) under nitrogen.

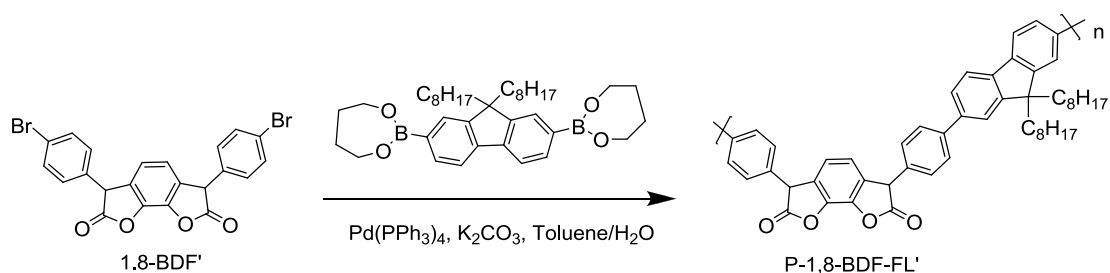
Then cesium carbonate (310 mg, 0.95 mmol) was added and the mixture was allowed

to stir for 48 hours under nitrogen at 90 °C. After completion of the reaction, the dark blue solution was treated with DCM, washed three times with water and once with brine. Then the organic layer was dried over anhydrous magnesium sulfate, and the solvent was removed at reduced pressure. Subsequently the crude product was dissolved in a minimal amount of DCM and precipitated in methanol. The product s was btained as a dark solid (90.5 mg, yield: 31 %).

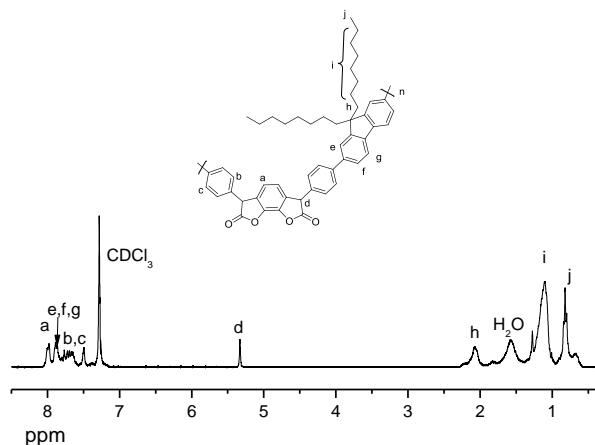


5.3.2.2 Conjugated polymers based on 1,8-BDF via Suzuki coupling

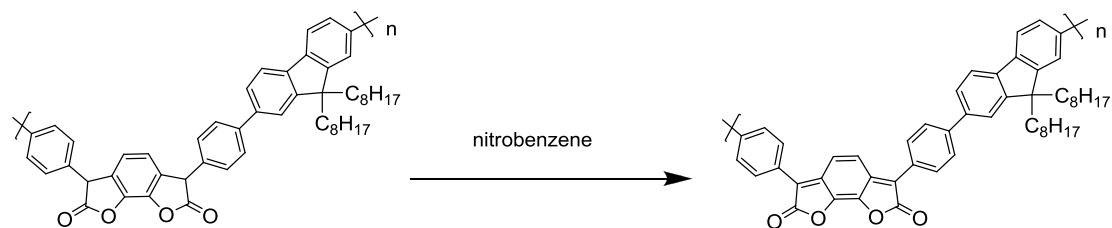
Polymer P-1,8-BDF-FL'



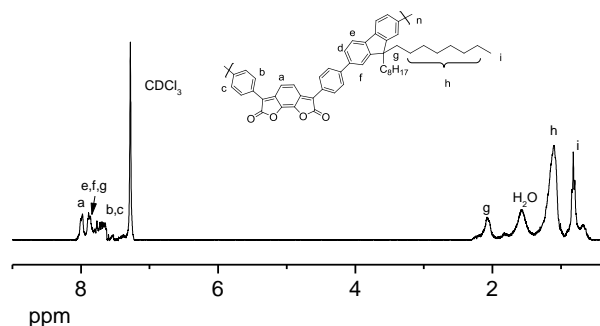
1,8-BDF' (0.2 g, 0.40 mmol), 2,2-(9,9-dioctyl-9H-fluorene-2,7-diyl-bis(4,4,5,5-tetramethyl-1,3,2-dioxaborolane)) (0.2345 g, 0.40 mmol) and tetrakis-(triphenylphosphino)-palladium(0) (22.31 mg, 0.02 mmol) were dissolved in toluene (10 ml) and purged with nitrogen for 15 min. A degassed solution of Na₂CO₃ (0.15 g, 1.4 mmol) in Milli-Q_{plus}-water (3 ml) was added, and the mixture was stirred at 100 °C for 24 hours. After cooling the purple solution was diluted with DCM (50 ml), and extracted with brine (2×50 ml) and water (50 ml). The organic phase was dried with MgSO₄, and filtered with Celite. The solvent was evaporated and the title product was obtained (0.21 g, 74.8 %). ¹H-NMR (300 MHz, d₁-CHCl₃) δ ppm: 7.82-8.03 (br, 8H), 7.48-7.79 (br, 8H), 5.31-5.35 (s, 2H), 1.98-2.18 (br, 4H), 0.98-1.31 (br, 24H), 0.74-0.93 (br, 6H).



Polymer P-1,8-BDF-FL'



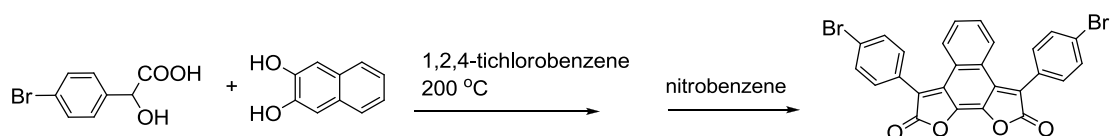
Polymer **P-1,8-BDF-FL'** was dissolved in toluene (20 ml) with 1 ml nitrobenzene at 100°C and stirred for one hour. After cooling the purple solution was diluted with DCM (50 ml), and extracted with brine (2×50 ml) and water (50 ml). The organic phase was dried with MgSO₄, and the solvent was evaporated. The polymer was dissolved again in DCM and precipitated with methanol giving a dark solid (0.16 g, yield: 76 %). Molecular weight (GPC, THF): $M_w = 21.4$ KDa, $M_n = 8.9$ KDa, PD = 2.4. ¹H-NMR (300 MHz, d₁-CHCl₃) δ ppm: 7.82-8.03 (br, 8H), 7.48-7.79 (br, 8H), 1.98-2.18 (br, 4H), 0.98-1.31 (br, 24H), 0.74-0.93 (br, 6H). UV/Vis (DCM): 555 nm; ε (555) = 54643 L mol⁻¹ cm⁻¹.



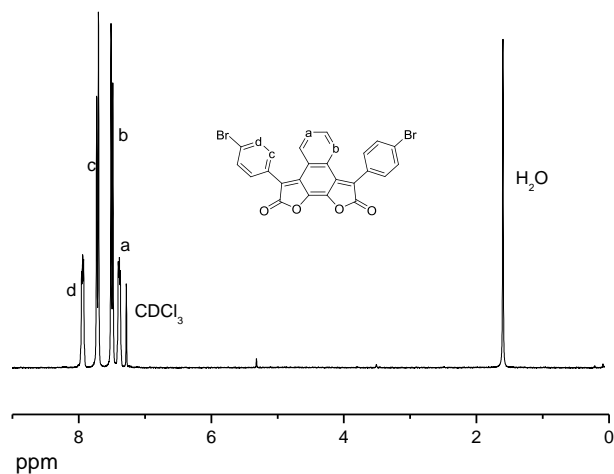
5.3.3 Conjugated polymers based on naphthodiones

5.3.3.1 Monomers and polymers based on NDF

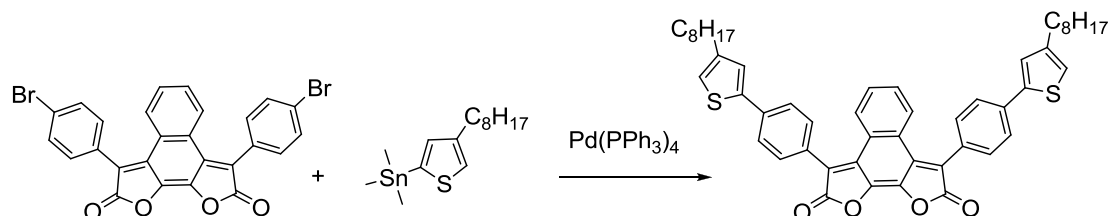
3,8-Bis(4-bromophenyl)naphtho[2,1-*b*:3,4-*b'*]difuran-2,9-dione (1,10-NDF)



Using a Dean-Stark apparatus, 2,3-dihydroxynaphthalene (0.8 g, 5 mmol) and 4-bromo-mandelic acid (2.31 g, 10 mmol) were dissolved in 1,2,4-trichlorobenzene (10 ml). The reaction mixture was stirred for 4 hours at 200 °C allowing formed water to distil off before it was cooled to room temperature. Then nitrobenzene (2.46 g, 20 mmol) was added. The mixture was stirred for another half an hour at 200 °C before it was cooled down, poured into methanol (50 ml), and filtered to recover the crude product. The crude product was dissolved in 1,2,4-trichlorobenzene at 200 °C, precipitated at room temperature, and digested in hot acetic acid. The product obtained was refluxed in methanol. After cooling an orange solid (1.91 g, yield: 70 %) was obtained. ¹H NMR (300 MHz, d₁-CHCl₃) δ ppm: 7.37-7.40 (m, 2H), 7.50 (d, J=8.1 Hz, 4H), 7.71 (d, J=7.8 Hz, 4H), 7.93-7.96 (m, 2H). Microanalysis found C, 56.89 %; H, 2.19 % (C, 56.97 %; H, 2.21 %). UV/Vis (DCM): 427 nm. ε (427) = 36620 L mol⁻¹ cm⁻¹. PL (DCM): 522 nm (excitation at 450 nm).

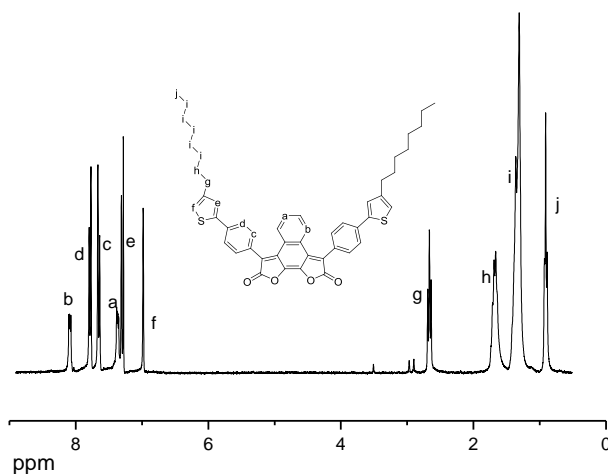


**3,8-Bis(4-(4-n-octylthiophen-2-yl)phenyl)naphtho[2,1-*b*:3,4-*b'*]difuran-2,9-dione
(Th-1,10-NDF)**

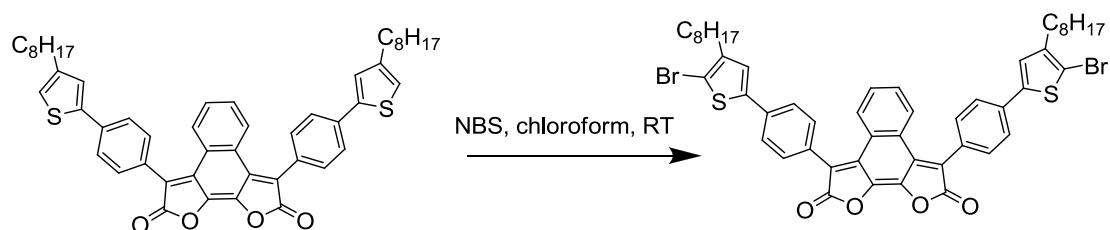


In a vial under nitrogen, **1,10-NDF** (1 g, 1.8 mmol), 4-n-octylthiophen-2-yl trimethylstannane (0.64 g, 1.8 mmol) and tetrakis(tri-phenylphosphine)palladium(0) (0.10 g, 0.09 mmol) were dissolved in dry DMF (10 ml) and stirred for 12 hours at 150 °C. After cooling the mixture was diluted with DCM (100 ml), washed three times with water, and once brine. The organic layer was separated, dried over magnesium sulfate and evaporated. Subsequently, the crude product was dissolved in a minimal amount of DCM and precipitated in methanol. The product was obtained as

a red solid (1.19 g, yield: 85 %). $^1\text{H-NMR}$ (300 MHz, $\text{d}_1\text{-CHCl}_3$) δ ppm: 8.07-8.10 (m, 2H), 7.78 (d, $J=8.1$ Hz, 4H), 7.65 (d, $J=8.1$ Hz, 4H), 7.35-7.38 (m, 2H), 7.31 (s, 2H), 6.98 (s, 2H), 2.67 (t, $J=7.5$ Hz, 4H), 1.66-1.68 (m, 6H), 1.34 (d, $J=15.6$, 20H), 0.91 (t, $J=6.1$, 6H). Microanalysis found C, 77.56 %; H, 6.64 % (C, 77.08 %; H, 6.47 %). UV/Vis (DCM): 484 nm

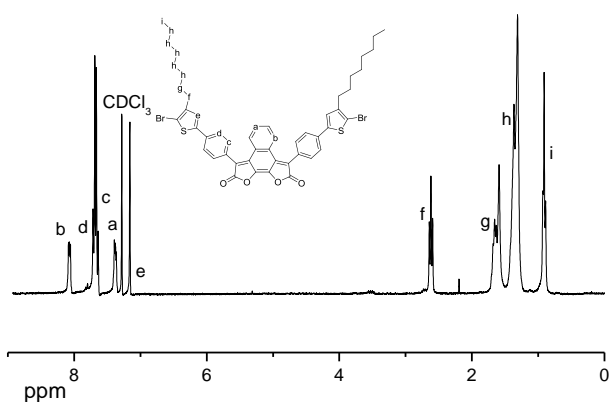


3,8-Bis(4-(5-bromo-4-n-octylthiophen-2-yl)phenyl)naphtho[2,1-*b*:3,4-*b'*]difuran-2,9-dione (Br-Th-1,10-NDF)

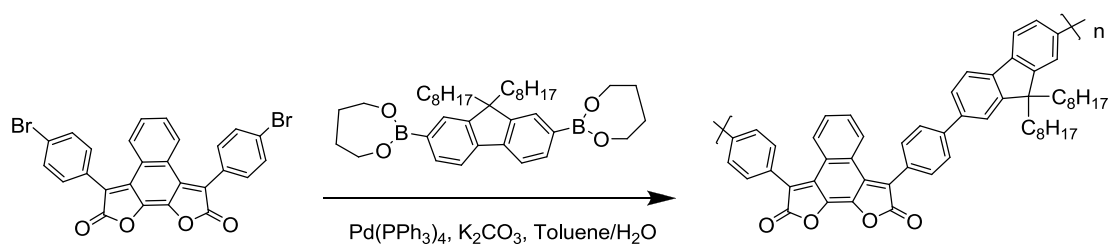


Under nitrogen, a flask was charged with **Th-1,10-NDF** (1 g, 1.28 mmol) in DCM (150 ml). Then NBS (0.57g, 3.2 mmol) was added and the reaction mixture was

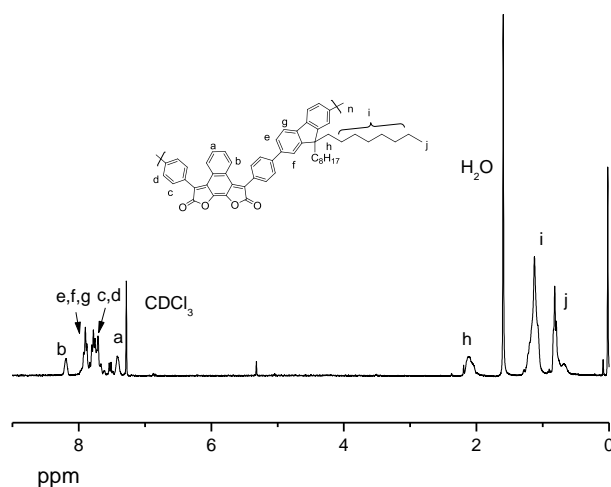
stirred at room temperature over night. The solution was washed with water (100 ml) three times, and the organic phase was dried over magnesium sulfate. After evaporating the solvent, the crude product was dissolved in a minimal amount of DCM, and precipitated in methanol. The product was obtained as a red solid (1.01 g, yield: 84 %). $^1\text{H-NMR}$ (300 MHz, $\text{d}_1\text{-CHCl}_3$) δ ppm: 8.06-8.09 (m, 2H), 7.14 (d, $J=8.4$ Hz, 4H), 7.13 (d, $J=8.4$ Hz, 4H), 7.36-7.39 (m, 2H), 7.16 (s, 2H), 2.62 (t, $J=7.6$ Hz, 4H), 1.63-1.68 (m, 4H), 1.34 (d, $J=15.6$, 20H), 0.91 (t, $J=6.3$, 6H). Microanalysis found C, 64.51 %; H, 5.09 % (C, 64.10 %; H, 5.16 %). UV/Vis (DCM): 487 nm. ϵ (487) = $36412 \text{ L mol}^{-1} \text{ cm}^{-1}$. PL (DCM): 661 nm (excitation at 450 nm).



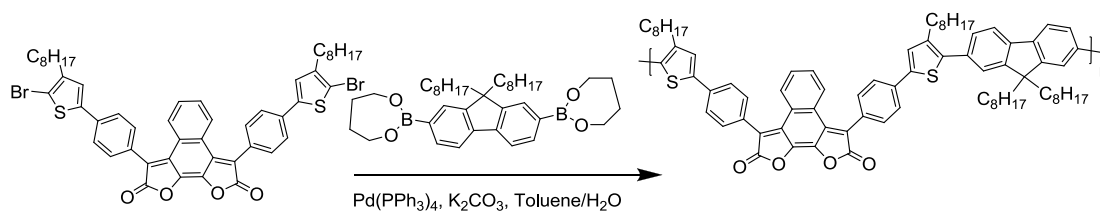
Polymer P-1,10-NDF-FL



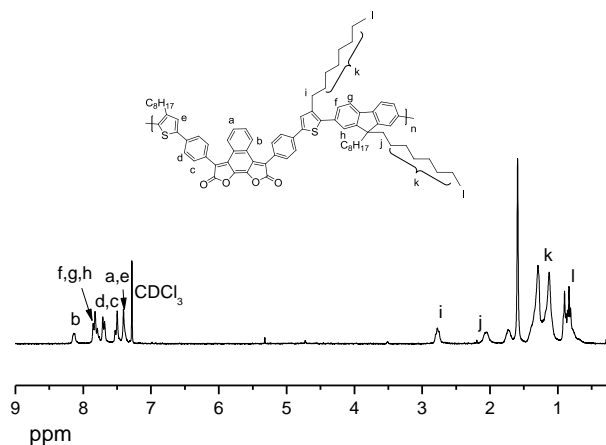
1,10-NDF (0.2 g, 0.36 mmol), 2,2-(9,9-dioctyl-9H-fluorene-2,7-diyl)bis(4,4,5,5-tetramethyl-1,3,2-dioxaborolane) (0.19 g, 0.36 mmol) and tetrakis-(triphenylphosphino)- palladium(0) (20.8 mg, 0.018 mmol) were dissolved in toluene (10 ml) and purged with nitrogen for 15 min. A degassed solution of Na₂CO₃ (0.14 g, 1.32 mmol) in Milli-Q_{plus}-water (3 ml) was added, and the mixture was stirred at 100 °C for 24 hours. After cooling the dark solution was diluted with DCM (50 ml), and extracted with brine (2×50 ml) and water (50 ml). The organic phase was dried with MgSO₄, and the solvent was evaporated. The polymer was dissolved again in DCM and precipitated with methanol giving a dark solid (0.16 g, yield: 58 %). Molecular weight (GPC, THF): *M_w* = 30.9 KDa, *M_n* = 10.1 KDa, PD = 2.98. ¹H-NMR (300 MHz, d₁-CHCl₃) δ ppm: 8.19 (s, 2H), 7.87-7.93 (m, 6H), 7.61-7.80 (br, 8H), 7.41-7.54 (br, 2H), 2.04-2.13 (br, 8H), 1.05-1.31 (br, 24H), 0.79-0.84 (br, 6H). UV/Vis (DCM): 482 nm; ε (482) = 38748 L mol⁻¹ cm⁻¹. PL (DCM): 686 nm (excitation at 450 nm); PL quantum yield Φ_f: 0.17 %.



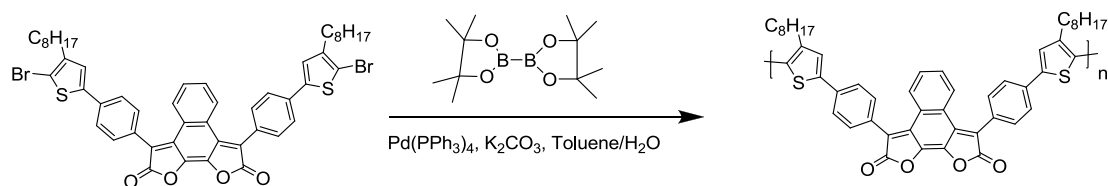
Polymer P-Th-1,10-NDF-FL



Br-Th-1,10-NDF (0.2 g, 0.21 mmol), 2,2-(9,9-dioctyl-9H-fluorene-2,7-diyl)bis(4,4,5,5-tetramethyl-1,3,2-dioxaborolane) (0.13 g, 0.21 mmol) and tetrakis(triphenylphosphino)- palladium(0) (12.3 mg, 0.011 mmol) were dissolved in toluene (10 ml) and purged with nitrogen for 15 min. A degassed solution of Na₂CO₃ (0.09 g, 0.84 mmol) in Milli-Q_{plus}-water (3 ml) was added, and the mixture was stirred at 100 °C for 24 hours. After cooling the dark solution was diluted with DCM (50 ml), and extracted with brine (2×50 ml) and water (50 ml). The organic phase was dried with MgSO₄, and the solvent was evaporated. The polymer was dissolved again in DCM and precipitated with methanol giving a dark solid (0.19 g, yield: 62 %). Molecular weight (GPC, THF): $M_w = 9.4$ KDa, $M_n = 5.16$ KDa, PD = 1.82. ¹H-NMR (300 MHz, d₁-CHCl₃) δ ppm: 8.11-8.14 (br, 2H), 7.76-7.85 (m, 6H), 7.69 (d, J=7.5 Hz, 4H), 7.51 (d, J=9.0 Hz, 4H), 7.41 (s, 4H), 1.66-2.06 (br, 8H), 1.12-1.29 (br, 48H), 0.81-0.90 (br, 12H). UV/vis (DCM): 522 nm; ε (522) = 25877 L mol⁻¹ cm⁻¹. PL (DCM): 680 nm (excitation at 450 nm); PL quantum yield Φ_F: 0.02 %.

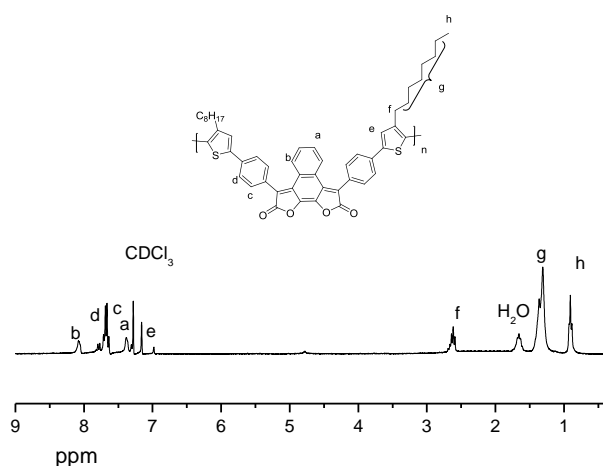


Polymer P-Th-1,10-NDF

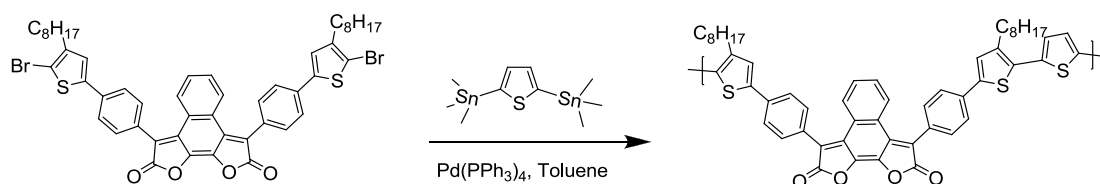


Br-Th-1,10-NDF (0.2 g, 0.21 mmol), bis(pinacolato)diboron (0.05 g, 0.21 mmol) and tetrakis(triphenylphosphino)- palladium(0) (12.3 mg, 0.011 mmol) were dissolved in toluene (10 ml) and purged with nitrogen for 15 min. A degassed solution of Na_2CO_3 (0.09 g, 0.84 mmol) in Milli-Q_{plus}-water (3 ml) was added, and the mixture was stirred at 100 °C for 24 hours. After cooling the dark solution was diluted with DCM (50 ml), and extracted with brine (2×50 ml) and water (50 ml). The organic phase was dried with MgSO_4 , and the solvent was evaporated. The polymer was dissolved again in DCM and precipitated with methanol giving a dark solid (0.10 g, yield: 57 %).

Molecular weight (GPC, THF): $M_w = 8.7$ KDa, $M_n = 4.10$ KDa, PD = 2.12. $^1\text{H-NMR}$ (300 MHz, $\text{d}_1\text{-CHCl}_3$) δ ppm: 8.07 (s, 2H), 7.74-7.59 (br, 8H), 7.45 (s, 2H), 7.20 (s, 2H), 2.58-2.69 (br, 4H), 1.16-1.46 (br, 24H), 0.82-0.94 (br, 6H). UV/vis (DCM): 522 nm; ϵ (482) = 25617 $\text{L mol}^{-1} \text{cm}^{-1}$. PL (DCM): 667 nm (excitation at 450 nm); PL quantum yield Φ_f : 4.7 %.

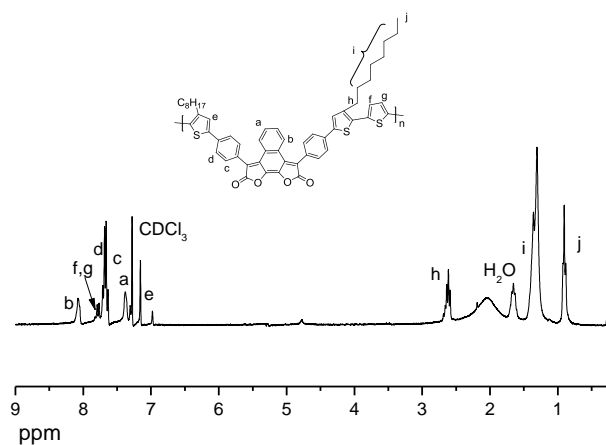


Polymer P-Di-Th-1,10-NDF

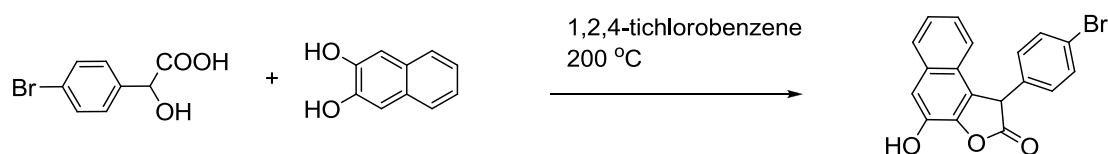


In a Schlenk flask, **Br-Th-1,10-NDF** (0.2 g, 0.21 mmol), 2,5-bis(tributylstannyl)thiophene (0.14 g, 0.21 mmol) and tetrakis(triphenylphosphine)palladium(0) (12.3 mg, 0.01 mmol) were dissolved in dry DMF (10 ml). Then the mixture was heated and

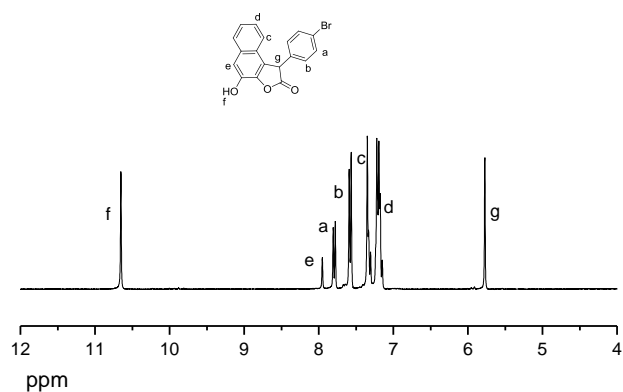
kept at 90 °C under nitrogen for 18 hours. After cooling, the dark solution was diluted with DCM (50 ml) and extracted with brine (2×50 ml) and water (50 ml). The organic phase was dried with MgSO₄, and the solvent was evaporated. The polymer was dissolved again in DCM and precipitated with methanol giving a dark solid (0.12 g, yield: 64 %). Molecular weight (GPC, THF): *M_w* = 5.6 KDa, *M_n* = 2.8 KDa, PD = 2.1. ¹H-NMR (300 MHz, d₁-CHCl₃) δ ppm: 8.09-8.12 (br, 2H), 7.77-7.81 (br, 4H), 7.61-7.69 (br, 8H), 7.26-7.29 (br, 2H), 7.16-7.19 (br, 2H), 2.78-2.89 (br, 4H), 1.34-1.78 (br, 24H), 0.82-0.91 (br, 6H). UV/Vis (DCM): 483 nm; ε (483) = 10734 L mol⁻¹ cm⁻¹. PL (DCM): 667 nm (excitation at 450 nm); PL quantum yield Φ_f: 4.8 %.



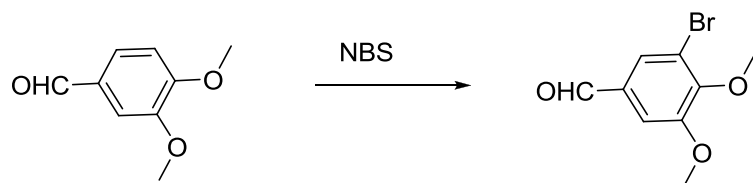
9-Hydroxy-2-oxo-3-(bromophenyl)-2,3-dihydro[1,2-*b*]furan



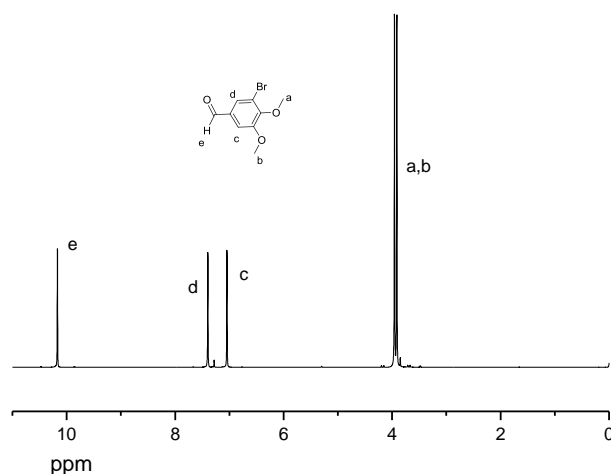
Using a Dean-Stark apparatus, 2,3-dihydroxynaphthalene (1.6 g, 10 mmol) and 4-bromo-mandelic acid (2.31 g, 10 mmol) were dissolved in 1,2,4-trichlorobenzene (20 ml). The reaction mixture was stirred for 2 hours at 200 °C allowing formed water to distil off before it was cooled to room temperature with nitrogen protection. The product began to precipitate during cooling and was stirred for a further 1 h at room temperature. The product was filtered off and washed with small amounts of toluene and hexane, respectively, giving a white solid. The crude product was dissolved in DMF and precipitated in water to yield a white solid. (1.89 g, yield: 65%) ^1H NMR (300 MHz, $\text{d}_1\text{-CHCl}_3$) δ ppm: 10.65 (s, 1H), 7.95 (s, 1H), 7.79 (d, $J=12$ Hz, 2H), 7.57 (d, $J=9$ Hz, 2H), 7.33 (m, 2H), 7.20 (m, 2H), 5.7 (s, 1H). Microanalysis found C, 74.01 %; H, 4.08 % (C, 73.97 %; H, 4.14 %).



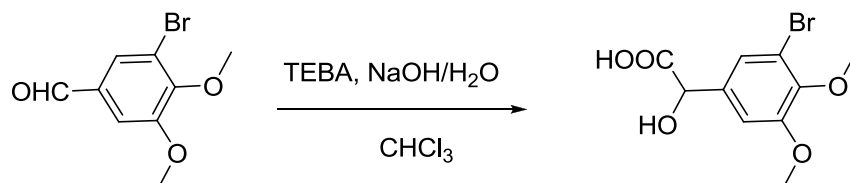
3-Bromo-4,5-dimethoxybenzaldehyde



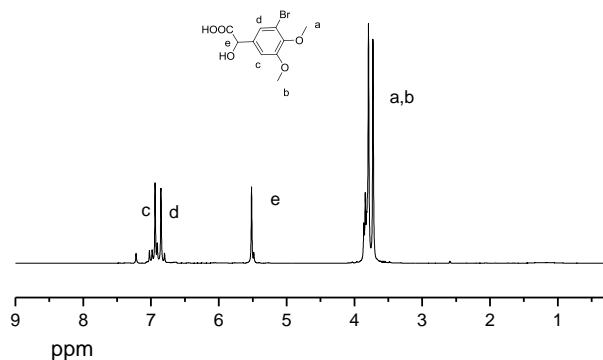
In a flask, 3,4-dimethoxybenzaldehyde (2.5 g, 15 mmol) was dissolved in acetonitrile (25 ml). The solution was cooled to 0 °C in an ice-water bath under N₂. NBS (2.9 g, 17 mmol) was added in small portions within a time period of 25 mins. The reaction mixture was stirred over night whilst slowly warming to room temperature. The reaction mixture was poured in water (20 ml). A white solid was precipitated. The crude product was dried in air. A pure product (3.2 g, yield: 87%) was obtained using recrystallization from methanol/DCM. ¹H-NMR (300 MHz, CDCl₃) δ ppm: 10.2 (s, 1 H); 7.41 (s, 1 H), 7.04 (s, 1 H), 3.95 (d, 6 H).



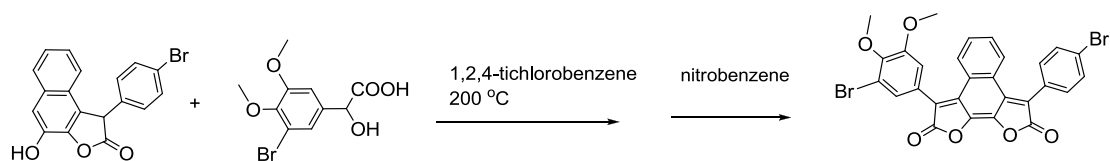
2-(3-Bromo-4,5-dimethoxyphenyl)-2-hydroxyacetic acid



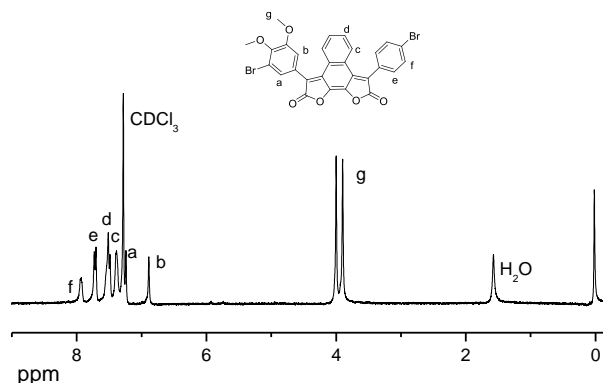
In a three necked flask, 3-bromo-4,5-dimethoxybenzaldehyde (3 g, 10.45 mmol) and TEBA (0.12 g, 0.5225 mol) were dissolved in chloroform (3.92 ml, 52.24 mmol) under N₂. The mixture was heated to 50 °C under stirring. A solution of NaOH (4.18 g, 104.5 mmol) in water (6.27 ml) was added dropwise. The reaction mixture was stirred at the same temperature for 15 h. After cooling, the mixture was diluted with 50 ml ethyl acetate. The aqueous phase was saved. A solution of 1 M HCl was added until a pH-value of 3 was reached. The product was extracted with EA and water. The organic phase was dried over MgSO₄, and the solvent was removed. The crude product was purified using column chromatography (DCM/hexane:1/4 and acetone//hexane:1/2). The title compound was obtained as a white solid (2.0 g, yield: 65.7%) ¹H-NMR (300 MHz, CDCl₃) δ ppm: 6.94 (s, 1 H); 6.04 (s, 1 H), 5.51 (s, 1 H), 3.79 (d, 6 H).



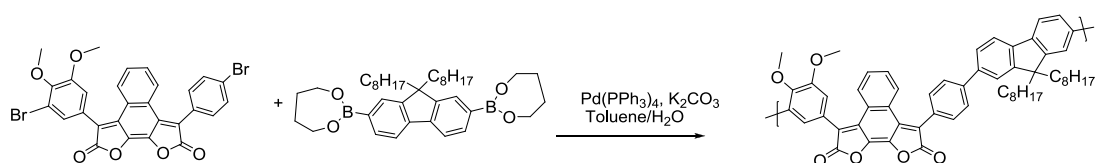
3-(4-Bromophenyl)-8-(3-bromo-4,5-dimethoxy-phenyl)-naphtho[2,1-*b*:3,4-*b'*]diferan-2,9-dione (1,10-uNDF).



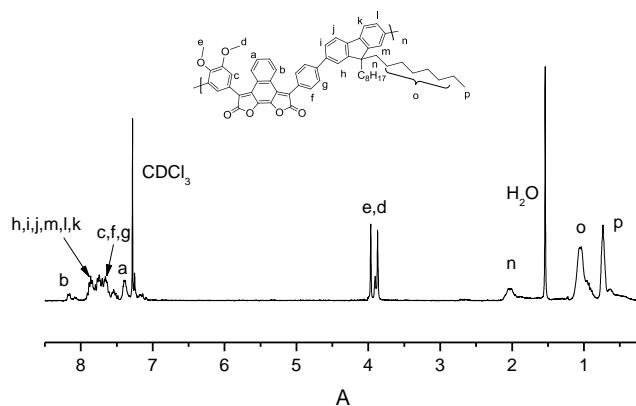
Using a Dean-Stark apparatus, 9-Hydroxy-2-oxo-3-(bromophenyl)-2,3-dihydronaphtho[1,2-*b*]furan (1.46 g, 5 mmol), and 3-bromo-4,5-dimethoxymandelic acid (1.39 g, 6 mmol) were dissolved in 1,2,4-trichlorobenzene (10 ml). The reaction mixture was stirred for 4 hours at 200 °C allowing formed water to distil off before it was cooled to room temperature. Then nitrobenzene (2.46 g, 20 mmol) was added. The mixture was stirred for another half an hour at 160 °C before it was cooled down, poured into methanol (50 ml), and filtered to recover the crude product. The crude product was dissolved in 1,2,4-trichlorobenzene at 160 °C, precipitated at room temperature, and digested in hot acetic acid. The product obtained was refluxed in methanol. After cooling an orange solid (1.91 g, yield: 63 %) was obtained. ¹H NMR (300 MHz, d₁-CHCl₃) δ ppm: 7.92 (s, 2H), 7.71 (d, J=6, 2H), 7.50 (d, J=9 Hz, 2H), 7.39 (s, 2H), 7.24 (s, 1H), 6.88 (s, 1H), 3.95 (d, J=33 Hz, 6H). Microanalysis found C, 55.48 %; H, 2.49 % (C, 55.29 %; H, 2.65 %). UV/Vis (DCM): 400 nm. ε (400) = 39250 L mol⁻¹ cm⁻¹.



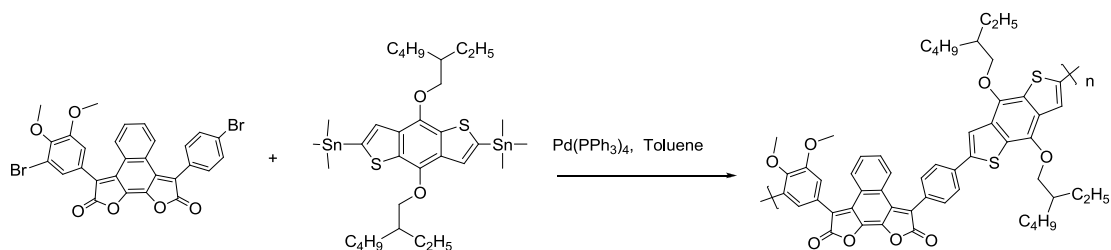
Polymer P-1,10-uNDF-FL



1,10-uNDF (0.2 g, 0.33 mmol), **2,2-(9,9-dioctyl-9H-fluorene-2,7-diyl)bis(4,4,5,5-tetramethyl-1,3,2-dioxaborolane)** (0.1928 g, 0.33 mmol) and **tetrakis(triphenylphosphino)-palladium(0)** (20.8 mg, 0.018 mmol) were dissolved in toluene (10 ml) and purged with nitrogen for 15 min. A degassed solution of Na_2CO_3 (0.14 g, 1.32 mmol) in Milli-Q_{plus}-water (3 ml) was added, and the mixture was stirred at 100 °C for 24 hours. After cooling the dark solution was diluted with DCM (50 ml), and extracted with brine (2×50 ml) and water (50 ml). The organic phase was dried with MgSO_4 , and the solvent was evaporated. The polymer was dissolved again in DCM and precipitated with methanol giving a dark solid (0.17 g, yield: 62 %). Molecular weight (GPC, THF): $M_w = 17.5$ KDa, $M_n = 8.3$ KDa, PD = 2.1. $^1\text{H-NMR}$ (300 MHz, $\text{d}_1\text{-CHCl}_3$) δ ppm: 8.10-8.23 (br, 2H), 7.58-7.89 (br, 12H), 7.33-7.46 (br, 2H), 3.88-4.03 (m, 6H), 1.98-2.17 (br, 4H), 1.07-1.17 (br, 24H), 0.72-0.84 (br, 6H). UV/vis (DCM): 464 nm; ϵ (464) = $39257 \text{ L mol}^{-1} \text{ cm}^{-1}$.

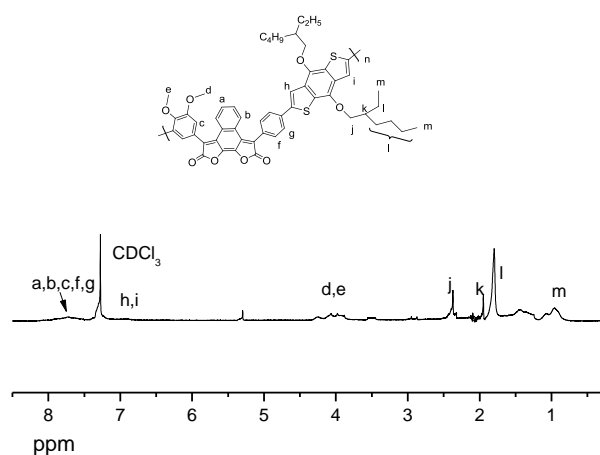


Polymer P-1,10-uNDF-BDT

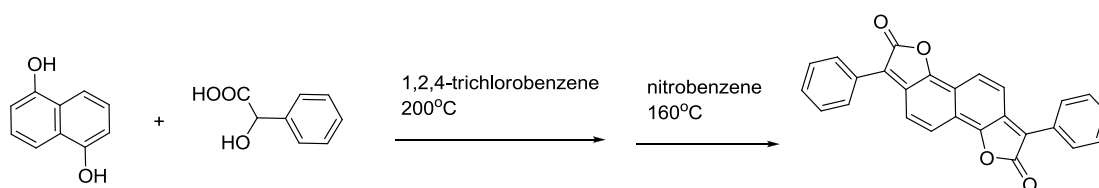


1,10-uNDF (0.2 g, 0.33 mmol), 2,2-(9,9-dioctyl-9H-fluorene-2,7-diyl)bis(4,4,5,5-tetramethyl-1,3,2-dioxaborolane) (0.2548 g, 0.33 mmol) and tetrakis-(triphenylphosphino)-palladium(0) (20.8 mg, 0.018 mmol) were dissolved in toluene (10 ml) and purged with nitrogen for 15 min. A degassed solution of Na_2CO_3 (0.14 g, 1.32 mmol) in Milli-Q_{plus}-water (3 ml) was added, and the mixture was stirred at 100 °C for 24 hours. After cooling the dark solution was diluted with DCM (50 ml), and extracted with brine (2×50 ml) and water (50 ml). The organic phase was dried with MgSO_4 , and the solvent was evaporated. The polymer was dissolved again in DCM

and precipitated with methanol giving a dark solid (0.16 g, yield: 54 %). Molecular weight (GPC, THF): $M_w = 9.6$ KDa, $M_n = 5.3$ KDa, PD = 1.8. $^1\text{H-NMR}$ (300 MHz, $\text{d}_1\text{-CHCl}_3$) δ ppm: 7.23-7.63 (br, 10 H), 6.81-6.98 (br, 2 H), 3.88-4.03 (m, 6 H), 2.21-2.23 (br, 4 H), 1.87-1.98 (br, 2 H), 1.72-1.84 (br, 16H), 0.85-0.98 (br, 12 H). UV/vis (DCM): 487 nm; ϵ (487) = 40254 $\text{L mol}^{-1} \text{cm}^{-1}$.



3,8-Bisphenylnaphtho[1,2-b:5,6-b']difuran-2,7-dione (1,6-NDF1)

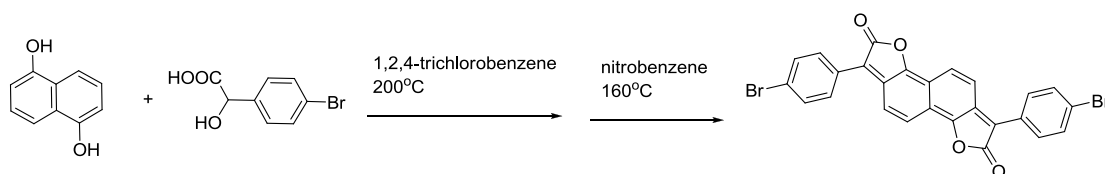


Using a Dean-Stark apparatus, 1,5-dihydroxynaphthalene (0.8 g, 5 mmol) and mandelic acid (1.52 g, 10 mmol) were dissolved in 1,2,4-trichlorobenzene (10 ml).

The reaction mixture was stirred for 4 hours at 200 °C allowing formed water to distil

off, before it was cooled to room temperature. Then nitrobenzene (0.67 g, 5 mmol) was added. The mixture was stirred for another half an hour at 200 °C and allowed to cool. A precipitate was formed, which was filtered off, and washed with methanol. The crude product was dissolved in 1,2,4-trichlorobenzene at 200 °C, precipitated at room temperature, and digested in hot acetic acid. The product obtained was refluxed in methanol giving a deep purple solid (1.35 g, yield: 69 %). Microanalysis found C, 78.05 %, H, 3.62% (C, 79.99 %; H, 3.61 %). UV/vis (DCM): 552 nm. ϵ (552) = 54093 L mol⁻¹ cm⁻¹.

3,8-Bis(4-bromophenyl)naphtho[1,2-b:5,6-b']difuran-2,7-dione (1,6-NDF2)



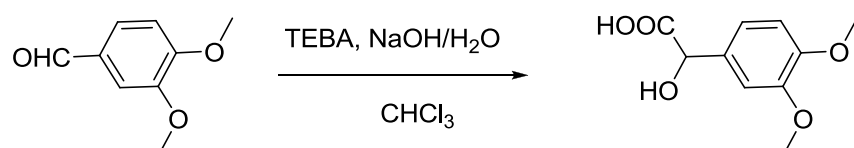
Using a Dean-Stark apparatus, 1,5-dihydroxynaphthalene (0.8 g, 5 mmol), and 4-bromo-mandelic acid (2.31 g, 10 mmol) were dissolved in 1,2,4-trichlorobenzene (10 ml). The reaction mixture was stirred for 4 hours at 200 °C allowing formed water to distil off, before it was cooled to room temperature. Then nitrobenzene (0.67 g, 5 mmol) is added. The mixture was stirred for another half an hour at 200 °C and allowed to cool. A precipitate was formed, which is filtered off, and washed with methanol. The crude product was dissolved in 1,2,4-trichlorobenzene at 200 °C, precipitated at room temperature, and digested in hot acetic acid. The product

obtained was refluxed in methanol giving a deep purple solid (1.69 g, yield: 62 %).

Microanalysis found C, 56.93 %, H, 2.59 % (C, 56.97 %; H, 2.21 %). UV/vis (DCM):

563 nm

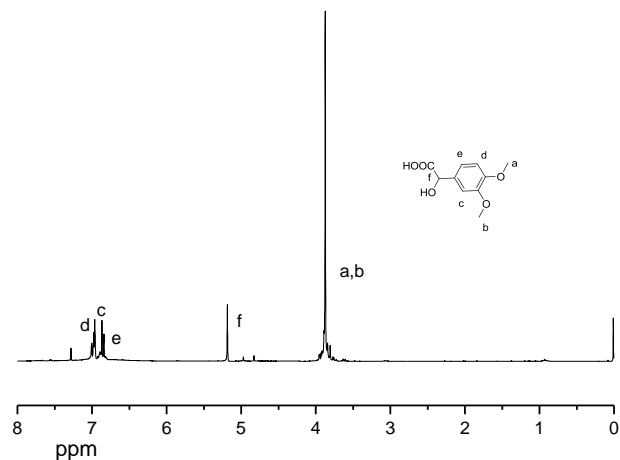
2-(3,4-dimethoxyphenyl)-2-hydroxyacetic acid



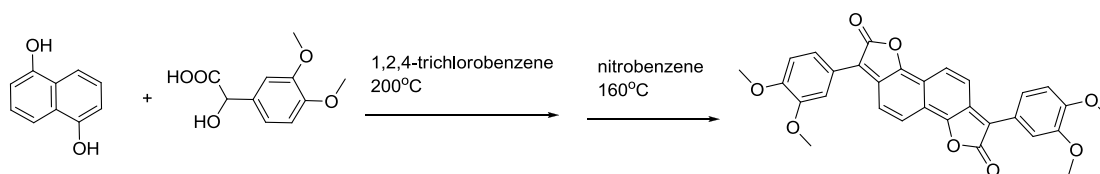
In a three neck flask, 3,4-dimethoxybenzaldehyde (1.68 g, 10.45 mmol) and TEBA (0.12 g, 0.5225 mol) were dissolved in chloroform (3.92 ml, 52.24 mmol) under N₂.

The mixture was heated to 50 °C under stirring. A solution of NaOH (4.18 g, 104.5 mmol) in water (6.27 ml) was added dropwise. The reaction mixture was stirred at the same temperature for 15 h. After cooling, the mixture was diluted with 50 ml ethyl acetate. The aqueous phase was saved. A solution of 1 M HCl was added until a pH-value of 3 was reached. The product was extracted with ethyl acetate and water.

The organic phase was dried over MgSO₄, and the solvent was removed. The crude product was purified using column chromatography (DCM/hexane:1/4 and acetone/hexane:1/2). The title compound was obtained as a white solid (1.40 g, yield: 63%). ¹H-NMR (300 MHz, CDCl₃) δ ppm: 6.97 (s, 1 H); 6.88 (s, 1 H), 6.84 (s, 1 H), 5.19 (d, 6 H), 3.85 (d, 2H).



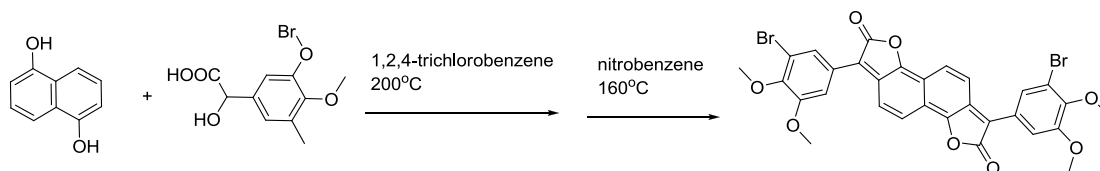
3,8-Bis(3,4-dimethoxyphenyl)naphtho[1,2-b:5,6-b']difuran-2,7-dione (1,6-NDF3)



Using a Dean-Stark apparatus, 1,5-dihydroxynaphthalene (0.8 g, 5 mmol) and 3,4-dimethoxy-mandelic acid (2.12 g, 10 mmol) were dissolved in 1,2,4-trichlorobenzene (10 ml). The reaction mixture was stirred for 4 hours at 200 °C allowing formed water to distil off, before it was cooled to room temperature again. Nitrobenzene (1.23 g, 10 mmol) was added and the mixture is stirred for another hour at 200 °C. After cooling to room temperature, 50 ml methanol were added. A precipitate was formed, which was filtered off, and washed with methanol. The crude product was dissolved in 1,2,4-trichlorobenzene at 200 °C, precipitated at room temperature, and digested in hot acetic acid. The product obtained was refluxed in

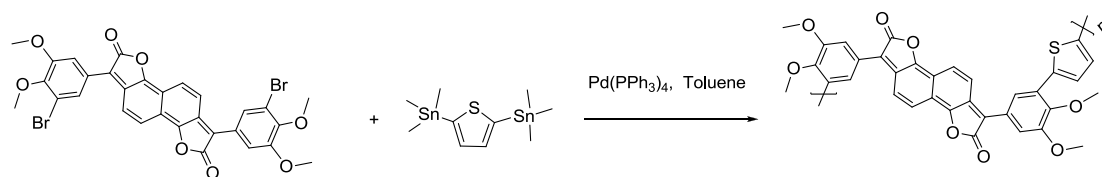
methanol giving a dark solid (1.07 g, yield: 42 %). Microanalysis found C, 70.31 %; H, 4.37 % (C, 70.58 %; H, 4.37 %). UV/vis (DCM): 635 nm. ϵ (635) /L mol⁻¹cm⁻¹: 102626.

**3,8-Bis(3-bromo-4,5-dimethoxyphenyl)naphtho[1,2-b:5,6-b']difuran-2,7-dione
(1,6-NDF4)**

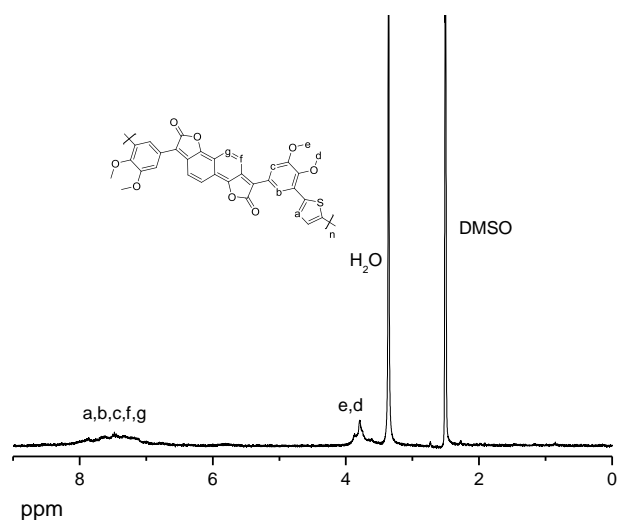


Using a Dean-Stark apparatus, 1,5-dihydroxynaphthalene (0.8 g, 5 mmol) and 3-bromo-4,5-dimethoxy-mandelic acid (2.92 g, 10 mmol) were dissolved in 1,2,4-trichlorobenzene (10 ml). The reaction mixture was stirred for 4 hours at 200 °C , allowing formed water to distil off, before it was cooled to room temperature. Nitrobenzene (1.23 g, 10 mmol) was added and the mixture is stirred for another hour at 200 °C. After cooling to room temperature, 50 ml methanol were added. A precipitate was formed, which was filtered off, and washed with methanol. The crude product was dissolved in 1,2,4-trichlorobenzene at 200 °C, precipitated at room temperature, and digested in hot acetic acid. The product obtained was refluxed in methanol giving a dark solid (1.57 g, yield: 47 %). Microanalysis found C, 52.01 %; H, 3.98 % (C, 53.92 %; H, 3.02 %). UV/Vis (DCM): 588 nm. ϵ (588) /L mol⁻¹cm⁻¹: 26208.

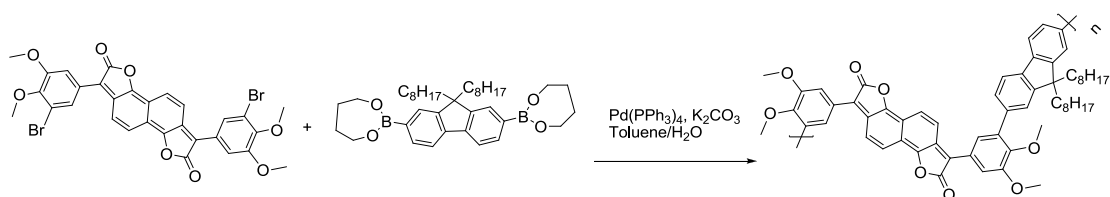
Polymer P-1,6-NDF-Th



In a Schlenk flask, **1,6-NDF4** (200.0 mg, 0.30 mmol), 2,5-bis-(trimethylstannyl)thiophene (122.6 mg, 0.30 mmol) and tetrakis(triphenylphosphine)palladium(0) (17.3 mg, 0.015 mmol) were dissolved in dry toluene/DMF(4/1, 10 ml). Then the mixture was heated and kept at 100 °C under nitrogen for 18 hours. After cooling to room temperature, methanol was added and a precipitate was formed. The precipitate was collected by filtration. Then the product was purified upon Soxhlet extraction with methanol and hexane. A dark solid was obtained (123 mg, yield: 45 %). ¹H NMR (300 MHz, DMSO): δ ppm 7.01-8.08 (br, 10 H), 3.59-3.91 (br, 12H). Molecular weight (GPC, THF): *M_w* = 7.9 kDa, *M_n* = 5.3 kDa, PDI = 1.5. UV/Vis (1,2,4-trichlorobenzene): 644 nm. UV/Vis (Thin film): 692 nm. ε (644) /L mol⁻¹cm⁻¹: 19425.



Polymer P-1,6-NDF-FL

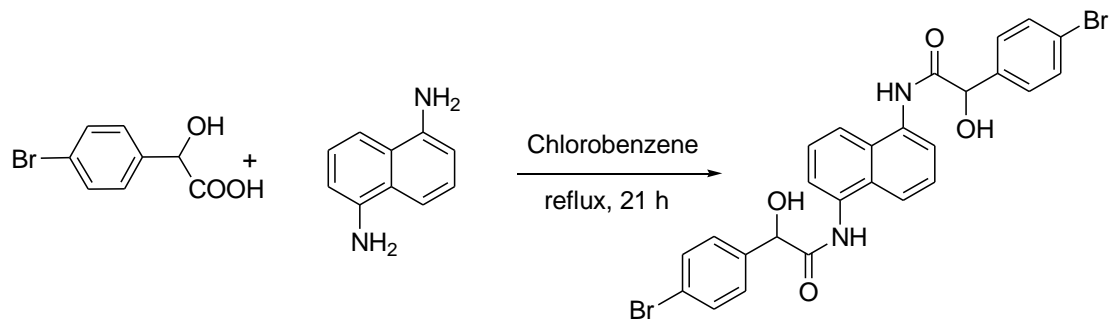


In a Schlenk flask, **1,6-NDF4** (200.0 mg, 0.30 mmol), 2,2'-(9,9-dihexyl-9H-fluorene-2,7-diyl)-bis(4,4,5,5-tetramethyl-1,3,2-dioxaborolane) (176 mg, 0.3 mmol) and tetrakis-(triphenyl-phosphine)palladium(0) (17.3 mg, 0.015 mmol) were dissolved in dry toluene (15 ml) under nitrogen. The reaction was degassed and heated to 50 °C. A degassed solution of potassium carbonate (137.8 mg, 1.3 mmol) in water (5 ml) is added. The mixture was stirred at 90 °C for 24 hours. After cooling to room temperature, the dark solution was diluted with DCM, washed three times with water and once with brine. Then the organic layer was dried over anhydrous magnesium sulfate and the solvent was removed by reduced pressure. After that, the crude product was dissolved in a minimal amount of DCM and precipitated in methanol. The product was obtained as a dark solid (43.6 mg, yield: 17 %).

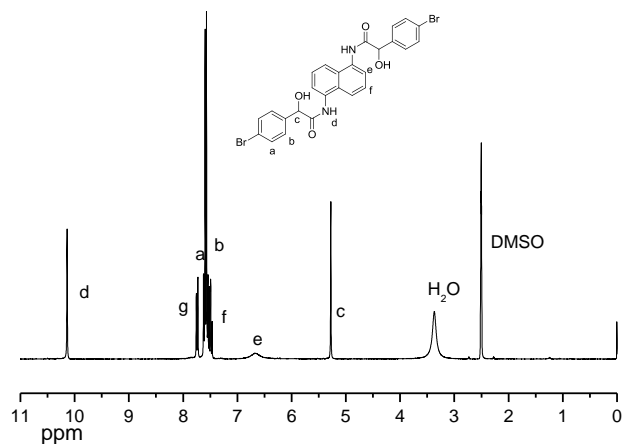
Molecular weight (GPC, THF): $M_w = 8.7$ kDa, $M_n = 4.0$ kDa, PD = 2.2. UV/vis (DCM): 620 nm. . UV/Vis (Thin film): 638 nm. ϵ (644) /L mol⁻¹cm⁻¹: 21364.

5.3.3.2 Conjugated polymers based on NDP

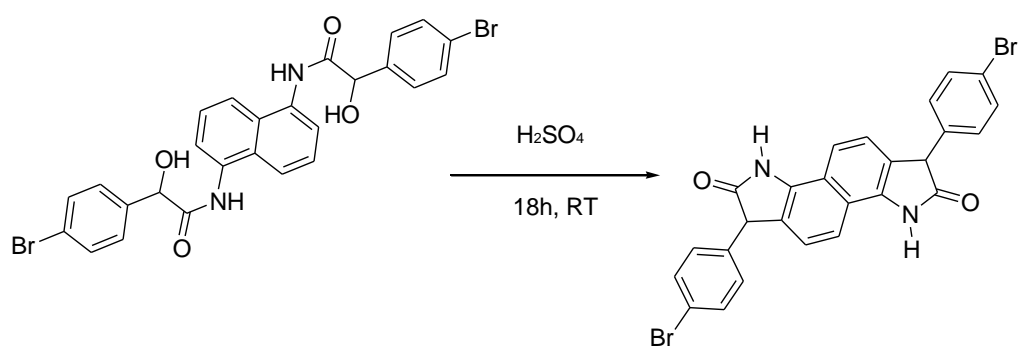
1,4-Bis(α -hydroxy(4-bromophenyl)acetyl-amino) naphthalene



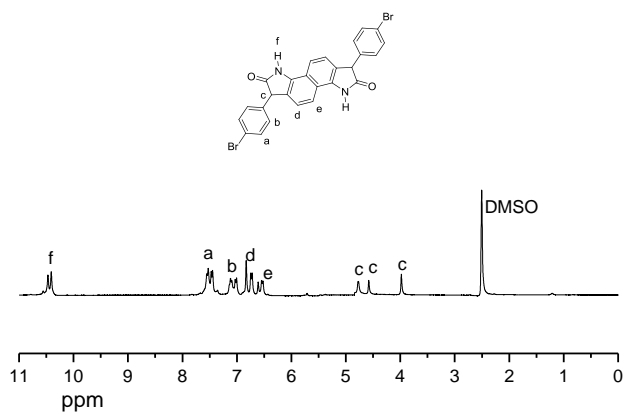
A mixture of 1,5-diaminonaphthalene (1.582 g, 10 mmol) and 4-bromo-mandelic acid (6.93 g, 30 mmol) in chlorobenzene (40 ml) was heated at 135 °C for 21 hours. On cooling to room temperature, the precipitate was filtered, washed with ethanol and dried in vacuo to yield the crude product (5.19 g, yield: 89 %). The crude product was suspended in chlorobenzene (20 ml), heated to 135 °C stirring for 20 minutes, and was then cooled to room temperature. The precipitated product was filtered off and washed with methanol. The product was dried in air giving a white solid (4.23 g, yield: 72 %). ¹H NMR (300 MHz, DMSO): δ ppm 10.13 (s, 2H), 7.74 (d, J=8.1 Hz, 2H), 7.60 (d, J=8.4 Hz, 4H), 7.55 (d, J=8.4 Hz, 4H), 7.49 (t, J=8.0 Hz, 2H), 6.67 (d, J=4.8 Hz, 2H), 5.27 (d, J=4.5 Hz, 2H). ¹³C NMR, (300MHz, CDCl₃): δ ppm 171.90, 140.89, 133.70, 131.56, 129.39, 129.31, 125.95, 122.80, 121.29, 120.72, 73.73. Microanalysis found C, 53.21 %; H, 3.68 %, N, 4.89 % (C, 53.45 %, H, 3.45 %, N, 4.79 %).



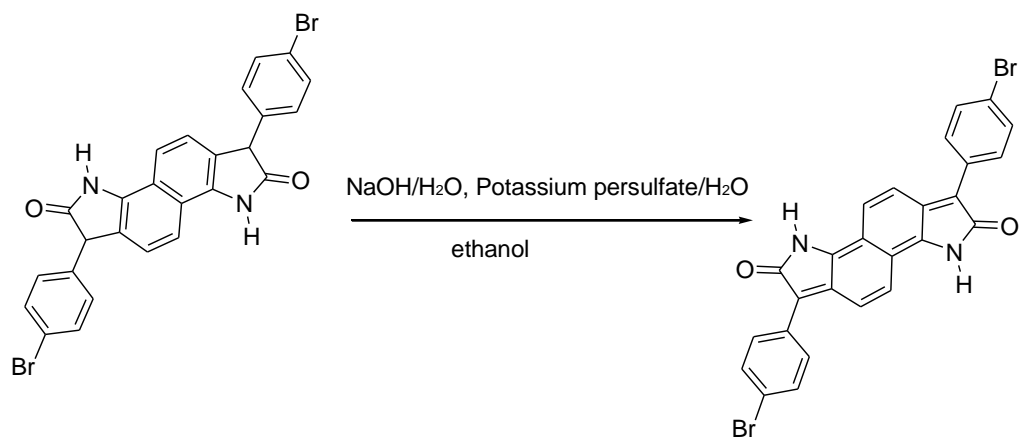
3,8-Di(4-bromophenyl)-2,7-dioxo-1,2,3,6,7,8-hexahydronaphtho[1,2-b:5,6-b']dipyrrole



1,4-Bis(α -hydroxy(4-bromophenyl)acetyl)amino)naphthalene (3.56 g, 6.1 mmol) was added to concentrated sulfuric acid (20 ml). After stirring at room temperature for 18 hours, the mixture was poured into ice water. The precipitate was filtered, washed with water and dried to yield the product (3.16 g, yield: 95 %). NMR (^1H , 300 MHz, DMSO): δ ppm 11.27-11.58 (m, 2H), 7.74-7.88 (m, 2H), 7.55-7.57 (m, 6H), 7.15-7.29 (m, 4H), 5.0 (m, 2H).



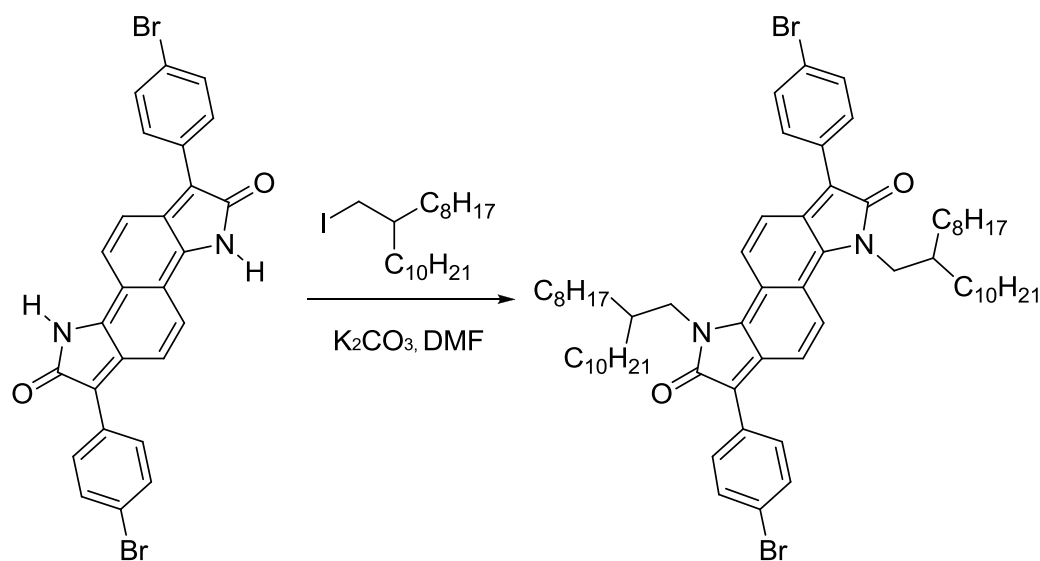
3,8-Di(4-bromophenyl)-2,7-dioxo-1,2,6,7-tetrahydronaphtho[1,2-b:5,6-b']dipyrrole



An aqueous sodium hydroxide solution (2.11 ml, 5 N) was dropwisely added to a suspension of 3,8-di(4-bromophenyl)-2,7-dioxo-1,2,3,6,7,8-hexahydronaphtho[1,2-b:5,6-b']dipyrrole (3.16 g, 5.8 mmol) in ethanol (18 ml). Then potassium persulfate (4.22 g, 15.7 mmol) in water (14 ml) is added. The resulting mixture was heated at reflux for 3 hours. The precipitate in the mixture was filtered, washed with water and ethanol, and dried to yield the product (2.88 g, yield: 91 %). The product was poor

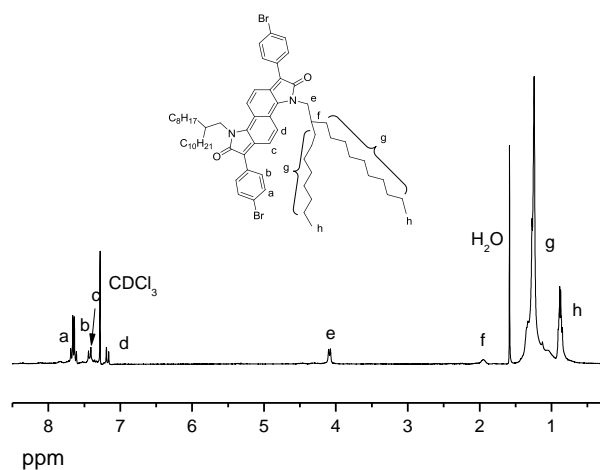
solubility, an spectrum could not be measured. Microanalysis found C, 58.01 %; H, 2.98 %, N, 9.89 % (C, 57.17 %, H, 2.58 %, N, 5.13 %). UV/Vis (DMF): 567 nm.

3,8-Di(4-bromophenyl)-1.6-bis-(2-octyl-dodecyl)-2,7-dioxo-1,2,6,7-tetrahydro-naphtho[1,2-b:5,6-b']dipyrrole (1.6-NDP1)

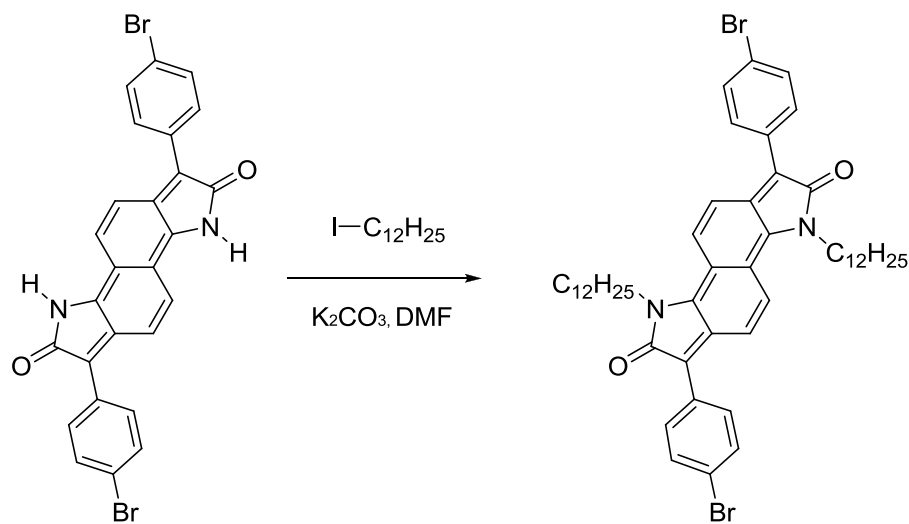


3,8-Di(4-bromophenyl)-2,7-dioxo-1,2,6,7-tetrahydro-naphtho[1,2-b:5,6-b']dipyrrole (1.5 g, 2.75 mmol) was dissolved in anhydrous dimethylformamide (40 ml) and then potassium carbonate (2.66 g, 19.25 mmol) and octyldodecyl iodide (4.49 g, 10.98 mmol) are added. After stirring for 7 hours at 50 °C, the mixture was poured into water and extracted with DCM. The organic layer was washed with brine and dried over anhydrous MgSO₄. On removal of the solvent, the crude solid product was obtained. Then the crude product was dissolved in a minimal amount of DCM and precipitated in methanol. The product was obtained as a dark solid (0.54 g, yield: 20 %). NMR (¹H, 300 MHz, DMSO): δ ppm 7.65 (d, J=8.7 Hz, 4 H), 7.60 (d, J=8.7 Hz, 4 H), 7.40 (d, J=9.6 Hz, 2H), 7.15 (d, J=9.6 Hz, 2H), 4.07 (d, J=7.2 Hz, 4H), 1.93

(s, 2H), 1.15-1.35 (br, 64 H), 0.83-0.89 (m, 12 H). UV/Vis (DCM): 571 nm. ϵ (571) /L mol⁻¹cm⁻¹: 48716.

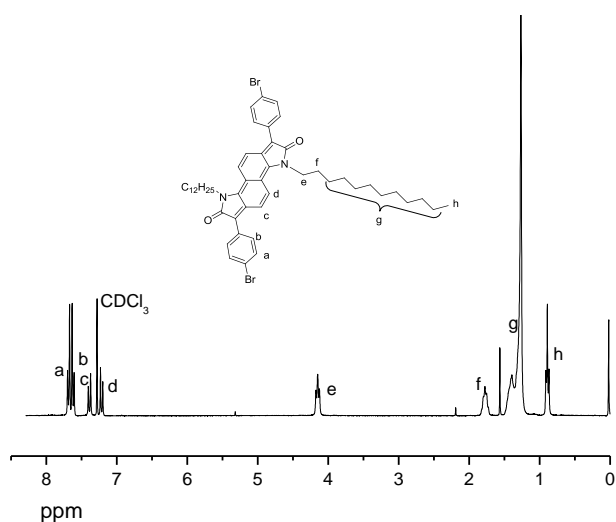


3,8-Di(4-bromophenyl)-1.6-bis-dodecyl-2,7-dioxo-1,2,6,7-tetrahydro-naphtho[1,2-*b*:5,6-*b'*]dipyrrole (1.6-NDP2)

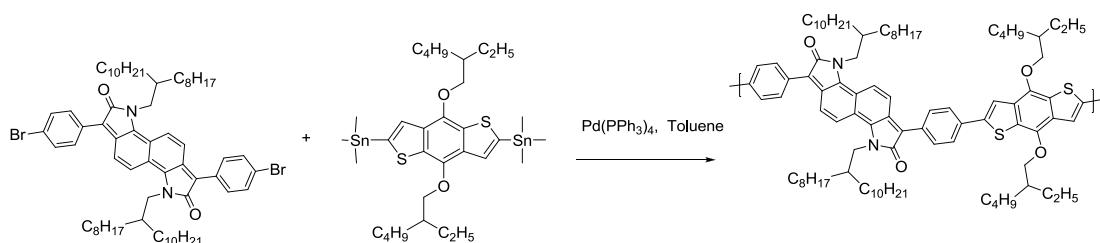


3,8-Di(4-bromophenyl)-2,7-dioxo-1,2,6,7-tetrahydro-naphtho[1,2-*b*:5,6-*b'*]dipyrrole (1.5 g, 2.75 mmol) was dissolved in anhydrous dimethylformamide (40 ml) and then

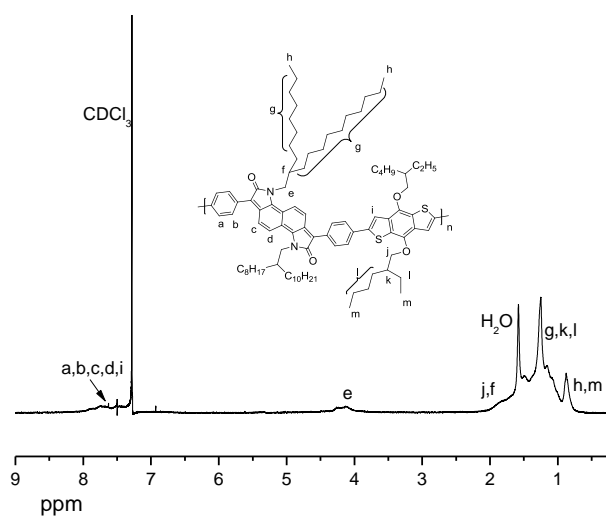
potassium carbonate (2.66 g, 19.25 mmol) and 1-iodododecane (3.39 g, 10.98 mmol) are added. After stirring for 12 hours at 50 °C, the mixture was poured into water and extracted with DCM. The organic layer was washed with brine and dried over anhydrous MgSO₄. On removal of the solvent, the crude solid product was obtained. Then the crude product was dissolved in a minimal amount of DCM and precipitated in methanol. The crude product was obtained as a dark solid (1.41 g, yield: 52 %). The crude product was purified by column chromatography on silica gel with hexane:DCM=1:2 as eluent to yield the product (0.54 g, 20%).¹H NMR (300 MHz, DMSO): δ ppm 7.65 (d, J=8.7 Hz, 4 H), 7.60 (d, J=8.7 Hz, 4 H), 7.40 (d, J=9.6 Hz, 2H), 7.15 (d, J=9.6 Hz, 2H), 4.07 (t, 4H), 1.77 (m, 4H), 1.15-1.35 (br, 36 H), 0.87-0.91 (t, 6 H). Microanalysis found C, 67.95 %; H, 7.12 %, N, 3.19 % (C, 68.02 %, H, 7.08 %, N, 3.17 %). UV/vis (DCM): 571 nm. ε (571) /L mol⁻¹cm⁻¹: 46423.



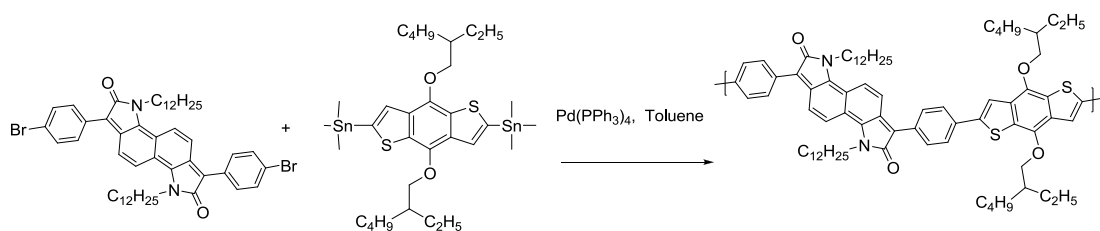
Polymer P-1,6-NDF-BDT1



In a Schlenk flask, **1,6-NDP1** (200.0 mg, 0.18), (4,8-bis(2-ethylhexyloxy)benzo[1,2-*b*:4,5-*b'*]dithiophene-2,6-diyl)bis(trimethylstannane) (139.5 mg, 0.18 mmol) and tetrakis(triphenylphosphine)palladium(0) (8.2 mg, 0.007 mmol) were dissolved in dry toluene (10 ml). Then the mixture was heated and kept under nitrogen at 100 °C for 18 hours. After cooling to room temperature, methanol was added and a precipitate was formed. The precipitate was collected by filtration. Then the product was purified upon Soxhlet extraction with methanol and hexane. A dark solid was obtained (148.5 mg, yield: 58 %). Molecular weight (GPC, THF): $M_w = 21.6$ kDa, $M_n = 10.3$ kDa, PD = 2.1. UV/vis (DCM): 659 nm, UV/Vis (thin film): 684 nm; ϵ (659) /L mol⁻¹cm⁻¹: 43521.

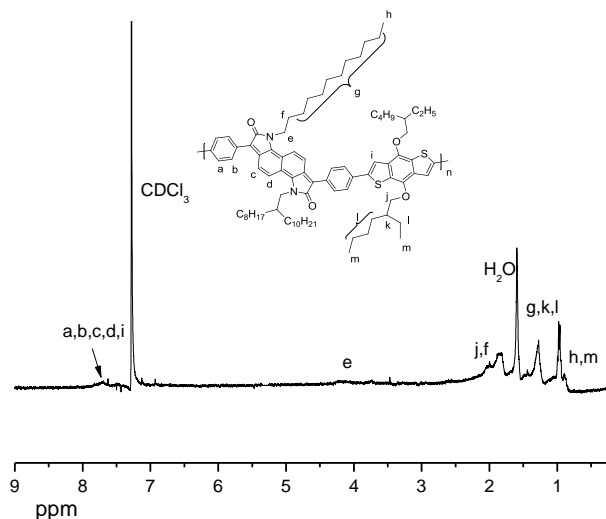


Polymer P-1,6-NDF-BDT2

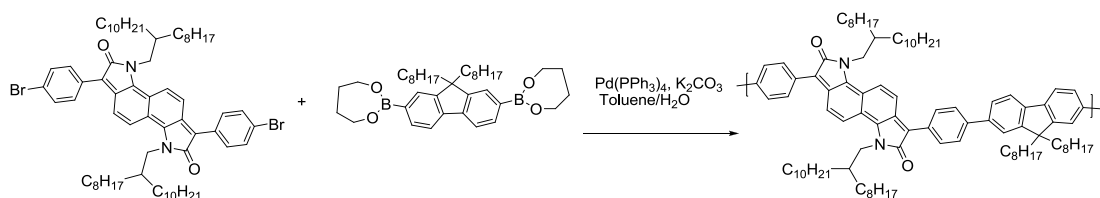


In a Schlenk flask, **1,6-NDF2** (200.0 mg, 0.23), (4,8-bis(2-ethylhexyloxy)benzo[1,2-*b*:4,5-*b'*]dithiophene-2,6-diyl)bis(trimethylstannane) (174.9 mg, 0.23 mmol) and tetrakis(triphenylphosphine)palladium(0) (10.4 mg, 0.009 mmol) were dissolved in dry toluene (10 ml). Then the mixture was heated and kept under nitrogen at 100 °C for 18 hours. After cooling to room temperature, methanol was added and a precipitate was formed. The precipitate is collected by filtration. Then the product was purified upon Soxhlet extraction with methanol and hexane. A dark solid was obtained (173.5 mg, yield: 63 %). Molecular weight (GPC, THF): $M_w = 14.2$

kDa, $M_n = 7.9$ kDa, PD = 1.8. UV/vis (DCM): 666 nm, UV/Vis (thin film): 696 nm; ϵ (666) /L mol⁻¹cm⁻¹: 45254.

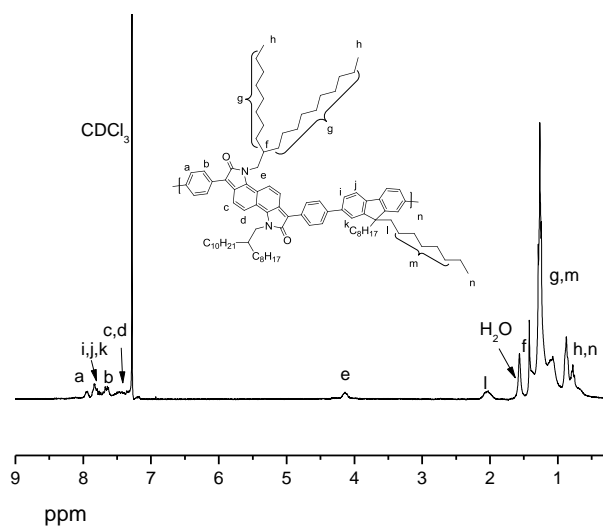


Polymer P-1,6-NDF-FL1

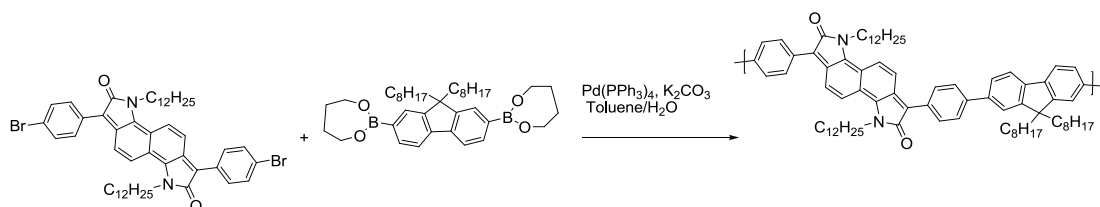


In a Schlenk flask, **1,6-NDF1** (200.0 mg, 0.18 mmol), 2,2-(9,9-dioctyl-9H-fluoren-2,7-diyl)bis(4,4,5,5-tetramethyl-1,3,2-dioxaborolane) (105.5 mg, 0.18 mmol) and tetrakis(triphenyl-phosphine)palladium(0) (8.2 mg, 0.007 mmol) were dissolved in dry toluene (10 ml) under nitrogen. The reaction was degassed and heated to 50 °C. A degassed solution of potassium carbonate (82.68 mg, 0.78 mmol) in water (3 ml) was added. The mixture is stirred at 90 °C for 24 hours. After cooling to room temperature, the dark solution was diluted with DCM, washed three times

with water and once with brine. Then the organic layer was dried over anhydrous magnesium sulfate and the solvent was removed at reduced pressure. After that the crude product was dissolved in a minimal amount of DCM and precipitated in methanol. The product was obtained as a dark solid (43.6 mg, yield: 17 %). Molecular weight (GPC, THF): $M_w = 25.6$ kDa, $M_n = 8.0$ kDa, PD = 3.2. UV/vis (DCM): 612 nm, UV/Vis (thin film): 639 nm; ϵ (615) /L mol⁻¹cm⁻¹: 85625.

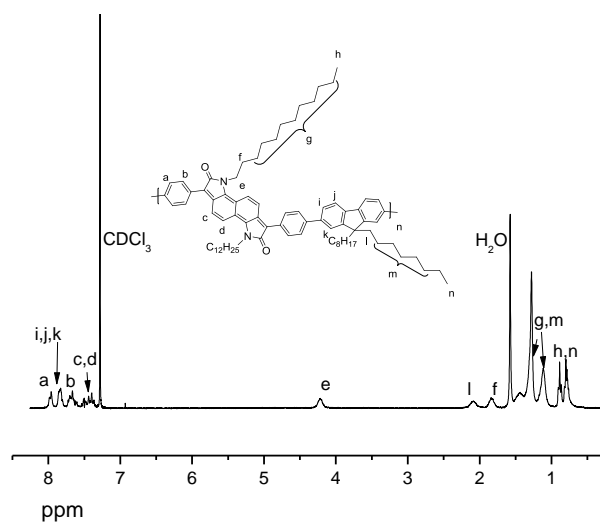


Polymer P-1,6-NDF-FL2

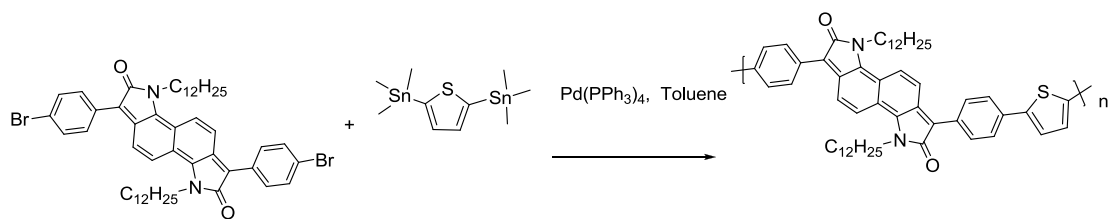


In a Schlenk flask, **1,6-NDF2** (200.0 mg, 0.23 mmol), 2,2-(9,9-dioctyl-9H-fluoren-2,7-diyl)bis(4,4,5,5-tetramethyl-1,3,2-dioxaborolane) (132.8 mg, 0.23

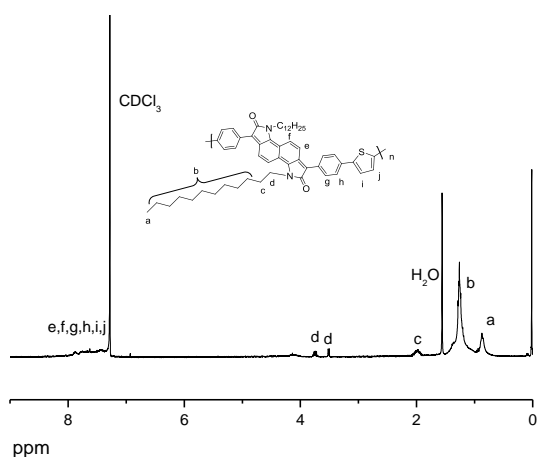
mmol) and tetrakis(triphenyl-phosphine)palladium(0) (10.4 mg, 0.009 mmol) were dissolved in dry toluene (10 ml) under nitrogen. The reaction was degassed and heated to 50 °C. A degassed solution of potassium carbonate (105.6 mg, 1.0 mmol) in water (3.5 ml) was added. The mixture was stirred at 90 °C for 24 hours. After cooling to room temperature, the dark solution was diluted with DCM, washed three times with water and once with brine. Then the organic layer was dried over anhydrous magnesium sulfate and the solvent was removed at reduced pressure. After that the crude product was dissolved in a minimal amount of DCM and precipitated in methanol. The product was obtained as a dark solid (128.6 mg, yield: 49 %). Molecular weight (GPC, THF): $M_w = 14.8$ kDa, $M_n = 5.5$ kDa, PD = 2.7. UV/vis (DCM): 603 nm, UV/Vis (thin film): 624 nm; ϵ (603) /L mol⁻¹cm⁻¹: 87623.



Polymer P-1,6-NDF-Th



In a Schlenk flask, **1,6-NDF2** (200.0 mg, 0.23), 2,5-bis(trimethylstannane)thiophene (92.8 mg, 0.23 mmol) and tetrakis-(triphenyl-phosphine)palladium(0) (10.4 mg, 0.009 mmol) were dissolved in dry DMF (10 ml). Then the mixture was heated and kept under nitrogen at 100 °C for 18 hours. After cooling to room temperature, methanol was added and a precipitate was formed. The precipitate was collected by filtration. Then the product was purified upon Soxhlet extraction with methanol and hexane. A dark solid was obtained. (96.3 mg, yield: 52 %). ¹H NMR (300 MHz, CDCl₃): δ ppm 7.02-8.04 (br, 14 H), 3.66-3.79 (m, 3H), 3.51 (d, J=6 Hz, 1H), 1.87-2.08 (s, 4H), 0.99-1.49 (s, 36H), 0.77-0.99 (s, 6H). Molecular weight (GPC, THF): *M_w* = 12.9 kDa, *M_n* = 3.8 kDa, PD = 2.0. UV/vis (DCM): 615 nm, UV/Vis (thin film): 678 nm; ε (615) /L mol⁻¹cm⁻¹: 28456.



6 References

- 1 A. Iqbal, M. Jost, R. Kirchmayr, J. Pfenniger, A. Rochat, O. Wallquist, *Bull. Soc. Chim. Belg.* 1988, **97**, 615-643.
- 2 A. Iqbal, L. Cassar, A. C. Rochat, J. Pfenninger, O. Wallquist, *J. Coat. Technol.* 1988, **60**, 37-45.
- 3 W. Kylberg, P. Sona, J. Heier, J.-N. Tisserant, C. Mueller, F. Nuesch, Z.-K. Chen, A. Dodabalapur, S. Yoon, R. Hany, *Energy Environ. Sci.*, 2011, **4**, 3617-3624.
- 4 A. Tang, L. Li, Z. Lu, J. Huang, H. Jia, C. Zhang, Z. Tan, Y. Li, J. Yao, *J. Mater. Chem. A*, 2013, **1**, 5747-5757.
- 5 M. Chen, W. Fu, M. Shi, X. Hu, J. Pan, J. Ling, H. Li, H. Chen, *J. Mater. Chem. A*, 2013, **1**, 105-111.
- 6 S.-Y. Liu, M.-M. Shi, J.-C. Huang, Z.-N. Jin, X.-L. Hu, J.-Y. Pan, H.-Y. Li, A. K.-Y. Jen, H.-Z. Chen, , *J. Mater. Chem. A*, 2013, **1**, 105-111.
- 7 D. G. Farnum, G. Metha, G. G. I. Moore, F. P. Sigal, *Tetrahedron Lett.* 1974, **29**, 2549-2552.
- 8 A. Iqbal, L. Cassar, U.S. Patent 4, 415, 685, 1983
- 9 A. C. Rochat, L. Cassar. A. Iqbal, EP 94911, 1983.
- 10 W. K. Chan, Y. Chen, Z. Peng, L. Yu, *J. Am. Chem. Soc.* 1993, **115**, 11735.
- 11 B. Thomas, T. Bernd, *Macromol. Rapid Commun.* 2000, 190, **21**, 182-189.
- 12 A. R. Rabindranath, Y. Zhu, I. Heim, B. Tieke, *Macromolecules*, 2006, **39**, 8250-8256.
- 13 Y. Zhu, A. R. Rabindranath, T. Beyerlein, B. Tieke, *Macromolecules*, 2007, **40**,

- 6981-6989.
- 14 Y. Zhu, K. Zhang, B. Tieke, *Macromol. Chem. Phys.* 2009, **210**, 431-439.
- 15 J. Louie, J. F. Hartwig, *J. Am. Chem. Soc.* 1997, **119**, 11695-11696.
- 16 F. Paul, J. Patt, J. F. Hartwig, *Macromolecules*, 1998, **31**, 1700-1704.
- 17 J.-F. Marcoux, S. Wagaw, S. L. Buchwald, *J. Org. Chem.* 1997, **62**, 1568-1569.
- 18 A. S. Guram, R. A. Rennels, S. L. Buchwald, *Angew. Chem. Int. Ed. Engl.* 1995, **34**, 1348-1350.
- 19 Y. P. Zou, D. Gendron, R. Badrou-Aich, A. Najari, Y. Tao, M. Leclerc, *Macromolecules*, 2009, **42**, 2891-2894.
- 20 Y. P. Zou, D. Gendron, R. Neagau-Plesu, M. Leclerc, *Macromolecules*, 2009, **42**, 6361-6365.
- 21 L. Buergi, M. Turbiez, R. Pfeiffer, F. Bienewald, H.-J. Kirner, C. Winnewisser, *Adv. Mater.* 2008, **20**, 2217-2224.
- 22 E. Zhou, S. Yamakawa, K. Tajima, C. Yang, K. Hashimoto, *Chem. Mater.* 2009, **21**, 4055-4061.
- 23 C. Kanimozhi, D. Balaru, G. D. Sharma, S. Patil, *J. Phys. Chem. B.* 2010, **114**, 3095-3103.
- 24 L. Huo, J. Hou, H.-Y. Chen, S. Zhang, Y. Jiang, T. Chen, Y. Yang, *Macromolecules*, 2009, **42**, 6564-6571.
- 25 G. Li, R. Zhu, Y. Yang, *Nature Photonics*, 2012, **6**, 153-161.
- 26 E. Guo, P. Ren, Y. Zhang, H. Zhang, W. Yang, *Chem. Commun.* 2009, 5859-5861.

- 27 B. Zhang, H. Zhang, X. Li, W. Li, P. Sun, W. Yang, *J. Polym. Sci. Part A: Polym Chem.*, 2011, **49**, 3048–3057.
- 28 P. Langr, J. Wuckelt, M. Doering, H. Goerls, R. Beckert, *Liebigs Ann./Recueil* 1997, 2553-2561.
- 29 M. Kirkus, S. Knippenberg, D. Beljonne, J. Cornil, R. A. J. Janssen, S. C. J. Meskers, *J. Phys. Chem. A*, 2013, **117**, 2782-2789.
- 30 I. Welterlich, Ph.D. *Thesis, University of Cologne*, 2013.
- 31 H. Faerstenwerth, Ger. Offen. DE 3 525 109 AI, Bayer AG, 1987.
- 32 Y. Z. Solberg, *Naturforsch*, 1977, **32c**, 292-295.
- 33 A. C. Rochat, A. Iqbal, J. Pfenninger, L. Casser, Eur. Pat. Appl. EP. 016 309, Ciba-Geigy, 1984.
- 34 J. Wuckelt, M. Doering, P. Langer, H. Goerls, R. Beckert, *Tetrahedron Lett.*, 1977, **38**, 5269-5272.
- 35 P. Langer, J. Wuckelt, M. Doering, *J. Org. Chem.*, 2000, **65**, 729-734.
- 36 R. Schroeder, *Synlett*, 2003, **15**, 2389-2391.
- 37 I. Welterlich, O. Charov, B. Tieke, *Macromolecules*, 2012, **45**, 4511-4519.
- 38 S. Lu, A. Facchetti, Y. Yao, M. Dress, H. Yan, US 2011/0 226 338 A1, 2011.
- 39 S. Lu, M. Dress, Y. Yao, D. Boudinet, H. Yan, H. Pan, J. Wang, Y. Li, H. Usta, A. Facchetti, *Macromolecules*, 2013, **46**, 3895-3906.
- 40 C. W. Greenhalgh, J. L. Carey. D. F. Newton, *Dyes Pigm.*, 1980, **1**, 103-120.
- 41 C. W. Greenhalgh, J. L. Carey, N. Hall. D. F. Newton, *J. Soc. Dyes Colour.*, 1994, **110**, 178-183.

- 42 British Patent, 1 568 231, ICI, 1976.
- 43 British Patent, 2 055 881, ICI, 1979.
- 44 British Patent, 2 068 402, ICI, 1980.
- 45 British Patent, 2 103 231, ICI, 1981.
- 46 European Patent, 0 182 507, ICI, 1984.
- 47 European Patent, 0 252 406, Bayer, 1985.
- 48 European Patent, 0 294 029, ICI, 1987.
- 49 European Patent, 0 333 337, ICI, 1988.
- 50 European Patent, 0 363 034, ICI, 1988.
- 51 European Patent, 0 371 223, NSK, 1988.
- 52 European Patent, 0 397 170, NSK, 1989.
- 53 European Patent, 0 436 940, NSK, 1990.
- 54 S. J. Bentley, D. J. Milner, *Syn. Commun.* 1996, 95-100.
- 55 A. A. Gorman, M. Hutchings, P. D. Wood, *J. Am. Chem. Soc.*, 1996, **118**, 8497-8498.
- 56 A. Oehlke, K. Hofmann, S. Spange, *New J. Chem.*, 2006, **30**, 533-536.
- 57 S. Spange, S. Prause, E. Vilsmeier, W. R. Thiel, *J. Phys. Chem. B*, 2005, **109**, 7280-7289.
- 58 P. A. Ulmann, H. Tanaka, Y. Matsuo, Z. Xiao, I. Soga, E. Nakamura, *Phys. Chem. Chem. Phys.*, 2011, **13**, 21045-21049.
- 59 J. P. C. Carrasco, A. Ripoché, F. Odobel, D. Jacquemin, *Dyes and Pigments*, 2012, **92**, 1144-1152.

- 60 Z. Cai, J. Gao, X. Li, B. Xiang, *Opticals Commun.*, 2007, 503-508.
- 61 K. Zhang, B. Tieke, *Macromolecules*, 2011, **44**, 4596-4599.
- 62 K. Zhang, B. Tieke, J. C. Forgie, F. Viela, P. J. Skabara, *Macromolecules*, 2012, **45**, 743-750.
- 63 K. Zhang, *Ph.D thesis, University of Cologne*, 2010.
- 64 H. Zhang, J. Zhang, B. Tieke, *Polym. Chem.*, DOI: 10.1039/C3PY01101A,
- 65 W. Cui, J. Yuen, F. Wudl, *Macromolecules*, 2011, **44**, 7869-7873.
- 66 P. Deng, L. Liu, S. Ren, H. Li, Q. Zhang, *Chem. Commun.*, 2012, **48**, 6960-6962.
- 67 W. Hong, B. Sun, C. Guo, J. Yuen, Y. Li, S. Lu, C. Huang, A. Facchetti, *Chem. Commun.*, 2013, **49**, 484-486.
- 68 W. Yue, X. Huang, J. Yuan, W. Ma, F. C. Krebs, D. Yu, *J. Mater. Chem. A*, 2013, **1**, 10116-10119.
- 69 J. W. Rumer, M. Levick, S.-Y. Dai, S. Rossbauer, Z. Huang, L. Biniek, T. D. Anthopoulos, J. R. Durrant, D. J. Procter, I. McCulloch, *Chem. Commun.*, 2013, **49**, 4465-4467.
- 70 J. L. Carey, C. A. Shand, R. H. Thomson, *J. Chem. Soc. Perkin Trans. I*, 1984, 1957-1962.
- 71 P. A. Smith, *PhD thesis, University of Leeds*, 1995
- 72 G. Hallas, C. Yoon, *Dyes and Pigments*, 2011, **48**, 107-119.
- 73 G. Hallas, C. Yoon, *Dyes and Pigments*, 2011, **48**, 121-132.
- 74 C. Yoon, G. Hallas, *Color. Technol.*, 2002, **118**, 125-130.
- 75 S. Ghasimi, *Master Thesis, University of Cologne*, 2012.

- 76 W. L. Ma, C. L. Yang, X. Gong, K. Lee, A. Heeger, *Adv. Funct Mater.* 2005, **15**, 1617-1622.
- 77 G. Li, V. Shrotriya, J. Huang, Y. Yao, T. Moriarty, K. Emery, Y. Yang, *Nat. Mater.* 2005, **4**, 864-868.
- 78 Y. Zhang, J. Zou, C. Cheuh, H. Yip, A. K. Jen, *Macromolecules* 2012, **45**, 5427-5435.
- 79 H. Tan, X. Deng, J. Yu, J. Chen, K. Nie, Y. Huang, Y. Liu, Y. Wang, M. Zhu, M. Zhu, *J. Polym. Sci. Part A: Polym. Chem.* 2013, **51**, 1051-1057.
- 80 L. Huo, L. Ye, Y. Wu, Z. Li, X. Guo, M. Zhang, S. Zhang, J. Hou, *Macromolecules* 2012, **45**, 6923-6929.
- 81 E. Zhou, J. Cong, K. Hashimoto, K. Tajima, *Macromolecules* 2013, **46**, 763-768.
- 82 R. S. Kularatne, H. D. Magurudeniya, P. Sista, M. C. Biewer, M. C. Stefan, *J. Polym. Sci. Part A: Polym. Chem.* 2013, **51**, 743-768.
- 83 G. C. Welch, R. C. Bakus, S. J. Teat, G. C. Bazan, *J. Am. Chem. Soc.* 2013, **135**, 2298-2305.
- 84 A. Lyer, J. Bjorgaard, T. Anderson, M. E. Koese, *Macromolecules* 2012 **45**, 6380-6389.
- 85 S.-W. Chang, H. Waters, J. Kettle, Z.-R. Kuo, C.-H. Li, C.-Y. Yu, M. Horie, *Macromol. Rapid Commun.* 2012, **33**, 1927-1932.
- 86 H. Zhou, Z. Li, F. Deledalle, E. C. Fregoso, M. Shahid, Z. Fei, C. B. Nielsen, G. N. Yacob, S. Rossbauer, T. D. Anthopoulos, *J. Am. Chem. Soc.* 2013, **135**, 2040-2043.

- 87 J.-H. Huang, C.-M. Teng, Y.-S. Hsiao, F.-W. Yen, P. Chen, F.-C. Chang, C.-W. Chu, *J. Phys. Chem. C* 2011, **115**, 2398-2405.
- 88 J. S. Kim, Z. Fei, D. T. James, M. Heeney, J.-S. Kim, *J. Mater. Chem.* 2012, **22**, 9975-9982.
- 89 T.-Y. Chu, J. Lu, S. Beaupre, Y. Zhang, J.-R. M. Pouliot, S. Wakim, J. Zhou, M. Leclerc, Z. Li, J. Ding, Y. Tao, *J. Am. Chem. Soc.* 2011, **133**, 4250-4253.
- 90 Y. Liang, Z. Xu, J. Xia, S.-T. Tsai, Y. Wu, G. Li, C. Ray, L. Yu, *Adv. Mater.* 2010, **22**, E135-E138.
- 91 M. A. Naik, N. Vemlatramaiah, C. Kanimozhi, S. Patil, *J. Phys. Chem. C* 2012, **116**, 26128-26137.
- 92 H. Usta, G. Lu, A. Facchetti, T. J. Marks, *J. Am. Chem. Soc.* 2006, **128**, 9034-9035.
- 93 G. Lu, H. Usta, C. Risco, L. Wang, A. Facchetti, M. A. Ratner, T. J. Marks, *J. Am. Chem. Soc.* 2008, **130**, 7670-7685.
- 94 I. Welterlich, B. Tieke, *Polym. Chem.*, 2013, **4**, 3755-37645.
- 95 K. Z. Chen, W. Huang, H. L. Wang, E. T. Kang, B. J. Chen, C. S. Lee, S. T. Lee, *Macromolecules* 2000, **33**, 9015-9025.
- 96 D. S. Surry, S. L. Buchwald, *Chem. Sci.* 2011, **2**, 27-50.
- 97 C. Reichardt, *Chem. Rev.* 1994, **94**, 2319-2385.
- 98 P. Mueller, *Pure Appl. Chem.* 1993, **22**, 409-416.
- 99 M. J. Kamlet, T. N. Hall, J. N. Hall, J. Boykin, R. Taft, W. J. *Org. Chem.* 1979, **44**, 2599-2604.
- 100 R. W. Taft, M. J. Kamlet, *J. Am. Chem. Soc.* 1976, **98**, 2866-2894.

- 101 M. J. Kamlet, R. W. Taft, *J. Am. Chem. Soc.* 1976, **98**, 377–383.
- 102 J. Catalán, C. Díaz, *Liebigs Ann.* 1997, 1941–1949.
- 103 J. Catalán, C. Díaz, *Eur. J. Org. Chem.* 1999, 885–891.
- 104 J. Catalán, V. López, P. Pérez, *Liebigs Ann.* 1995, 793–795.
- 105 J. Catalán, C. Díaz, V. López, P. Pérez, J.-L. G. d. Paz, J. G. Rodríguez, *Liebigs Ann.* 1996, 1785–1794.
- 106 J. Catalán, J. Palomar, C. Díaz, J.-L. G. d. Paz, *J. Phys. Chem. A* 1997, **101**, 5183–5189.
- 107 J. Catalán, H. Hopf, *Eur. J. Org. Chem.* 2004, 4694–4702.
- 108 J. Catalán, *Phys. J. Chem. B* 2009, **113**, 5951–5960.
- 109 K. Hofmann, S. Brumm, C. Mende, K. Nagel, A. Seifert, I. Roth, D. Schaarschmidt, H. Lang, S. Spange, *New J. Chem.*, 2012, **36**, 1655–1644.
- 110 B. C. Thompson, Y. G. Kim, J. R. Reynolds, *Macromolecules* 2005, **38**, 5359–5362.
- 111 L. D. M. De, M. M. J. Simenon, A. R. Brown, R. E. F. Einerhand, *Synth. Met.* 1997, **87**, 53–59.
- 112 D. D. Perrin, W. L. F. Armarego, *Purification of Laboratory Chemicals*. 3th ed.; Pergamon 1988.
- 113 M. J. Frisch, G. W. Trucks, H. B. Schlegel, G. E. Scuseria, M. A. Robb, J. R. J. Cheeseman, J. A. Montgomery, T. Vreven, K. N. Kudin, J. C. Burant, J. M. Millam, S. S. Iyengar, J. Tomasi, V. Barone, B. Mennucci, M. Cossi, G. Scalmani, N. Rega, G. A. Petersson, H. Nakatsuji, M. Hada, M. Ehara, K. Toyota, R. Fukuda,

J. Hasegawa, M. Ishida, T. Nakajima, Y. Honda, O. Kitao, H. Nakai, M. Klene, X. Li, J. E. Knox, H. P. Hratchian, J. B. Cross, V. Bakken, C. Adamo, J. Jaramillo, R. Gomperts, R. E. Stratmann, O. Yazyev, A. J. Austin, R. Cammi, C. Pomelli, J. W. Ochterski, P. Y. Ayala, K. Morokuma, G. A. Voth, P. Salvador, J. J. Dannenberg, V. G. Zakrzewski, S. Dapprich, A. D. Daniels, M. C. Strain, O. Farkas, D. K. Malick, A. D. Rabuck, K. Raghavachari, J. B. Foresman, J. V. Ortiz, Q. Cui, A. G. Baboul, S. Clifford, J. Cioslowski, B. B. Stefanov, G. Liu, A. Liashenko, P. Piskorz, I. Komaromi, R. L. Martin, D. J. Fox, T. Keith, M. A. Al-Laham, C. Y. Peng, A. Nanayakkara, M. Challacombe, P. M. W. Gill, B. Johnson, W. Chen, M. W. Wong, C. Gonzalez, J. A. Pople, Gaussian 03, Revision C.02. Gaussian, Inc.: Wallingford, CT, 2004.

7 Acknowledgements

First of all, I am very grateful to my doctor supervisor Prof. Dr. Bernd Tieke for the opportunity to work in his fantastic group, giving me an interesting research topic and patience and support with my work. I enjoy everyday in this group even sometimes is very busy.

My warmest thanks go to Prof. Wenjun Yang and Prof. Dr. Xuegang Chen, Qingdao University Science and Technology, China, for their guidance, encouragement, and hospitality in Qingdao. Prof. Wenjun Yang is a very nice and friendly person and for work with him during my master thesis is a pleasure.

I would like to thank Prof. Dr. Ulrich K. Deiters, Prof. Dr. Sanjay Mahur and Dr. Dirk Hertel for their attendance as a referee. Especially thank Prof. Dr. Ulrich K. Deiters for helping me to write a recommendation letter to apply for DAAD scholarship.

I thank Dr. Welterlich and Mr. Ghasimi for supplying monomers of isoDPP and ABDF, Dr. Kai Zhang for helpful advice and support in my beginning time in the group and Dr. Pascal Hayoz, BASF, Switzerland for cooperation and helpful discussions. I would like to thank Ms. Sara Sahm for her kind help in translation of the abstract into German. I also thank Prof. Dr. Stefan Spange and Mr. A. Kuchenbuch for measuring the solvatochromic properties of monomer and polymer based on ABDF.

Many thanks to Mr. Jun Zhang for computer calculation of the HOMO/LUMO structure and Dr. J. Neudörfl for analyzing the crystal structures of some monomers.

I thank all my colleagues in my group, K. Cheng, G. Krieger, K. Kraus for the pleasant and inspiring atmosphere.

I also thank the students, C. Xu, J. Wolf, O. Chedati, C. Dittmer, K. Korsching and S. Lülldorf, whom I co-supervised during their laboratory internships, for their good performances and help.

Finally but not least I would like to express my heartfelt thanks to my parents for their invaluable advice, encouragement, and unconditional love. Their constant push for me to excel academically led to my choice of chemistry as a career.

Financial support by the German Academic Exchange Service (DAAD), China Scholarship Council (CSC), and BASF Schweiz AG, Basel, Switzerland, are gratefully acknowledged.

8 List of publications and conferences

- 1 Haichang Zhang, Irina Welterlich, Joerg-Martin Neudoerfl, Bernd Tieke, Chao Yang, Xuegang Chen, Wenjun Yang. "Synthesis and Characterization of 1,3,4,6-Tetraarylpyrrolo[3,2-*b*]-pyrrole- 2,5-dione (isoDPP)-based Donor-Acceptor Polymers with Low Band Gap". *Polym. Chem.*, 2013, **4**, 4682-4689.
- 2 Haichang Zhang, Joerg-Martin Neudoerfl, Bernd Tieke. "Naphthodifuranone- Based Monomers and Polymers". *Macromolecules*, 2013, **46**, 5842-5849.
- 3 Haichang Zhang, Jun Zhang, Bernd Tieke. "Comparative study of polymers containing naphthodifuranone and benzodifuranone units in the main chain". *Polym. Chem.* 2013, DOI: 10.1039/C3PY01101A.
- 4 Haichang Zhang, Saman Ghasimi, Bernd Tieke, Alexander Schade, Stefan Spanger. "Aminobenzodione-based polymers with low band gap and solvatochromic behavior".(Article, submitted in *Polym.Chem.*)
- 5 Haichang Zhang, Bernd Tieke, "1,6-Naphthodione based monomers and polymers".(Communication, manuscript submitted in ACS Macroletters)
- 7 Haichang Zhang, Bernd Tieke, "Polymers based on benzodiones and naphthodiones".(Review, manuscript is in preparing)
- 8 Irina Welterlich, Haichang Zhang, Kai Zhang, Bernd Tieke, "Low band gap polymers based on dithioketopyrrolopyrrole and benzodifuranone unit". Macromolecule conference, Freiburg, Germany, 2012.
- 9 Bernd Tieke, Irina Welterlich, Haichang Zhang, Kai Zhang, "Polymer for electronic applications based on pyrroloprrolediones and other high performance pigments". Macromolecule conference, Freiberg, Germany, 2014.

Patent

Pascal Hayoz, Bernd Tieke, Haichang Zhang. "Polymers based on Naphthodiones".
PF EP/US 74482 (BASF)

Ich versichere, daß ich die von mir vorgelegte Dissertation selbständig angefertigt habe, die benutzten Quellen und Hilfsmittel vollständig angegeben und die Stellen der Arbeit einschließlich Tabellen, Karten und Abbildungen, die anderen Werken im Wortlaut oder dem Sinn nach entnommen sind, in jedem Einzelfall als Entlehnung kenntlich gemacht habe, dass diese Dissertation noch keiner anderen Fakultät oder Universität zur Prüfung vorgelegen hat; dass sie abgesehen von vorner angegebenen Teilpublikationen noch nicht veröffentlicht worden ist. sowie das ich eine solche Veröffentlichung vor Abschluss des Promotionsverfahrens nicht vornehmen werde. Die Bestimmungen dieser Promotionsordnung sind mir bekannt. Die von mir vorgelegte Dissertation ist von Professor Dr. B. Tieke betreut worden.

Ich versichere, dass ich alle Angaben wahrheitsgemäß nach bestem Wissen und Gewissen gemacht habe und verpflichte mich, jedmögliche, die obigen Angaben betreffenden Veränderungen, dem Dekanat unverzüglich mitzuteilen.

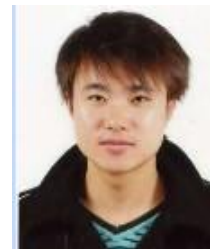
Haichang Zhang

Köln. Den 13.11.2013

Curriculum Vitae

Personal Data

Name Haichang Zhang
Date of birth 20.07.1984
Place of birth Liaoning, P. R. China
Family state Single, without child
Nationality P. R. China



Univeristy Education

09/2003 – 07/2007

Shenyang University of Chemical Technology, P.R.China

Degree: Bachelor's Degree in Chemistry engineering

09/2007 – 07/2010

Qingdao University of Science and Technology, P. R. China

Degree: Master's Degree in Chemistry engineering

04/2011-01/2014

Doctor thesis at University of Cologne, Cologne, Germany

Title: Low bang gap polymer Based on Isodiketopyrrolopyrroles,
aminobenzodiones, 1,8-benzodifuranones and naphthodiones